University of Kentucky

UKnowledge

2018

THE ROLE OF PRO-INFLAMMATORY MEDIATORS IFN**β** AND PROSTAGLANDIN E2 IN SUPPRESSION OF INNATE IMMUNITY TO LISTERIA MONOCYTOGENES

Michelle G. Pitts

University of Kentucky, michelle.pitts@uky.edu
Digital Object Identifier: https://doi.org/10.13023/ETD.2018.127

Right click to open a feedback form in a new tab to let us know how this document benefits you.

STUDENT AGREEMENT:

I represent that my thesis or dissertation and abstract are my original work. Proper attribution has been given to all outside sources. I understand that I am solely responsible for obtaining any needed copyright permissions. I have obtained needed written permission statement(s) from the owner(s) of each third-party copyrighted matter to be included in my work, allowing electronic distribution (if such use is not permitted by the fair use doctrine) which will be submitted to UKnowledge as Additional File.

I hereby grant to The University of Kentucky and its agents the irrevocable, non-exclusive, and royalty-free license to archive and make accessible my work in whole or in part in all forms of media, now or hereafter known. I agree that the document mentioned above may be made available immediately for worldwide access unless an embargo applies.

I retain all other ownership rights to the copyright of my work. I also retain the right to use in future works (such as articles or books) all or part of my work. I understand that I am free to register the copyright to my work.

REVIEW, APPROVAL AND ACCEPTANCE

The document mentioned above has been reviewed and accepted by the student's advisor, on behalf of the advisory committee, and by the Director of Graduate Studies (DGS), on behalf of the program; we verify that this is the final, approved version of the student's thesis including all changes required by the advisory committee. The undersigned agree to abide by the statements above.

<div align="right">

Michelle G. Pitts, Student

Dr. Sarah E. F. D'Orazio, Major Professor

Dr. Kenneth Fields, Director of Graduate Studies

</div>

THE ROLE OF PRO-INFLAMMATORY MEDIATORS
IFNβ AND PROSTAGLANDIN E2
IN SUPPRESSION OF INNATE IMMUNITY TO
LISTERIA MONOCYTOGENES

DISSERTATION

A dissertation submitted in partial fulfillment of

the requirements for the degree of

Doctor of Philosophy in the

College of Medicine at the

University of Kentucky

By: Michelle Georgiana Pitts

Director: Dr. Sarah E.F. D'Orazio, Associate Professor of

Microbiology, Immunology, and Molecular Genetics

Lexington, Kentucky

2018

ABSTRACT OF DISSERTATION

THE ROLE OF PRO-INFLAMMATORY MEDIATORS
IFNβ AND PROSTAGLANDIN E2

IN SUPPRESSION OF INNATE IMMUNITY TO
LISTERIA MONOCYTOGENES

As a foodborne pathogen, *Listeria monocytogenes* (*Lm*) encounters many barriers to invasion and dissemination in the host that may change the nature of host response. *Lm* has been most commonly studied using intravenous (i.v.) inoculation, however, a method that delivers a bolus of bacteria directly to the bloodstream. Thus, little is known about what systemic and local mediators are triggered during the natural course of infection and how these may impact susceptibility. Our laboratory used foodborne transmission of *Lm* in mice to assess whether the method of transmission and the specific organ microenvironment could affect infection-induced secretion of type I interferon or prostaglandin E2. Type I interferon is a pro-inflammatory effector secreted in response to viruses that has been proposed to paradoxically down-regulate innate immunity to intracellular bacteria. In contrast to i.v. infection, type I interferon was not detrimental to the immune response when *Lm* were acquired orally. In fact, most of the anti-inflammatory effects of type I interferon in the spleen were attributable to i.v. but not foodborne infection. Importantly however, downregulation of the receptor for interferon gamma (IFNGR1), previously ascribed to the type I interferon response, was found to be a consequence of infection and unrelated to type I interferon. In the liver, robust recruitment and activation of neutrophils (PMN) is thought to be required for initiation of *Lm* immunity. Prostaglandin E2 (PGE2) is a lipid mediator most commonly associated with pain and fever that has also been demonstrated to have anti-inflammatory or tolerogenic effects. It is unknown, however, whether foodborne infection induces PGE2 in the liver and if PGE2 then down-regulates PMN activities. Recruitment of PMN to the liver following foodborne infection was robust in both susceptible and resistant animals. Bone marrow PMN from each killed *Lm ex vivo* with similar efficiency, thus suggesting that if PMN were dysfunctional during the course of natural infection, they were responding to cues in the microenvironment. Accordingly, significantly more PGE2 was made *ex vivo* by cells from the livers of susceptible animals than from resistant animals. When PGE2 was applied to naïve PMN prior to exposure to *Lm*, it consistently dampened the killing efficiency of these cells, suggesting that this lipid better known for its pro-inflammatory roles might have anti-inflammatory effects during *Lm* infection. Overall, these studies indicate that mediators produced

as a result of infection may have very different roles dependent on route of inoculation, timing, and the specific organ examined.

Michelle G. Pitts
_____

04.13.18
_____

Date

THE ROLE OF PRO-INFLAMMATORY MEDIATORS
IFNβ AND PROSTAGLANDIN E2

IN SUPPRESSION OF INNATE IMMUNITY TO
LISTERIA MONOCYTOGENES

By

Michelle G. Pitts

Sarah D'Orazio

———————————————————

Director of Dissertation

Kenneth Fields

———————————————————

Director of Graduate Studies

04.13.18

———————————————————

Date

This work is dedicated to the animals who kept me sane over the past years. They know who they are. I hope that someday my work helps them as much as they have helped me.

Acknowledgements

First of all, this dissertation would not have been possible without the guidance of my mentor, Sarah D'Orazio. Sarah accepted me into her lab and life, and her mentorship has been an enormous part of my development as a scientist. She pushed me to think more critically, to speak more clearly, and to be a better scientist. I'm very grateful for her help and support and glad I chose the D'Orazio lab back in 2013.

Beyond a doubt, I would not be here without the help and support of former lab member Tanya Myers Morales. From teaching me math that I had forgotten with being out of school for so long, to starting early morning cultures, to helping me when my experiments were too big for one person to handle, Tanya was there for me from day one. More than anything, though, Tanya helped me navigate this winding path of graduate school by being a friend when I needed one. I'm so glad that when she had to leave our lab, she joined the one right next door.

My husband Mark played has also played a very important role in this journey. A PhD himself, Mark understood the evenings, the weekends, the early mornings, and the late nights of writing without ever missing a beat. I'm thankful for having such a supportive partner in my life.

I would also like to acknowledge several people in the MIMG department and beyond. Former lab member Grant Jones was a great person to bounce ideas off of, and seemingly was always in a good mood. Travis Combs, the first student I ever supervised, showed me that I could teach others. Jessica Ferrell, a relatively new person in our lab, was a great set of hands to have around as I frantically tried to finish my work. Melissa Hollifield was pretty much the resource for anything, from information to materials to advice. Dr. Jeff Rush in the Biochemistry department graciously allowed me to use his lab's nitrogen evaporator and provided excellent advice.

Lastly, I would like to recognize the support of Dr. Pam Robinson and her husband Jim, owners of Brandywine Farm. I was employed by them when I made the decision to go back to school, and Pam and Jim have always been supportive of me. They allowed me to spend time with horses whenever I needed to breathe, and I appreciate that more than words can say. Free access to their horses has also allowed me to develop my photography talents, and I would not be anywhere near the skill level I am today without their kindness.

Table of contents

List of Figures

1. Introduction

1.1 Epidemiology

Listeria monocytogenes (*Lm*) is a gram-positive facultative anaerobe often found in the soil and decaying vegetation (1, 2). *Lm* is the causative agent of listeriosis, a rare but very serious disease that may afflict humans and grazing mammals. In addition to *Lm*, more than ten other members of the *Listeria* genus have been identified, but only *Listeria ivanovii* is recognized as pathogenic. Thirteen serotypes of *Lm* have been described, with four causing most cases of human disease. The commonly used laboratory strain EGDe is one of these four, serovar 1/2a. A recent study, however, found that the reference strains EGD, EGDe, 10403s, and LO28 may all be hypovirulent in comparison to clinical isolates belonging to other clonal complexes (3).

It is estimated, using fecal carriage studies, that most people will consume *Lm*-contaminated foods between 5 and 9 times a year (4). *Lm* is a common contaminant of fresh produce, nuts, smoked fish, and dairy, and is annually responsible for many national and international recalls of both human and animal food products. In late 2017-early 2018, a massive outbreak occurred in South Africa that as of April 2018 had cause 189 deaths from an astounding 982 laboratory-confirmed cases (5). The outbreak was associated with consumption of a food product called polony, and whole genome sequencing of bacteria isolated from both the production plant and the finished product confirmed genetic relatedness of the isolated bacteria. In 2016, *Lm* accounted for a staggering 81% (47 million out of 58 million total pounds) of the total amount of food recalled by the USDA, thanks in large part to contamination of frozen vegetable products produced by one company (6). Nine people in four states were hospitalized and diagnosed with listeriosis linked to the isolates from these products with three deaths, one of which was confirmed to be directly caused by listeriosis (7). Another notable recall occurred in

2015, when Blue Bell Creameries voluntarily recalled all of its products and shut down production following a multi-state outbreak with three deaths. All of the diagnoses, 10 in total, were made in patients who were already hospitalized for unrelated conditions and six of these people were positively determined to have consumed products made from the contaminated ice cream (8). This outbreak underscored the idea that although *Lm* is commonly consumed, some level of immune compromise or genetic predisposition is generally required for invasive disease to develop.

1.2   Clinical disease and treatment

For the majority who ingest *Lm*, the only symptoms that materialize will be self-limiting gastroenteritis or flu-like symptoms (9). In the elderly, however, or in patients with comorbidities such as HIV, cancer, diabetes mellitus, and those on immunosuppressive therapies, the disease may progress to invasive listeriosis, characterized by septicemia, meningitis, and/or encephalitis, before diagnosis is made (9). A recent study found that because a diagnosis of invasive listeriosis generally results in admission to intensive care, it is the third most costly foodborne pathogen in the US (10). Fortunately, *Lm* is susceptible to a wide range of antibiotics, including trimethoprim–sulphamethoxazole and β-lactams, and provided that proper treatment is initiated early, many who are diagnosed will recover. Once the bacteria have crossed the blood-brain barrier, however, treatment becomes more difficult and outcomes are generally less favorable (11).

In humans, listeriosis presents most often in immunocompromised or elderly individuals as sudden-onset meningitis or septicemia and has an annual mortality rate averaging 25% of all diagnosed cases (12, 13). There are also cases noted in adults with no known pre-disposing conditions and otherwise healthy immune systems, suggesting that a genetic component may contribute to susceptibility, or that a dose threshold exists, below which most symptoms will be

self-limiting in immunocompetent individuals. The infectious dose needed for listeriosis to develop is not well understood overall. The recent ice cream outbreak, however, provided investigators with an opportunity to assess *Lm* levels in a frozen product, where *Lm* is fully capable of persisting but does not grow. Testing products manufactured before the outbreak on the same production line as the implicated products found an average of 380-2100 CFU per 80-gram unit of product (14). This is a startlingly low number; previously the infectious dose for healthy individuals was estimated to be 10 to 100 million organisms, and for immunocompromised people was estimated at 0.1 to 10 million (15). The incubation period, or the time between ingestion of *Lm* and illness, is also not well-understood, thanks in large part to the wide variety of foods which *Lm* can be found in. A recent French study which identified 37 cases from investigations carried out by the French National Institute for Public Health Surveillance found a wide range of incubation periods. Gastroenteritis was observed in as little as 24 hours, central nervous system and bacteremia cases in 1-14 days, and pregnancy-associated cases presented between 17-67 days after suspected ingestion of contaminated foods (16).

Listeriosis is a serious concern during pregnancy, necessitating a long list of foods that are "off limits" during pregnancy. Pregnant women may themselves only develop flu-like symptoms; however, spontaneous abortion, pre-term birth, and neonatal infection are all potential complications for the pregnancy (9, 11, 13). Recently, a cohort study encompassing 818 cases found that one-quarter of diagnosed pregnant women experienced fetal loss prior to 29 weeks of gestation (11).

1.3 Virulence characteristics

Environmental adaptations

Lm has evolved characteristics that make it both environmentally hardy and insidious in human disease. A saprophyte, *Lm* has been found in a variety of soils and tested to survive under a wide range of soil conditions (1, 2, 17). As such, it is commonly found contaminating dairies, fresh produce, and silage (fermented ruminant feed). *Lm* is able to rapidly transition from its environmental state into an infective state, a process that requires multiple changes in gene regulation in response to changes in temperature, pH, oxygen saturation, and osmolarity. Two transcription factors- the stress response alternative sigma factor σ^B, and PrfA, control the majority of these adaptations (18, 19).

Johannson et al. showed that PrfA was controlled by a 5' UTR thermosensor, which adopted secondary structures at various temperatures to ensuring that the virulence genes regulated by PrfA are upregulated at 37°C (20). However, this thermoregulation is thought to produce a low, basal level of PrfA only, as intracellular conditions further upregulate PrfA and transcription of the virulence genes that it controls (21). PrfA regulates genes encoding two phospholipases; *actA,* which encodes the actin-polymerizing protein ActA; *hly,* which encodes the cholesterol-dependent pore-forming toxin listeriolysin O (LLO), and *mpl*, a metalloprotease. Loss of any of these genes significantly attenuates *Lm* virulence; for example, Δ*hly* mutants cannot escape from the phagosome and thus are completely avirulent (22).

The transcription factor σ^B regulates a number of genes useful in environmental stress responses, including a glutamate decarboxylase, involved in acid resistance, and a bile sale hydrolase (21). Additionally σ^B was shown by Nadon, et al. to regulate transcription of one of the *prfA* promoters *in vitro*, thus the expression of *prfA*- mediated virulence genes is at least partially dependent on σ^B (23).

4

Invasion factors

   Lm appears to use two primary invasion factors, known as internalins (Inl), to gain access to cells. Although there are more than 20 cataloged internalins, InlA and InlB are the two major invasion factors (24-27).   InlA is a cell-wall anchored protein that interacts with E-cadherin to facilitate uptake into enterocytes and goblet cells (27). Addition of InlA to *Listeria innocua*, a normally non-invasive member of the genus, allowed this bacteria to gain receptor-mediated entry into Caco-2 cells, which are similar to human intestinal epithelial cells (24). E-cadherin, however, is a major component of adherens junctions, the side-to-side connections of epithelial cells, and is not normally accessible from the intestinal lumen. Pentecost et al. showed that rather than disrupting epithelial barrier integrity in the intestine to access E-cadherin, *Lm* instead uses the self-renewing nature of enterocytes to its advantage (28). When a cell is normally extruded, E-cadherin is transiently exposed to the lumen and becomes accessible to *Lm*. Thus, the bacteria triggers its own uptake without activating host surveillance mechanisms.   InlA- E-cadherin interactions are very species-specific, however, and wild type mice do not express the form of E-cadherin that InlA naturally binds (29, 30), making oral infection of mice inefficient. Experimental methods used to alleviate this difficulty are discussed further under section 1.4, "Transmission method."

   InlB binds Met, a receptor tyrosine kinase, on a variety of cells including hepatocytes, and also activates cell signaling mechanisms not triggered by InlA (24, 31, 32). *In vitro*, *inlB* expression was found to be necessary for hepatocyte tropism; however, Gregory et al. showed that the *inlAB* operon was not necessary *in vivo* for infection of hepatocytes (33). It remains unclear, however, what other routes *Lm* might use to access hepatocytes.

   Deletion of *inlA* was shown not to affect bacteria levels in the spleen and liver following oral infection of mice (34, 35). *Lm* have also been shown *in vitro* to translocate across intestinal M cells independent of internalin function or secretion of the pore-forming toxin LLO (36). This

suggested that *Lm* utilize other methods to gain access to the intestinal lamina propria. Drolia et al. recently reported that LAP (*Listeria* adhesion protein) binding of HSP-60 on intestinal epithelial cells triggers NFκB signaling in the cell and rearrangement of cell-to-cell adhesion proteins, thus allowing *Lm* to translocate across the epithelium (37). In this study, Δ*lap Lm* exhibited a significant defect in dissemination to the spleen and liver, more so than the Δ*inlA* strain.

Cell-to-cell spread

In vitro infections as well as extensive work done using i.v. infection of mice has shown much of how *Lm* escapes from the phagosome and begins cell-to-cell spread. Key virulence factors LLO and PLC function in a complementary manner to facilitate *Lm* vacuolar escape. If not rapidly killed once internalized, *Lm* utilizes LLO and PLC to lyse the vacuole membrane and escape to the cell cytosol (38-41). Secreted PLC also induces phagosomal assembly of NADPH oxidase, a process which secretion of LLO was also recently shown to prevent (42). To move from one adjacent cell to another, *Lm* uses ActA to polymerize host cell globular actin into filamentous F-actin, forming the "comet tails" commonly seen in micrographs and immunofluorescent images of intracellular *Lm* (43, 44). Extensive work by several groups including Tilney and Portnoy (44) showed that actin was polymerized on one pole of the bacterium, thus allowing *Lm* to move away from the building actin tail. In confluent or adjoining cells, once the tail reaches the cell membrane, *Lm* protrudes into a neighboring cell and is eventually taken into that cell, forming a double-membrane vacuole which is again lysed by LLO and PLC (41, 44). This is a particularly useful trait in tissues such as the hepatic parenchyma, where it can infect large areas of hepatocytes without needing to encounter complement or phagocytic cells.

1.4   Mouse Model

Differential susceptibility in mice

In order to compare characteristics that might affect infection in susceptible and resistant individuals, two mouse strains are commonly used: susceptible BALB/cBy/J (BALB) and comparatively resistant C57BL/6. (B6) Using intravenous (i.v.) infection, Cheers et al. found that the LD_{50} for B6 mice was 100-fold greater than that of BALB mice. When these two strains were crossed, approximately half of the offspring became resistant, leading to the idea that there was a dominant resistance gene in the B6 mouse (45). Later, the same group showed that overall clearance kinetics in the spleen and liver were slowed in the BALB mouse and that early bacterial burdens grew differently in the liver than in the spleen (46). At 24 hours post infection with 10^4 *Lm*, approximately 10-fold more bacteria were present in the livers of BALB mice than in B6, whereas burdens were very similar at this point in the spleen. This suggested that a differential early clearance response had taken place in the liver, and the authors speculated that macrophage uptake of *Lm* in the BALB liver could be deficient (46).

Overall, most susceptibility differences between mouse strains have been attributed to facets of innate immunity, including differential expression of STAT4 and reduced or delayed secretion of TNFα, IL-12, and IFNγ (47-50). The conventional view is that when infected with *Lm*, BALB mice initially tend to produce a Th2 response, which is useful for extracellular pathogens and parasites, while B6 mice respond with secretion of Th1 cytokines including IFNγ. Both BALB and B6 mice carry a non-functional allele for NRAMP1, a protein associated with natural resistance to intracellular bacteria, and are complement-sufficient (51, 52). A study utilizing F2 progeny of BALB and B6 matings mapped susceptibility loci to chromosomes 5 and 13, designated *Listr1* and *Listr2* (53). Later, expression of CXCL11 was mapped to the *Listr1* loci on chromosome 5. (54) Mice carrying the locus had significantly higher hepatic bacterial burdens at 24 hours post infection than the control strain, a difference thought to be due to the

presence of fewer CD14+ liver-resident mononuclear phagocytes. Notably, this locus had no effect on bacterial burdens in the spleen. Another study co-localized the diabetes susceptibility allele *Idd14* in non-obese diabetic (NOD) mice with *Listr2* (55), thus adding NOD mice to the list of *Lm*-susceptible animals.   In general, however, the majority of studies of *Lm* susceptibility have used BALB or B6 mice and their derivatives, as these two display the largest difference in susceptibility. Despite extensive study over the past several decades, though, many important components of innate immunity to *Lm* such as the neutrophil response have not been compared in these mice.

Sex-based susceptibility

Sex-based susceptibility of mice to *Lm* has not been as clearly defined as strain susceptibility. In humans, gender is often identified as a risk factor for many diseases including those of infectious origin; however, a clear gender preference has not been identified in listeriosis cases. An early study by Cheers et al. found no difference in susceptibility in any of the mice tested (45), while a much more recent investigation showed that female mice of any strain were significantly more susceptible to *Lm* infection than males. This difference was thought to be a result of increased serum IL-10 (56). When foodborne infection was used, BALB females were more susceptible than males, but interestingly, no sex-based differences were seen in B6 mice (35). For ease of study and to lessen the chances of fighting amongst cage mates, female mice were often used in the studies detailed in the later chapters. However, male mice were also used where available or appropriate, and no significant differences in susceptibility, cell function, or cell yield per gram of body weight were noted between sexes in these studies.

Transmission method

Lm has long been studied as a model intracellular pathogen in mice by using intravenous infection, a highly reproducible method that has led to the advancement of knowledge in many areas of immunology. Intraperitoneal infection has also been widely used because of its ease and reproducibility. However, with the exception of maternal-fetal vertical transmission, *Lm* is exclusively acquired in humans by the consumption of contaminated food. Oral infection of mice is most commonly done by intragastric (i.g.) inoculation, a process that is extremely investigator-dependent, and may even induce rapid blood borne spread by esophageal tearing (57). Furthermore, i.g. inoculation is thought to decrease transit time through the stomach and small intestine, resulting in a large percentage of the inoculum being shed in the feces. Lecuit et al. observed that a single amino acid in E-cadherin was responsible for the species specificity of InlA (30). Shortly thereafter, this group created a mouse expressing human E-cadherin in enterocytes and observed that this single change allowed significantly more bacteria to translocate across the intestinal epithelium, creating immune responses and pathologies not seen with the Δ*inlA* mutant (29). More recently, *inlA* was murinized by point mutation, creating "*inlA^m*" (58). This allowed interaction with mouse E-cadherin and therefore the use of lower and presumably more physiologic doses. However, murinization was also found to increase the receptor repertoire of InlA^m by allowing binding of N-cadherin and furthermore to create inflammation not previously noted (59, 60). It is unclear though what effect this altered tropism has, as murinized and non-murinized strains of *Lm* were recently found to spread beyond the intestine in a similar manner (61).

In order to study natural dissemination, Bou Ghanem et al. developed a foodborne method of *Lm* transmission that more accurately recapitulates the events of infection than other transmission methods (35). After i.v. infection, approximately 90% of the original inoculum is found in the liver only minutes after infection (62-64). The burden quickly begins to grow,

peaking at approximately day 3 before clearance mechanisms overcome the rapid bacterial growth. Cheers et al. showed in 1979 that an i.v. dose of 1.2 x 10^3 *Lm* yielded an infection that peaked at day 2-3 in the spleens and livers of BALB and B6 mice. Clearance was observed in the spleen by day 6 in both mice, but BALB livers were still significantly infected at day 6 when the burden in B6 livers had dropped below the limit of detection (46). D'Orazio et al. showed later that an i.v. infection of BALB mice with 2 x 10^3 CFU yielded a similar peak day, although burdens were approximately 10-fold higher (65). However, this study showed that burdens were not cleared from either organ until approximately day 14. This is a striking difference from the earlier study, one that might potentially be explained by the *Lm* strain used; however, it is unknown what strain was actually used in the 1979 study.

Using foodborne transmission and a dose of ~5 x 10^8- 1 x 10^9 CFU, a very low number of bacteria are sometimes found in the liver at 6 hpi, with burdens below the limit of detection at 24 hpi, indicating that early innate clearance mechanisms are sufficient to remove low numbers of bacteria (D'Orazio, SEF, unpublished data). This is likely due to direct transit from the intestinal tissues to the liver via the portal vein. The burden does not grow to appreciable numbers until at least 48 hpi with a peak typically at 5 dpi ((35), Pitts unpublished observations). This difference is because *Lm* must cross many barriers to dissemination and either establish a fulminant infection in the intestinal tissues followed by spread to the liver or be carried to the liver via portal vein circulation (depicted in Fig. 1.1 and discussed further in "Spread beyond the intestine"). Clearance after the peak burden is achieved is relatively rapid in the B6 mouse, happening at approximately eight dpi in most tissues. In the BALB, the comparatively higher burdens are cleared more slowly, with most organs still bearing high burdens at eight dpi, especially if the infection is done during the mouse's dark cycle (35). In order to observe similar bacterial burdens in the spleen when comparing i.v. and foodborne infection, it is necessary to modulate the dose and timing as was done in Chapter 3. Here, B6 were either infected i.v. with

10^4 CFU and spleens were harvested at 1 dpi or infected by foodborne transmission with 10^9 CFU and spleens were harvested at 3 dpi. Although not identical, this produced similar CFU burdens in the spleen at harvest because of the different kinetics of each infection.

Although foodborne transmission of *Lm* is much more relevant to study of the natural course of infection than other methods, it is not without hurdles, particularly with regard to natural variation from mouse-to-mouse. CFU burdens within a group of mice may vary by 10-fold or more, for example. Simple techniques to overcome some of these hurdles, such as fasting mice overnight prior to infection and housing mice for the duration of the infection on raised wire floors to prevent coprophagy, can overcome these issues however.

1.5   Innate immunity to *Lm*

Uptake

Lm may be phagocytosed by professional phagocytes such as neutrophils (PMN) and macrophages or taken up by activating internalin- dependent mechanisms in non-phagocytic cells (32, 66). Complement opsonization, the decoration of the surface of a pathogen with phagocytosis-enhancing proteins, is not necessary for phagocytosis of *Lm* but was shown to greatly improve phagocytosis efficiency of human cells (67). Some discrepancies between work done with mouse and human cells exist, however. Baker et al. showed that cell wall components of *Lm* activate the complement system via the alternative pathway in mouse serum (68). Activation of the complement by the alternative pathway in human serum has also been described (69), but another group found no role for the heat labile component of serum in opsonization (70). A role for complement and IgM, but not IgG, in opsonization of *Lm* was also described by Bortolussi et al. (67). Regardless of any potential differences between mouse and man, however,

11

complement appears to play a major role in opsonization of *Lm* where *Lm*-specific antibodies are not present.

Spread beyond the intestine

Orally acquired *Lm* must first pass through the acidic environment of the stomach, thought to kill the majority of bacteria, and then gain access to the intestinal lamina propria (35, 71) before being transported to the liver via the portal vein or the lymphatics (depicted in Fig. 1.1). Melton-Witt et al. used signature-tagged infection of guinea pigs to estimate that only 1 in 10^6 ingested bacteria reach the lamina propria (72), therefore, portal vein transport of large numbers of intact bacteria simultaneously from the intestine to the liver is likely to be a rare event. *Lm* not transported through portal circulation must disseminate to the mesenteric lymph nodes, avoid killing by phagocytes, and then move into general circulation through the lymphatic fluid before accessing the liver and spleen.

It is unclear how *Lm* spread from the intestine to the mesenteric lymph nodes. *Lm* is considered a primarily intracellular pathogen, yet studies have found significant percentages of extracellular bacteria after both i.v. and foodborne infection. Glomski et al. showed that many bacteria in both the spleen and the liver after i.v. infection were sensitive to both gentamicin and the presence of neutrophils, indicating that the bacteria were extracellular (73). The bacteria may also replicate extracellularly in the gall bladder, allowing them to re-seed the intestine as bile is released with each meal (71). Jones et al. observed that the majority of the intestinal burden after foodborne infection was extracellular and that likewise, most of the bacteria in the lymph nodes were not inside a cell (74). *Lm* was also found to primarily associate with monocytes in the intestine and mesenteric lymph nodes, but the cells were not efficiently infected, casting doubt that intracellular transport in monocytes was a primary route of dissemination (75).

I.v., i.p. (intraperitoneal), and i.g. methods all fail to replicate the natural course of infection and therefore, little is actually known about the immune response to ingested *Lm*. I.v. infection rapidly seeds the liver with up to 90% of the inocula, with the remainder largely entering the spleen (62-64). Studies using i.v. infection have found that bloodborne *Lm* are initially trapped by resident macrophages in the liver and spleen (63, 64, 76). Kupffer cells (KC), the resident macrophages of the liver, trap up to 90% of bloodborne bacteria, with the remainder trapped by marginal zone macrophages of the spleen (64). KC were shown to inactivate the majority of the bacteria ingested, while marginal zone macrophages do not do so until they encounter IFNγ (64). Regardless, as a result of encountering sequential bottlenecks, ingested *Lm* are likely to arrive at the liver and spleen asynchronously and in much smaller numbers than after i.v. infection and activate innate immunity more slowly. If i.g. inoculation is employed, or if very high doses are used, rapid seeding of the liver may be observed. This has been speculated to be a result of direct bloodstream invasion after esophageal tearing, in the case of i.g. inoculation, or due to large numbers of bacteria gaining access to portal circulation if overwhelming doses are used (77).

Innate immunity in the spleen

The spleen is not required for the initial stages of the immune response to *Lm*; however, splenectomized mice fail to develop adaptive immunity to i.v. *Lm* and are thus susceptible to reinfection (76). Splenic marginal zone macrophages, which recognize bacteria through several receptors, move into the white pulp after ingesting *Lm*, where they begin to establish foci of infection characterized by recruitment of PMN and monocytes (76, 78). *Lm*-specific CD4 and CD8 T cells can be found in the white pulp after 24 h of infection, indicating rapid antigen processing once the phagocytes move into the white pulp (76). When mice were given a very high dose i.v. infection in order to more effectively visualize bacteria, PMN began to accumulate

in the marginal zone and red pulp of the spleen within 6 h of infection and continued to infiltrate until 2 dpi, extending into the white pulp as the CFU burden grew (76).

Large numbers of splenic lymphocytes undergo apoptosis as *Lm* enters the white pulp, a process attributed to induction of type I interferon (discussed in section 1.7 and chapter 3) (79). Carrerro et al. showed that SCID mice, which lack lymphocytes, were paradoxically more resistant to i.v. *Lm*, suggesting that the lymphocyte apoptosis induced in the spleen was negatively regulating immunity. This study also found that IL-10 induced after apoptosis was a key regulator of anti-*Lm* immunity (79).

As with most intracellular pathogens, interferon gamma (IFNγ) is critical for innate immunity to *Lm* and is secreted by CD8+ T cells and NK T cells following infection in an IL-12 and IL-18-dependent manner. In wild-type *Lm*, the pore-forming toxin LLO allows the bacteria to escape the phagosome and move to the cytosol, thus inducing rapid secretion of IL-12 and IL-18 (80). CD8+ T cells are recruited to the red pulp after i.v. infection, localizing around large numbers of *Lm* and nascently-infected monocytes and macrophages (81). In agreement with previous work using i.v. *Lm,* several studies have indicated that the interferon gamma receptor (IFNGR1), expressed on most myeloid cells and lymphocytes, is critical for immunity to *Lm* (82, 83) primarily because of its role in activating macrophages.

Tolerance and innate immunity in the liver

The liver is unique in that it receives both portal vein blood, carrying antigens derived from the intestinal contents and microbiota, as well as oxygenated arterial blood. Its structure is highly conducive to filtration and allows extremely large amounts of blood flow; however, inflammation in the organ is tightly regulated so as to prevent inappropriate reactions to nonpathogenic food-derived antigens (84). Blood flow slows in the liver due to the narrow,

honeycomb-like sinusoids, allowing extensive contact between antigens, as well as circulating T cells, with the phagocytes and antigen-presenting cells of the liver (84, 85).

Although not tightly bound like other endothelial layers, liver sinusoidal endothelial cells (LSEC) physically separate the sinusoidal blood from the hepatocyte plates, forming a fenestrated layer, under which is known as the space of Disse. LSEC, which make up nearly 50% of the non-parenchymal cells of the liver, play a central role in hepatic tolerance. These cells express several Toll-like receptors, scavenger receptors, MHC I and II, costimulatory molecules CD80 and 86, and lymphocyte adhesion molecules (86). Internalized antigen cross-presented on MHC I induces antigen-specific T cell tolerance, of high importance because the liver contains a larger concentration of T cells than even lymphoid organs. Antigens can also be transcytosed and released into the space of Disse, exposing hepatocytes to antigen too large to pass through the fenestrated endothelium. Furthermore, T cell recognition of antigen presented on MHC I results in a reciprocal signal that induces upregulation of PD-L1 on LSEC. Thus, CD8 T cells rapidly proliferate but do not secrete IFNγ and are tolerized.

Kupffer cells (KC), the liver's resident macrophages, exist in the sinusoidal lumen and comprise approximately 35% of the steady-state non-parenchymal cells of the liver (86). These cells secrete IL-10 and prostaglandins, suppressing antigen-specific T cell activation, but are required for clearance of even low doses of *Lm* (85, 86). KC are not a homogenous population of cells, and opinions differ on both their lifespan and whether they are bone marrow-monocyte derived or are repopulated by hepatic stem cells. KC express high levels of complement receptor CR-1 and capture C3b-coated bacteria under flow conditions, but they do not always internalize captured bacteria. Gregory et al. showed that while critical for immunity to *Lm,* KC did not internalize this bacterium. Instead, *Lm* remained bound extracellularly and PMN were recruited to the site, killing the bacteria (63).

1.6 PMN and their role in hepatic listeriosis

The fenestrated endothelium of the liver sinusoids and expression of hyaluronan on sinusoidal endothelial cells allows PMN to enter the liver via CD44-hyaluronan interaction, which can further be augmented during bacterial inflammation by production of serum-derived hyaluronan associated protein (87). Gregory et al. found a 7-fold increase in liver PMN between 10 min and 6 hours after i.v. injection of *Lm*, which corresponded with a 10-fold reduction in CFU over the same time-period (63). This demonstrated that upon acute insult, PMN could be recruited rapidly to the liver, overcoming the tolerogenic environmental cues. Senescent PMN taken up by KC have also been paradoxically suggested to suppress release of cytokines and chemokines by KC (88).

Direct killing by PMN plays a primary role in hepatic clearance of *Lm*. PMN in the liver could either kill bacteria released from apoptotic hepatocytes or may directly lyse infected hepatocytes, releasing the bacteria from a protective niche and allowing killing (62, 89, 90). Neutrophil extracellular traps (NETs) in the liver have also been demonstrated to enhance bacterial capture by KC (86). Carr et al. also demonstrated that PMN were a major contributor to TNFα production in the liver (91). TNFα was previously shown to directly lyse infected hepatocytes (92), and another study correlated hepatocyte lysis with PMN being in close proximity (93). While the growth of *Lm* itself is also thought to lyse infected hepatocytes (90), these results are suggestive that TNFα-mediated lysis of infected hepatocytes is a critical role of PMN.

Depletion studies

Early work to determine the role of PMN in murine listeriosis relied on antibody-mediated depletion using a clone (RB6-8C5) that was subsequently shown to bind both PMN and

monocytes (94-98). More recent depletion strategies designed to avoid this issue yielded conflicting results about the importance of PMN for clearance from the liver (91, 99). Carr et al. demonstrated that specific depletion of hepatic PMN beginning one day prior to infection yielded more pronounced susceptibility in the liver than the spleen (91). This supported previous studies which showed an increase in CFU in the liver, but not the spleen, at one day after i.v. infection of RB6-8C5-depleted mice (94). Shi et al. found that PMN localized around foci of infection in the liver, but that their specific depletion, beginning immediately post-infection, did not negatively impact survival (99). The major difference in these studies appears to be the timing of PMN depletion; removal of PMN after the infection by Shi et al. could plausibly have allowed PMN to begin killing *Lm* before the effects of the antibody became apparent.

PMN recruitment to the infected liver

Ly6G$^+$ PMN make up less than 1% of the total steady state non-parenchymal cell population of the liver (63, 88); however, PMN rapidly increase following infection and PMN-rich hepatic abscesses have been observed in both BALB/c and B6 mice after i.v. infection (53, 99). PMN develop in the bone marrow and are retained by interaction of CXCR4 with CXCL12 (SDF-1α) and the integrin VLA-4 with endothelial cell VCAM-1, remaining in the marrow for up to two days after full maturation (87, 100, 101). During inflammation, a variety of chemotactic factors including leukotriene B4 (LTB4), C5a, IL-8 (CXCL-8 in mice), CXCL1, and CXCL2, may stimulate PMN egress to the blood (100, 102). Hepatic PMN recruitment after i.v. *Lm* infection is sustained by the IL-23/IL-17 axis (103). After infection, IL-17A is produced by the γδ T cell population of the liver (104) and influences several cytokines and chemokines that impact PMN recruitment, including IL-6, G-CSF, and GM-CSF (103, 104). IL-23 is an IL-12 family member previously demonstrated to maintain IL-17-producing cells and play a PMN-dependent protective role in several other infection models (103, 105). Meeks et al. found that

IL-23 was required for protection against i.v. *Lm*, but that its effects were only apparent after several days of infection, indicating that redundant factors played a role in early PMN recruitment to the liver (103).

Leukotriene B4 (LTB4), a lipid derived from arachidonic acid, is a powerful chemotactic signal for PMN (106, 107). Upon initial PMN encounter with apoptotic cells or bacteria, it is secreted by the PMN themselves. It then serves as a signal relay molecule, creating a PMN swarm that is sustained until factors produced within the swarm initiate its dispersal (108, 109). Formylated peptide receptors (FPR) also play a local role in PMN recruitment within the infected tissue. Mice lacking FPR were significantly more susceptible to i.v. *Lm* infection than wild type controls when CFU were assessed at 2 dpi (110-112). PMN were still found in the livers of these mice, however, again suggesting that redundancy amongst chemotactic factors was important for PMN migration into the liver, but that other factors could play very specific, non-overlapping roles in recruitment to foci of *Lm* infection.

Use of human vs. murine PMN

Significant differences in mouse and human physiology have historically presented some barriers to the experimental use of mouse PMN. Although many of these differences can easily be overcome, perception has led to human peripheral blood PMN being used even in studies where the question primarily relates to a mouse phenotype, such as susceptibility to bacterial disease. As the largest population of cells in human blood, PMN are easily obtained from a peripheral blood sample. In contrast, they only account for about 15% of circulating immune cells in the mouse (102, 113). Mouse bone marrow, however, is an abundant source of morphologically mature PMN that release both primary and secondary granules and are suitable for functional assays including adoptive transfer (114, 115). Murine PMN do possess some functional differences compared to human PMN; they lack defensins and respond poorly to the formylated

18

peptide fMLF, although they do possess a strong affinity for penta- and tetra-formylated peptides from *Lm and Staphylococcus aureus* (110, 112, 116). Murine PMN have also been shown to migrate more slowly than human blood PMN in chemotaxis assays (117, 118).

1.7   Type I Interferons

Receptor and signaling

Type I IFNs (IFNα/β) are multifunctional cytokines with both pro- and anti-inflammatory roles in immunity. The role of these substances in the progression or control of listeriosis is thus complex and most studies have failed to appreciate that the way in which infection is performed may complicate the final result. They were first characterized over sixty years ago as substances that could "interfere" in viral infections (119). Over a dozen IFNα subtypes as well as a single IFNβ subtype have been identified, and all of these bind the common type I IFN receptor (IFNAR), a heterodimer composed of IFNAR1 and IFNAR2 (120, 121) (Fig. 1.2). The predominant signaling pathway activated by ligation of IFNAR involves activation of tyrosine kinases JAK1 and TYK2, which in turn phosphorylate STAT1 and STAT2. Once phosphorylated, STAT1 and STAT2 bind interferon response factor (IRF) 9 and translocate to the nucleus, where they bind interferon stimulated response elements in DNA to stimulate transcription. Several other STATs, mitogen activated protein kinases (MAPK) and p38, and PI3K are also activated by ligation of IFNAR (120, 121). IFNAR1 is expressed on all nucleated cells and binds IFNβ with a higher affinity than any of the IFNα subtypes, and strong similarities in expression have been shown between human and mouse cells (122).

Expression and secretion

Secretion of type I IFN is induced by ligation of Toll-like receptors (TLR) and cytosolic sensors such as DDX41 and stimulator of interferon genes (STING) (123, 124). Cytosolic DDX41 senses production of the bacterial second-messengers cyclic di-AMP and GMP, acting as a pattern-recognition receptor. STING is embedded in the endoplasmic reticulum and can act as an adaptor protein for DDX41 but also can directly sense cytosolic dinucleotides as well as DNA and RNA. In *Lm,* cyclic-di-GMP is secreted through multi-drug resistance pumps (125); strains that overexpress MDR-T have been characterized as hyper-inducers of IFNβ (126). Mice in which STING has been knocked out produced significantly less type I IFN in response to *Lm* infection than wild type mice; however, this did not affect susceptibility measured by CFU in the spleen (127).

During viral infection, type I IFNs are secreted by plasmacytoid dendritic cells (pDC) after stimulation of endosomal TLR7 and TLR9 together with the MyD88 adaptor (128). Stockinger et al. sorted spleen cells to determine that macrophages produce type I IFN 24h after intraperitoneal (i.p.) *Lm* infection (129). Another study determined that a subtype of TNF and iNOS-producing dendritic cells (Tip-DC) made IFNβ in the spleen after i.v. and i.p. *Lm* infection (130).

Influence on immunity to viral challenge

Mice lacking the common type I IFN receptor (IFNAR1$^{-/-}$) were found to be highly susceptible to even low-titer challenge with vesicular stomatitis virus, Semliki Forest virus, and vaccinia virus, thus demonstrating that IFNα/β signaling was essential for immunity to acute viral infection (131). Type I IFN can prevent or restrict viral replication through a variety of means, such as induction of cyclin-dependent kinase inhibitors, upregulation of apoptosis promoters

TRAIL and FAS/FASL, and increasing expression of Mx-1, a GTPase which blocks viral transcription through interactions with viral proteins (132, 133). These cytokines also have diverse pro-inflammatory effects on the host, such as stimulation of dendritic cell maturation; upregulation of MHC-I, MHC-II and costimulatory molecules CD80 and CD86; and increasing secretion of antibodies from B cells (134, 135). It is somewhat unexpected, therefore, that a robust type I IFN response may also promote more severe disease during influenza virus infection (136, 137).

Influence on susceptibility to bacterial challenge

The role of type I IFN in the response to bacterial challenge is likely to be considerably more complex than what has been observed in viral infections. Type I IFN signaling improved disease resistance in mice infected with extracellular encapsulated bacteria Group B streptococci, *Streptococcus pneumoniae,* and *E. coli* (138). In fact, mice deficient for IFNα/β or IFNAR1 were hyper-susceptible to these bacteria, thought to be due to a failure of macrophages to produce TNFα and IFNγ (138). This same study also suggested that in the case of these bacteria, IFNα/β and IFNγ synergized for bacterial clearance.

In contrast, the presence of type I IFNs during infection with intracellular bacterial pathogens such as *Mycobacterium tuberculosis* (139, 140), *Francisella tularensis* (105), *Salmonella enterica* (141), and *Lm* (142-145) has been generally shown to be detrimental to the host. Like the initial viral studies, studies using IFNAR1$^{-/-}$ mice suggested that IFNα/β signaling modulates multiple facets of innate immunity to bacteria. Down-regulation of IFNGR1, which inhibits macrophage responsiveness to IFNγ, was found to be a major consequence of *Lm* infection (82, 83, 146). Type I IFN also was shown to cause mass apoptosis of splenic T cells by sensitizing the cells to *Listeria*-induced apoptotic signals (144). In models of both *Francisella tularensis* and i.v. *Lm* infection, IFNAR1$^{-/-}$ mice recruited more PMN to the spleen (105, 147). Another study using i.v. *Lm* infection found more robust recruitment to TNFα-producing CD11b$^+$

21

cells to the spleens of *Lm*-infected IFNAR1^{-/-} mice (142).   In all of these examples, a lack of type

I IFN signaling resulted in improved bacterial clearance in comparison to wild type mice.

1.8   Prostaglandin E2

Prostaglandin E2 (PGE2) is a lipid derived enzymatically from arachidonic acid present

in the cell membrane. It is a member of a family of signaling lipids called eicosanoids which

encompasses leukotriene B4 (LTB4), thromboxane A4, and prostacyclins. Although well-known

as a pro-inflammatory mediator, PGE2 and the pathways that cause its induction have also been

widely studied for their role in aberrant polarization of T cell responses and inhibition of

macrophage function (148-151). The role of PGE2 in the body seems to depend strongly on the

tissue, the stimulus causing its induction, and the timing of secretion. For example, PGE2 plays a

homeostatic role in maintenance of barrier integrity of the gastric mucosa (152), but is also made

in response to commensal bacteria and limited PMN activation in response to acute mucosal

infection with *Toxoplasma gondii* (153).   PGE2 plays a maintenance role in normal kidney

function and blood pressure (152), but it has also been shown to drive IL-10 secretion in the liver

after infection or inflammatory stimulus (154, 155).   Suppression of innate immunity by PGE2

may outweigh its induction of pro-inflammatory pathways in many situations.

Production

PGE2 secretion can be stimulated by mechanical trauma and inflammatory stimuli

including bacteria (156). It is derived from a series of enzymatic reactions (depicted in Fig. 1.3)

beginning with release of arachidonic acid from the cell membrane by one of three phospholipase

A2 enzymes, a calcium-dependent cytosolic PLA2 (cPLA2), a secreted pLA2 (sPLA2), and a

calcium-independent pLA2 (iPLA2). cPLA2 and sPLA2 are inducible and activated by microbial

components, including secretion of LLO, which causes an intracellular calcium flux (157). Once

22

arachidonic acid is liberated, it may be oxidized by the cyclooxygenase enzymes (COX-1 and COX-2) or by lipoxygenase. COX modification produces an intermediate product that is further enzymatically modified by prostaglandin E synthase (PGES) to produce PGE2. Three isoforms of PGES exist- microsomal PGES (mPGES) 1 and 2 and cytosolic PGES (cPGES). A study using peritoneal macrophages of BALB/c and B6 mice found that BALB/c macrophages express higher levels of mPGES and thus produce more PGE2 when stimulated with LPS (150). Since the discovery of the two isoforms in the 1990s, COX-1 has been considered the "housekeeping" COX and COX-2 the inducible isoform. Some studies have contradicted this convention, however, and shown that both isoforms are present at homeostasis and induced by inflammation (158). If free arachidonic acid is metabolized by 5-lipoxygenase, this ultimately results in leukotrienes including LTB4, a lipid with chemotactic properties for PMN (106, 107). Activation of the 15-lipoxygenase pathway results in secretion of lipoxin A4 (LXA4), a pro-resolution lipid produced during the plateau phase of PMN swarming (109, 159, 160). Using human PMN, Levy et al. showed that PGE2 exposure switched lipoxygenase activity from predominately 5-lipoxygenase, producing LTB4, to 15-lipoxygenase, making LXA$_4$, within 5 hours (160). This study provided strong evidence that PGE2 could induce downregulation of the PMN immune response.

Receptors and signaling

PGE2 can be produced by most nucleated cells, with the notable exception of B lymphocytes, and is secreted to the extracellular environment by multidrug resistance transporter 4 (156, 161, 162). It is rapidly removed from circulation, making serum measurements difficult, and may also be degraded by a dehydrogenase, forming inactive 15-keto PGE2, or albumin, forming 15-keto PGA2 and PGB2 (162-165). In general, PGE2 acts locally, with autocrine and paracrine functions noted in many cell types (156). PGE2 binds four G-protein coupled receptors

expressed on a variety of tissues and cells (EP1-EP4) (Fig. 1.4) (152, 166, 167). EP2 and EP4 are coupled to $G_{\alpha s}$ in the cytoplasm and stimulate an increase in cyclic adenosine monophosphate (cAMP) through activation of adenylate cyclase (168). EP4 can also stimulate a PI3K-dependent ERK1/2 pathway and both EP2 and EP4 have been shown to activate GS3K/β catenin signaling, demonstrating potential roles in the pathogenesis of certain cancers (162). Although EP4 has a higher affinity for PGE2 than EP2, stimulation of EP2 stably transfected in HEK cells resulted in accumulation of more cAMP, speculated to be a result of faster desensitization of EP4 due to receptor internalization (168, 169). Conversely, EP1 and EP3 stimulation results in a decrease in cAMP and an increase in intracellular calcium (170). Dendritic cells were shown to express all four EP receptor subtypes, while mouse peritoneal PMN were found to express EP2 and EP4, but not EP1 and EP3 (171). T and B cells also express PGE2 receptors, with both immune stimulatory and inhibitory effects reported depending on cellular context (152, 172).

Pro-inflammatory roles of PGE2

PGE2 is involved in the classic symptoms of inflammation- warmth, redness, and fever, through its roles in vasodilation and lymphocyte recruitment and induction of IL-6 (173, 174). It is considered a strong pro-inflammatory mediator, and as such has quite a number of drugs directed at it. Non-steroidal anti-inflammatory drugs (NSAIDS) such as ibuprofen broadly target all prostaglandin production through suppression of both COX-1 and COX-2, thus leading to some of their negative side effects such as gastrointestinal bleeding (152). COX-2 specific drugs such as celecoxib, on the other hand, target the inflammatory induction of only COX-2 and have fewer side effects (152). For the purposes of this document, however, the focus will be on the anti-inflammatory effects of PGE2.

Anti-inflammatory or immunosuppressive roles of PGE2

Numerous studies have examined the effect of PGE2 on both T cell responses and phagocyte functions and concluded that it is an immunosuppressive compound with a role in Th1/Th2 polarization. PGE2 was shown to suppress IFNγ and IL-2 from Th1 clones, induce *FOXP3* expression, and prevent anti-CD3-induced proliferation (148, 175). Recently, outer membrane vesicles released by *Helicobacter pylori* were shown to induce COX-2 expression and robust PGE2 secretion in human peripheral blood monocytes. In turn, this strongly inhibited T cell proliferation without stimulating apoptosis (176). Hutchison and Myers identified PGE2 in splenocyte culture supernatants as a factor that suppressed peritoneal macrophage phagocytosis of *Lm* (177). Using splenocytes stimulated with *S. aureus* Cowan 1, Kuroda et al. found that PGE2 strongly suppressed Th1 activation and IFNγ secretion, but that PGE2 secretion in response to *in vitro* stimulation was not significantly different amongst different mouse strains. From these results, they concluded that BALB/c cells were in fact more sensitive to the effects of PGE2 and that this sensitivity played a pivotal role in Th2 polarization in BALB/c mice (149). Later, the same group found that LPS or *S. aureus*-stimulated BALB/c macrophages produced more PGE2 than B6 macrophages, and that this PGE2 suppressed Th1 activation in an EP-4 dependent and self-regulatory manner (150). Thus, PGE2 modulates aberrant Th2 activation in BALB/c myeloid cells *in vitro* through both differential production and increased sensitivity compared to B6 cells.

EP2 and EP4-mediated accumulation of intracellular cAMP is thought to result in some of the immunosuppressive effects of PGE2 (151, 152, 171, 178-180). In *Histoplasma capsulatum*-infected macrophages, ligation of EP2 and EP4 resulted in lower levels of phagocytosis, decreased phosphorylation of NFκB, and lower secretion of TNFα (178). In alveolar macrophages, EP2 and EP4 ligation inhibited phagocytosis of *Klebsiella pneumoniae* in a cAMP-dependent manner and inhibited killing through effects on NADPH oxidase (151, 179).

25

In activated dendritic cells, PGE2 or EP4 agonism resulted in lower secretion of pro-inflammatory chemokines, but also upregulated receptors necessary for migration to lymph nodes (152). Also somewhat contradictory, PGE2 treatment of mouse peritoneal PMN resulted in accumulation of cAMP and lower TNFα secretion than control cells but enhanced IL-6 production when the cells were also treated with LPS (171). This result was suggested to be caused by differential signaling of EP2 and EP4.

Monocytes and PMN are rapidly recruited to sites of infection, including the intestinal lamina propria, mesenteric lymph nodes, the spleen, and the liver (75, 147). Although many cells secrete PGE2, Grainger et al. recently showed that monocytes recruited to the murine intestinal lamina propria produced PGE2, thus modulating PMN function in response to *T. gondii* (153). Application of PGE2 to human PMN was shown to inhibit superoxide production in a cAMP- and EP2-dependent manner and inhibited chemotaxis to fMLP independent of cAMP accumulation (180). It is largely unknown, however, how PGE2-dependent decrease in one or more killing mechanisms might impact the overall ability of PMN to kill pathogenic bacteria.

1.9 Overall hypothesis

The release of cytokines, chemokines, and signaling lipids during natural infection with foodborne pathogens is an understudied area of microbiology and immunology. The use of intravenous and intragastric infection, while efficient and reproducible for the most part, has hampered the synthesis of knowledge of how a relatively mild infection originating from the gastrointestinal tract produces life-threatening disseminated infection in vulnerable populations.

In this study, foodborne transmission and *in vitro* infection were used to assess how two mediators not classically thought of as part of bacterial infection, IFNα/β and PGE2, impact early immunity to *Lm*. I hypothesized that IFNα/β, while clearly capable of modulating immune

responses, was induced as a result of the infection method and was specifically a consequence of a very large number of bacteria initiating colonization of the spleen simultaneously. Additionally, I hypothesized that foodborne infection triggered a condition in the livers of susceptible BALB/c mice, namely overproduction of PGE2, which led to modulation of PMN clearance of *Lm*. As predicted, results showed that foodborne infection elicited little production of IFNα/β. Additionally, mice lacking the common type I IFN receptor were not more resistant to foodborne *Lm* infection, a sharp contrast to the phenotype observed with these mice using i.v. infection. These data suggested that most of the detrimental effects attributed to type I IFN during listeriosis may actually be an artifact of the i.v. infection model.

Furthermore, results demonstrated that murine PMN efficiently kill serum-opsonized *Lm* using both oxidative and non-oxidative mechanisms. This led to the conclusion that there were no intrinsic differences in the capacity of PMN from susceptible BALB/c and resistant B6 mice to kill *Lm* and suggested that if PMN in the BALB/c liver were deficient, they were responding to the hepatic microenvironment. Accordingly, more PGE2 was found in cells removed from infected BALB/c livers. When exogenous PGE2 was applied to bone marrow PMN, it significantly decreased their killing efficiency, thus suggesting that overproduction of PGE2 under infection conditions could modulate the PMN response to *Lm*.
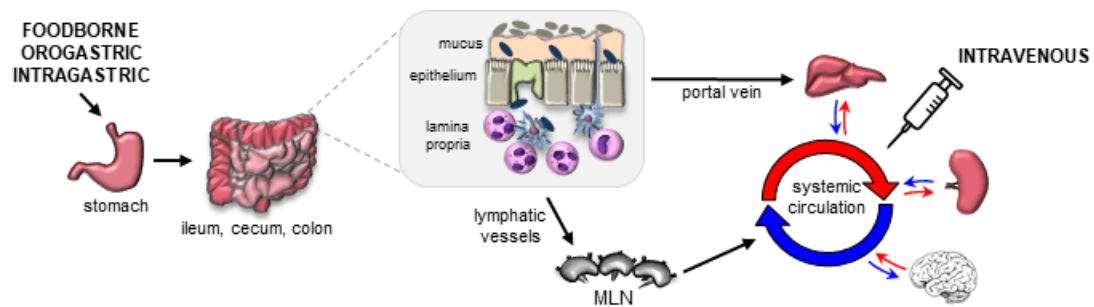
Figure 1.1 Orally-acquired Lm must pass through sequential anatomical barriers and bottlenecks to cause infection.

Up to 90% of an ingested *Lm* inoculum is either killed in the stomach or shed in feces within a few hours (35, 71). *Lm* that survive must compete with the gut microbiota to gain access to the epithelium (181, 182); it has been estimated that invasion of the mucosal barrier is a rare event, with only 1 in 10^6 bacteria reaching the underlying lamina propria (72). If i.g. inoculation is used, or if an overwhelmingly large dose ($\geq 10^9$ CFU) is used with any oral infection method, rapid dissemination to the liver, presumably via the portal vein, is observed. *Lm* not transported through portal circulation must disseminate to the mesenteric lymph nodes (MLN), avoid killing by activated phagocytes, and then gain access to the blood circulation. Given the number of barriers faced, it is likely that small numbers of *Lm* reach the spleen and liver asynchronously. In contrast, *Lm* that are i.v. injected seed the spleen and liver as a large bolus within 10-15 minutes after administration (63, 64, 183).

This figure was published as part of reference (184) (Pitts, et al. 2018). DOI: 10.3390/pathogens7010013

28
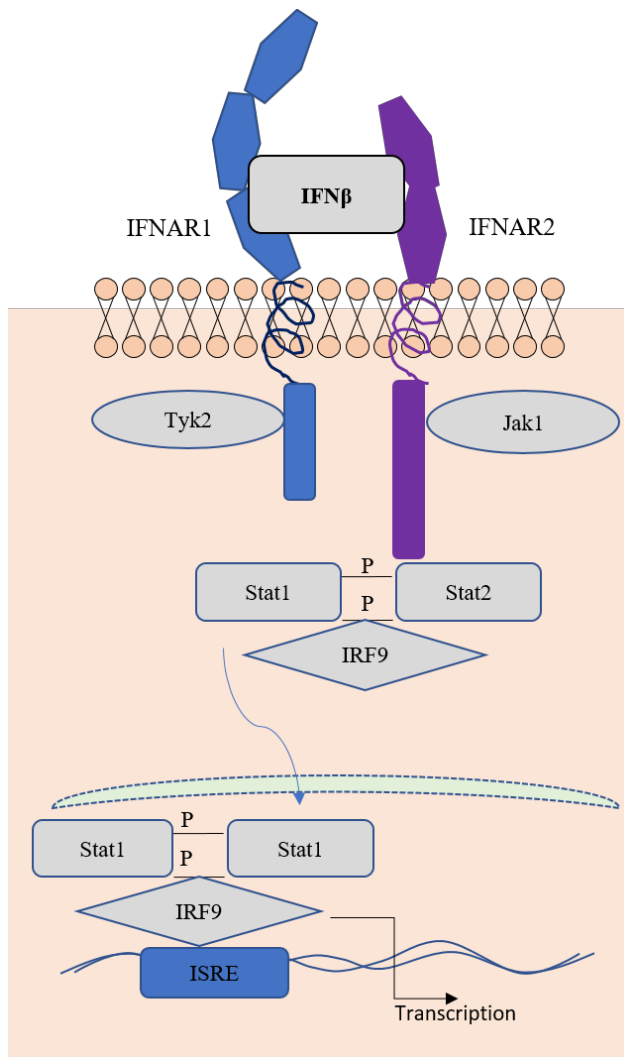
Figure 1.2 Model of type I interferon signaling

For type I IFN signaling to occur, IFNα or IFNβ must bind IFNAR1, which then recruits IFNAR2 to form a heterodimer. These two extracellular-facing proteins are coupled to Tyk2 and Jak1 in the cytoplasm, which phosphorylate Stat1 and Stat2, causing them to dimerize, bind interferon response factor (IRF9), and then translocate into the nucleus. Once in the nucleus, an interferon response element (ISRE) is bound on DNA, causing transcription.
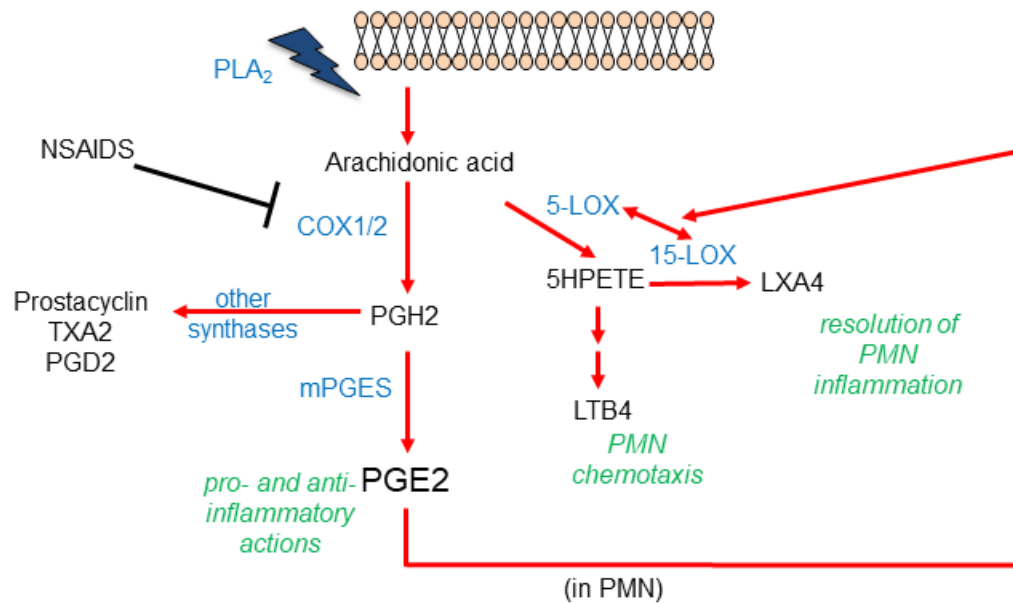
Figure 1.3 Scheme of eicosanoid production

Arachidonic acid is released from membrane phospoholipids by activated by phospholipase A2 (PLA$_2$). If acted upon by cyclooxygenase enzymes (COX1/2), an intermediate prostaglandin is produced that may then be further modified by tissue or cell-specific synthases such as microsomal PGE synthase (mPGES). If arachidonic acid is acted upon by the lipoxygenase enzymes (5-LOX and 15-LOX), leukotriene B4 (LTB4) and lipoxin A4 (LXA4) are produced. PGE2 exposure in PMN may also trigger a switch from 5-LOX to 15-LOX, inducing secretion of pro-resolving LXA4 (160). Non-steroidal anti-inflammatory drugs (NSAIDS) act on the COX1 and COX2 enzymes. The intermediate PGH2 may also be acted on by other specific synthases to produce other eicosanoid family members, including prostacyclin, thromboxane (TXA2), and prostaglandin D2 (PGD2)
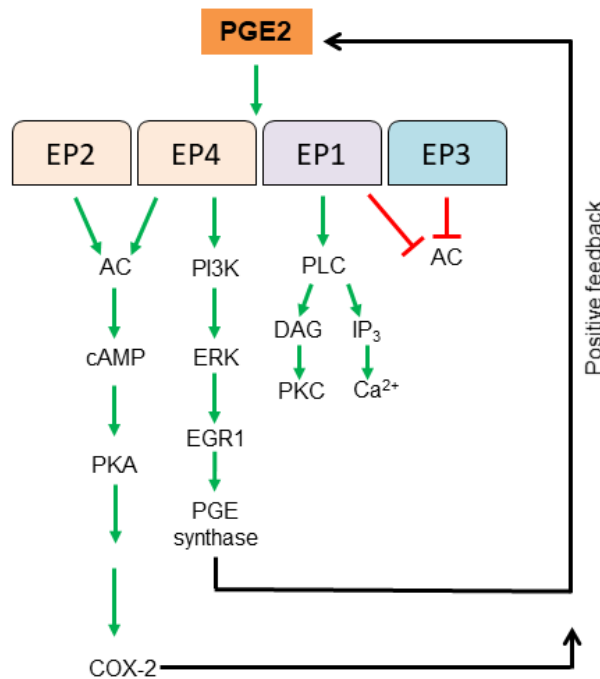
Figure 1.4 PGE2 receptors

PGE2 binds four 7-transmembrane spanning G-protein coupled receptors (EP1-EP4). EP2 and EP4 stimulate adenylate cyclase (AC), causing an accumulation of intracellular cyclic adenosine monophosphate (cAMP) and activation of protein kinase A (PKA). One of the downstream consequences of this pathway is transcription of COX-2, stimulating a positive feedback loop (168). Ligation of EP4 can also stimulated PI3 kinase (PI3K), causing downstream transcription of PGE synthase, also feeding into the positive feedback loop. Ligation of EP1 causes intracellular calcium flux and activation of protein kinase C (PKC) and can also directly block activation of AC, and EP3 ligation also directly blocks AC activation. ERK, extracellular signaling related kinase; EGR1, early growth response factor 1, PLC, phospholipase C; DAG, diacylglycerol; IP$_3$, inositoltriphosphate

2. Materials and Methods

Bacteria

Mouse-adapted (inlA^m-expressing) *L. monocytogenes* (*Lm*) EGDe derivatives SD2000, SD2001 (kanamycin-resistant) and SD2710 (constitutive GFP) were used in these studies (61, 75). *Lm* EGDe and an isogenic *inlA* deletion (Δ*inlA*) mutant were provided by Cormac Gahan (University College Cork, Ireland). Expression of the modified inlA^m surface protein allows the bacteria to efficiently bind murine E-cadherin, promoting invasion of the intestinal epithelium (58). *Lm* SD2000 was created by integrating inlA^m into the chromosome of *Lm* ΔinlA as described by Jones et al. (75). Kanamycin (50 μg/mL) was added to plates for selection of *Lm;* IPTG (isopropyl-β-D-thiogalactopyranoside; final concentration, 1 mM) was added to induce the expression of antibiotic resistance genes carried on pIMC3 derivatives.

Media

RP-5^- medium was comprised of RPMI 1640 [Life Technologies # 21870], 5% FBS [Gemini], 2.5 mM L-glutamine, 10 mM HEPES, 0.1 mM β2-mercaptoethanol [Sigma-Aldrich]. RP-10^- medium was identical to RP-5 except with the addition of 10% FBS. For bone marrow, RP-10^- was supplemented with 2 mM EDTA and 25 μg/mL gentamicin [Gibco]. RP10^+ contained 100U/mL penicillin and 0.1 mg/mL streptomycin [Sigma]. Flow cytometry buffer contained Ca^{2+}/Mg^{2+}-free HBSS, 25mM HEPES, 5mM EDTA, 1% FBS. Cells were sorted into a 1:1 mixture of buffer and sterile FBS with the addition of 25 μg/mL gentamicin.

Mice

BALBcBy/J (BALB/c; stock # 001026), C57BL/6J (B6; stock # 000664), and B6.129S-*Cybb^{tm1Din}*/J (gp91^phox-/-; stock # 002365), and IFNγ^-/- (stock #002287) mice were purchased from The Jackson Laboratory (Bar Harbor, ME) and housed in a specific pathogen-free facility. The IFNγ^-/- mice were crossed with Thy1.1/luciferase-expressing C57BL/6 mice (185) (originally

obtained from Dr. Robert Negrin, Stanford University) to obtain homozygous Thy1.1$^{+/+}$IFN$\gamma^{-/-}$ progeny. IFNAR1$^{-/-}$ mice were obtained from Dr. Jayakrishna Ambati (University of Kentucky). Both male and female animals were used in all experiments. Bone marrow was harvested from animals 8-16 weeks old; no significant differences were noted in PMN recovery per gram of weight between male and female mice. Animals used for *in vivo* infection were 6-12 weeks old at time of infection. Mice were euthanized by cervical dislocation. Blood was collected from the aorta immediately after euthanasia and transferred to a serum separator tube (BD), followed by centrifugation for 2 min at 20,000 *x g*. Serum was stored at 4°C for use the same day or at -80°C for later use. To pre-treat bacteria with serum, autologous mouse serum was added to *Lm* (10% final concentration) and the mixture was incubated at 37°C for 30 min. Pre-treatment with serum alone in the absence of PMN had no effect on *Lm* growth (data not shown). Serum was heat-inactivated by incubating at 55°C for 30 min. All procedures were approved by the Institutional Animal Care and Use Committee at the University of Kentucky.

In vivo infection

For *in vivo* infection, intestinally passaged *Lm* were grown to early stationary phase in Brain Heart Infusion (BHI) broth (Difco) shaking at 37° C (for i.v. infection) or standing at 30° C (for foodborne infection) and then aliquots were prepared and frozen at -80° C until use as described previously (186). An aliquot was thawed on ice and cultured for 1.5 h in BHI broth shaking at 37° C (i.v.) or standing at 30° C (foodborne). For i.v. infection, *Lm* were washed once, suspended in sterile PBS, and diluted to the appropriate concentration. A total volume of 200 µL was aseptically injected into the lateral tail vein. Uninfected mice received a 200 µL injection of sterile PBS via the lateral tail vein. For foodborne infection, *Lm* were washed twice and suspended in 5 µL of a salted butter (Kroger) plus sterile PBS mixture (3:2 ratio) and then added to a 2-3 mm piece of white bread (Kroger). Mice were fasted for 16-24 hours prior to ingestion of the *Lm*-contaminated bread and housed on raised wire flooring as described previously (187,

188). Uninfected mice were fasted and fed an uncontaminated piece of bread. For experiments requiring only CFU determination, spleens and livers were harvested aseptically and homogenized (Fisher PowerGen 1000, 60% power) in sterile water for 30 seconds. For all CFU determination, dilutions were prepared in sterile water (chapter 3) or PBS (chapters 4 and 5) and plated on BHI agar with or without Kanamycin and IPTG. Colonies were counted after 24 h incubation at 37°C.

In vitro infection

For *in vitro* infection of PMN, a glycerol stock of each *Lm* type was struck out onto BHI agar (Difco). After overnight growth, a freshly streaked colony was inoculated into BHI broth and grown shaking at 37˚C overnight (16 h). *Lm* were washed once with Ca^{2+}/Mg^{2+}-free HBSS and then diluted in the same buffer to the appropriate concentration for infection. For *in vitro* infection followed by COX-2 analysis (Fig. 5.1), cells were exposed to *Lm* SD2000 (MOI =1). 25 µg/mL gentamicin was added after 2 hr and incubation was continued overnight.

Isolation of splenocytes

Spleens were injected with 100 U of type IV collagenase (Worthington) in a total volume of 1 mL of HBSS. Spleens were minced, additional collagenase was added for a final concentration of 200 U/mL, and the samples were incubated for 30 min at 37°C in 7% CO_2. The digested tissue was pushed through a sterile screen (# 80 mesh), filtered, and red blood cells were lysed using an ammonium chloride buffer. For some experiments in Chapter 3 requiring only a single cell suspension, spleens were mechanically dissociated by pushing through mesh screens without collagenase treatment using a 3-mL syringe plunger. For CFU determination, a portion of the splenocyte single cell suspension was removed and diluted in sterile water prior to plating on BHI agar.

Liver non-parenchymal cell preparation

At indicated time points post-infection, mice were euthanized and livers were perfused via the hepatic portal vein with 11 mL of collagenase type IV solution (250 U/mL in HBSS), removing blood. The perfused tissue was cut into small pieces, transferred to a 50-mL tube containing DNase (10 U/mL; Worthington) and collagenase type IV (100 U/ mL) in 10 mL of RP-5⁻ and incubated for 35 min shaking at 37°C. The digested tissue was gently pushed through a mesh screen (no. 80 mesh) to create a single cell suspension. At this point, one tenth of the volume was removed for determination of CFU burdens. Non-parenchymal cells were enriched by allowing 2 min settling time followed by centrifugation for 1 min at 50 x g at 4°C. Supernatant was centrifuged at 300 x g at 4°C for 10 min, the pellet was suspended in 30 mL of RPMI 1640, and the prior two steps were repeated. Finally, the pellet was suspended in 1.6 mL cold RPMI 1640 followed by addition of 2.4 mL cold 40% Histodenz (Sigma) in PBS. The suspension was layered under 2 mL of cold RPMI 1640 in 15 mL polypropylene tubes that had been pre-coated with FBS. Samples were centrifuged for 20 min at 4°C at 1500 x g with no brake. The interface was collected and passed through a filter to remove clumps.

Type I IFN ELISA

For detection of type I IFN, lymphocytes were depleted from splenocyte suspensions using APC-conjugated anti-B220 (RA3-6B2) and anti-TCRβ (H57-597) antibodies (eBioscience) and IMag anti-APC magnetic beads (BD Biosciences). This protocol resulted in greater than 90% depletion of both B cells and T cells for all samples. APC-enriched splenocytes were cultured for 24 h at 37° C in 7% CO_2 at a density of 1.0 x 10⁶ cells/200 μL in 96-well flat bottom plates in RP10⁻ containing 12.5 μg/mL gentamicin. Cultured cells were centrifuged at 300 x g for 8 minutes and the supernatants were harvested and stored at -80° C. Cytokine concentrations were determined using the Verikine Mouse IFNβ ELISA kit (PBL Assay Science, Piscataway, NJ) and the Mouse IFNα Platinum ELISA kit (eBioscience).

IL-10 ELISA

For IL-10 detection, spleens were harvested aseptically and placed into 2 mL of ice-cold PBS, homogenized for 30 seconds (Fisher PowerGen 1000, 60% power), split into aliquots, and stored at -80° C. An aliquot was thawed on ice and centrifuged at 14,000 x g for 10 min, and the supernatant was collected. ELISA was performed using anti-mouse IL-10 capture antibody (JES5-16E3), biotin-conjugated anti-mouse IL-10 detection antibody (JES5-2A5), and mouse IL-10 standard (eBioscience).

PGE2 EIA

Prostaglandin E2 was measured using the Prostaglandin E2 Metabolite (PGEM) EIA kit (Cayman Chemical No. 514531) according to manufacturer instructions. Liver non-parenchymal cells were gradient-enriched and cultured overnight at a density of 2.5 x 10^5 cells per well in a final volume of 0.5 mL in 24-well low adherence dishes (Corning). Cells and supernatant from like samples were pooled, and proteins were precipitated using four volumes of ice-cold acetone followed by incubation at -20˚C for at least 2 hr. Samples were dried under nitrogen and suspended in the kit buffer according to instructions. Lipids were extracted using ethyl acetate according to the protocol supplied in the PGEM assay kit and samples were suspended in the kit assay buffer.

Bone marrow derived monocytes

BALB/c mice were euthanized and femurs and tibias were removed and flushed with 10 mL RP-10^+. Red blood cells were lysed by exposure to an ammonium chloride buffer and remaining cells were washed and counted. Cells were plated at 1 x 10^6 cells/mL in 16 mL in ultra-low attachment plates (Corning No. 3262) and m-CSF was added to each plate at a final concentration of 20 ng/mL. Cells were harvested on day 4 or day 5, washed with RP-10$^-$, and plated in low-adherence 24 well plates (Corning No. 3473) at 2.5 x 10^5 cells/mL in 1 mL RP-10$^-$.

Flow cytometry

Cells were stained using fluorescently-conjugated antibodies specific for the following molecules: CD64 (X-54-517.1), Ly6C (HK1.4), and Ly6G (1A-8), purchased from Biolegend; F4/80 (BM8), CD11c (HL3), CD11b (M1/70), CD19 (D3), B220 (RA3-6B2), CD3 (17A2), and streptavidin, purchased from eBioscience. Biotin-conjugated IFNGR1/CD119 (2E2; Biolegend) was detected with PE Cy5-conjugated streptavidin (eBioscience). Intracellular COX-2 was detected after incubation with fixation and permeabilization buffer (BD) according to manufacturer instructions using FITC-conjugated anti-COX-2 antibody purchased from Cayman Chemical. Dendritic cells were defined as $CD11c^{hi}F4/80^{-/lo}$, macrophages as $CD11c^{-/lo}$ and $F4/80^{hi}$ or $CD64^{hi}$; B cells as $CD3^-B220^+CD19^+$ or $Ly6G^-Ly6C^-CD19^+$, T cells as $CD3^+CD19^-$ or $B220^-CD3^+TCR\beta^+$; PMN as $Ly6G^{hi}Ly6C^{int}CD11b^+$ or $Ly6G^{hi}Ly6C^{+/-}$, monocytes as $Ly6G^-Ly6C^{hi}$, and B cells as $Ly6G^-$ $Ly6C^-$ $CD19^+$. Fluorescence was measured using an LSR II flow cytometer (BD Biosciences) or an iCyt Synergy sorter and analysis was performed using FlowJo v.10 (Tree Star). The sort gating strategy incorporated live cell and singlet gates prior to gating on individual markers; sort purities for PMN ranged from 92-99%. Following collection, cells were washed twice with RP-10$^-$ prior to use.

Bone marrow harvest for PMN enrichment

Marrow was flushed from femurs and tibias with RP10$^-$ supplemented with EDTA and 25 µg/mL gentamicin. Cells (two bones per tube) were passed through a sterile mesh filter into a 15 mL polyethylene terephthalate (PET) tubes (Corning) and pelleted by centrifugation at 400 x g. Erythrocytes were lysed by exposure to 0.2% NaCl for 20 sec followed by addition of an equal volume 1.6% NaCl.

Density gradient enrichment of PMN

Following erythrocyte lysis, PMN were enriched as described previously (115). Briefly, 3 mL Histopaque 1077 was gently layered onto 3 mL Histopaque 1119 in a 15 mL PET tube. Cells were resuspended in cold PBS at 8-12 x 10^6 cells/mL and overlayered on the Histopaque suspension at 8-12 x 10^6 cells per tube. Tubes were centrifuged according to author's instructions and the bottom layer of cells was recovered and suspended in RP-10⁻ or flow cytometry buffer.

***In vitro* killing assay**

PMN (10^5/well) were plated in 96-well flat-bottom tissue culture-treated plates in 100 μL in RP-10 and incubated at 37°C in 7% CO2 for 1 hour to allow a period of recovery. *Lm* was added at the indicated MOI in a volume of 20-40μL to 3-6 wells per sample group. In each experiment, a group of wells contained bacteria only (no PMN) to assess growth/survival. The plate was centrifuged at 300 x g for 5 min and then incubated at 37˚C in 7% CO2. At each time point, the contents of each well was transferred to an individual microcentrifuge tube and wells were vigorously washed 3x with PBS and examined microscopically to ensure that all cells were removed. Serial dilutions of each well were prepared in PBS and plated on BHI agar. The percentage of *Lm* killed was calculated by dividing the number of CFU from wells with PMN by the mean number of CFU from wells without PMN.

Gentamicin protection assay

Gradient-enriched PMN were plated and exposed to serum-opsonized *Lm* as described above. Gentamicin was added at a final concentration of 10 μg/ml at 10 minutes post infection (mpi). At indicated time points, the cells were washed once with RP-10⁻, lysed by addition of sterile water, and plated on BHI agar.

Chemotaxis assay

An under-agarose assay was used as described previously by Heit and Kubes (118), with the exception of the following modifications. Ultra-pure agarose (1%; Invitrogen) was dissolved in Ca^{2+}/Mg^{2+}-free HBSS and diluted with phenol red-free RPMI 1640 containing a final concentration of 2.5% FBS. FBS-coated 60 mm petri dishes were filled with 4.5 ml of the agarose mixture. 3 mm holes were cored 1 or 2 mm apart (indicated in figure legend) using a sterilized template made from a silicone sheet and a hollow punch tool. Either 1 µM formylated synthetic peptide (fMIVTLF plus fMIGWII; Bio-Synthesis, Inc.) or 100 nM leukotriene B4 (Cayman Chemical No. 20110) diluted in Ca^{2+}/Mg^{2+}-free HBSS was applied to the center well and allowed to diffuse into the agarose for 20 min prior to application of gradient-enriched PMN (1 x 10^5/well) to the outer wells. Dishes were incubated at 37°C in 7% CO_2 for 3 h. Images were acquired in DIC mode with a Nikon A1R confocal microscope, using a 10x air objective with a numerical aperture of 0.45 and the transmitted light detector. Image size was 4096 by 4096 pixels with a resolution of 0.31 micrometer/pixel. Distance traveled was determined using the manual measurement tool in the NIS-Elements software program (Nikon).

Immunofluorescent microscopy

Sorted PMN were plated in RP-10⁻, rested for 1 hr, and then Cytochalasin D [Sigma] (20 µM in DMSO) was added and cells incubated at 37°C in 7% CO_2. *Lm* SD2710 was added to the wells and the plate was centrifuged for 5 min at 300 *x g* followed by incubation for 5 min at 37°C in 7% CO_2. Difco *Listeria* O Antiserum Poly [BD Biosciences] and goat anti-rabbit IgG–Texas Red (Thermo Fisher) were used to perform differential "in/out" staining as described previously (75). Cells were visualized using a Zeiss Axio Imager.Z1 with a 100x/1.4 NA PlanApo oil immersion objective and analyzed with AxioVision software. Slides were blinded and examined by two different investigators; average values are reported.

Reactive oxygen species

Gradient-enriched PMN were plated in RP-10⁻, rested for 1 hr, and then centrifuged at 300 $x\ g$ and suspended in Ca^{2+}/Mg^{2+}-free HBSS. Dihydrorhodamine 123 (DHR, Cayman Chemical No. 85100) suspended in DMSO and diluted in HBSS was added to wells (final conc. 2.5 μg/mL) 15 min prior to addition of either *Lm* or 20 nM PMA diluted in HBSS (Sigma No. P1585). Plates were centrifuged at 300 $x\ g$ for 5 min and then incubated at 37°C in 7% CO_2. To scavenge reactive oxygen intermediates, cells were incubated for 90 min with 50 mM 4-hydroxy Tempo dissolved in HBSS [Tempol, Sigma No. 176141]. *Lm* was added at the indicated MOI and further incubated for 30 min. DHR was added during the final 15 min of incubation. In both cases, DHR fluorescence was analyzed by flow cytometry in the FL-1 channel after fixation using 1% paraformaldehyde.

Serine protease inhibition

Cells were treated with diisopropylfluorphosphate (DFP; Sigma No. D0879) suspended in isopropanol and diluted in HBSS for 30 min at 37°C in 7% CO_2. DHR was added to the wells prior to addition of *Lm* for ROS detection. For flow cytometry analysis, cells were washed, stained with fluorescently-tagged anti-Ly6G antibody, and fixed in 10% formalin after incubation with bacteria.

***In vitro* PGE2 and PGE2 receptor antagonist treatment**

Cells were treated with prostaglandin E2 (Cayman Chemical No. 14010) suspended in ethanol and diluted in RP1-⁻ for the indicated time periods prior to addition of bacteria and further assessment of functionality. For antagonist experiments, cells were treated with EP-2 antagonist PF-04418948 (Cayman Chemical No. 15016) or EP4-antagonist L-161,982 (Cayman Chemical No. 10011565) suspended in DMSO and diluted in RP10⁻ at a final concentration of 100 nM concurrently with 1 uM PGE2.

In vivo PGE2 and indomethacin treatment

For PGE2 supplementation, female B6 mice were injected i.p. with 40 μG 16,16 dM PGE2 (Cayman Chemical No. 14750) suspended in DMSO and diluted in sterile HBSS once daily, beginning immediately after infection. Organs were harvested on day 4, homogenized, and plated on BHI agar. For indomethacin challenge experiments, female BALB/c mice were injected i.p. twice per day with 2 mg/kg indomethacin (Cayman Chemical No. 70270) suspended in DMSO and diluted in sterile HBSS.

Statistical analysis

Statistical analysis was performed using Prism for Macintosh Version 6.0f (GraphPad). Significance was determined using unpaired T-test unless otherwise noted. P-values < .05 were considered significant and are indicated by * <.05, ** <.01, *** <.001, ****<.0001

3. **Type I IFN Does Not Promote Susceptibility to Foodborne *Listeria monocytogenes***

Summary

Type I IFN (IFNα/β) is thought to enhance growth of the foodborne intracellular pathogen *Listeria monocytogenes* (*Lm*) by promoting mechanisms that dampen innate immunity to infection. However, the type I IFN response has been studied primarily using methods that bypass the stomach and, therefore, fail to replicate the natural course of *Lm* infection. In this study, we compared i.v. and foodborne transmission of *Lm* in mice lacking the common type I IFN receptor (IFNAR1^{-/-}). Contrary to what was observed using i.v. infection, IFNAR1^{-/-} and wild type mice had similar bacterial burdens in the liver and spleen following foodborne infection. Splenocytes from wild type mice infected intravenously produced significantly more IFNβ than those infected by the foodborne route. Consequently, the immunosuppressive effects of type I IFN signaling, which included T cell death, increased IL-10 secretion, and repression of PMN recruitment to the spleen, were all observed following i.v., but not foodborne transmission of *Lm*. Type I IFN was also previously shown to cause a loss of responsiveness to IFNγ through down-regulation of the receptor IFNGR1 on macrophages and dendritic cells. However, we detected a decrease in surface expression of IFNGR1 even in the absence of IFNα/β signaling, suggesting that in vivo, this infection-induced phenotype is not type I IFN-dependent. These

results highlight the importance of using the natural route of infection for studies of host-pathogen interactions and suggest that the detrimental effects of IFNα/β signaling on the innate immune response to *Lm* may be an artifact of the i.v. infection model.

Introduction

Type I IFNs (IFNα/β) are multifunctional cytokines with diverse roles in anti-viral, anti-bacterial, and anti-tumor immunity. Over a dozen IFNα subtypes as well as a single IFNβ subtype have been identified, and all of these bind the common type I IFN receptor (IFNAR), a heterodimer composed of IFNAR1 and IFNAR2 (120, 121). Ligation of IFNAR, which is expressed on a variety of immune cells, triggers Jak-Stat signaling and can affect the expression of a diverse array of downstream genes (120). Secretion of type I IFN is induced by ligation of Toll-like receptors and cytosolic sensors such as DDX41 and stimulator of interferon genes (STING) (123, 124).

Studies using mice with a functionally inactivated type I IFN receptor (IFNAR1^{-/-}) demonstrated that IFNα/β signaling was essential for immunity to acute viral challenge. Despite otherwise normal immune responses, these animals were unable to restrict replication of vesicular stomatitis virus, Semliki Forest virus, or vaccinia virus after a low-titer challenge (131). Type I IFN can directly limit the intracellular niche for viral replication by inducing expression of cyclin-dependent kinase inhibitors, pro-apoptotic TRAIL and FAS/FASL, and the *Mx-1* gene (132, 133). These cytokines also stimulate dendritic cell maturation; upregulate expression of MHC-I, MHC-II and costimulatory molecules; and promote the production of anti-viral antibodies in B cells (134, 135). Although a robust type I IFN response is crucial for clearance of most viruses, it has also been correlated with the development of more severe disease during influenza virus infection (136, 137).

The role of type I IFN in the response to bacterial challenge is complex and appears to depend on the nature of the pathogen. Type I IFN signaling improved disease resistance in mice infected with Group B streptococci, *Streptococcus pneumoniae,* and *E. coli* (138). In contrast, type I IFNs have been characterized as detrimental to the host during infection with intracellular bacterial pathogens such as *Mycobacterium tuberculosis* (139), *Francisella tularensis* (105), *Salmonella enterica* (141), and *Lm* (142-144). Studies using IFNAR1$^{-/-}$ mice suggest that IFNα/β signaling can affect several key areas of innate immunity during infection with these bacteria. During *Lm* infection, IFNα/β signaling inhibited macrophage responsiveness to IFNγ and sensitized T cells to apoptotic signals (83, 144). Type I IFN also limited neutrophil recruitment to the spleen during both *Francisella* and *Lm* infection (105). Another study found a higher frequency of TNFα-producing CD11b$^+$ cells in the spleens of *Lm*-infected IFNAR1$^{-/-}$ mice (142). In each of these cases, mice that lacked type I IFN signaling resulted in infections had either reduced bacterial burdens or more rapid bacterial clearance compared to wild type mice.

Lm is transmitted to humans through the ingestion of contaminated food, but innate immunity to *Lm* is poorly understood because most studies have used either i.v. or i.p. inoculation, methods that result in robust systemic growth of *Lm* without encountering the harsh environment of the gastrointestinal tract. Some previous studies have used oral gavage to infect mice; however, this delivery method can result in more rapid spread of *Lm* to the blood, spleen, and liver with significant variability amongst investigators (57). All of these methods fail to replicate the natural course of infection and therefore, disparate effects on host innate immunity may be observed.

In this study, we compared foodborne transmission of *Lm* to i.v. infection to determine if type I IFN secretion was detrimental to the host when the bacteria were introduced by the natural route. We hypothesized that i.v. infection would trigger robust, rapid IFNβ secretion because a bolus of bacteria reached the spleen within minutes of inoculation. Conversely, during foodborne

infection, *Lm* would asynchronously arrive at the spleen over the course of two to three days. Therefore, it was expected that foodborne transmission of *Lm* would not trigger a robust IFNα/β response, and that the corresponding host-detrimental effects would not be observed. As predicted, we found that mice lacking the common type I IFN receptor were not more resistant to foodborne *Lm* infection, and that foodborne infection triggered significantly less production of IFNβ than i.v. infection. The data presented here suggest that most of the detrimental effects attributed to type I IFN during *Lm* infection may actually be an artifact of the i.v. infection model.

3.1 IFNα/β receptor deficiency is not beneficial during foodborne Lm infection

After i.v. inoculation of *Lm*, IFNα/β receptor-deficient (IFNAR1^{-/-}) mice resist high titer growth in the spleen and clear the infection more quickly than wild type mice (142, 143). Intravenously-injected *Lm* are quickly filtered from the blood by phagocytes in the spleen and liver, producing a rapid-onset infection in these organs (78). However, i.v.-infected IFNAR1^{-/-} and wild type mice do not show a significant difference in *Lm* burdens until 2 days post-infection (dpi), with maximal differences observed at 3 dpi (142). To find out if type I IFN signaling also promoted the growth of *Lm* after oral transmission, we used a natural feeding model of *Lm* infection. Groups of IFNAR1^{-/-} and wild type C57BL/6 mice were fed a sublethal dose of *Lm* or infected intravenously, and bacterial loads in the spleen and liver were compared. In agreement with previous reports, the livers from IFNAR1^{-/-} mice had more than 1000-fold fewer *Lm* compared to wild type mice three days after i.v. infection (Fig. 3.1). In the spleen, IFNAR1-deficient mice had 160-fold less *Lm* than wild type mice. In contrast, three days after foodborne infection there was no significant difference in bacterial burdens in the liver, and the spleens of IFNAR1^{-/-} mice had only 20-fold fewer *Lm* than wild type mice (Fig. 3.1). These results are similar to a recently published report by Kernbauer et al. who showed that i.g. infection of IFNAR1^{-/-} and wild type mice with *Lm* LO28 resulted in equivalent bacterial burdens in the

spleen and liver 3 dpi (189). Even when foodborne infection was allowed to proceed for up to 5 days, there remained no significant difference between CFU counts in the liver, and differences in the spleen were 5-fold or less. Notably, foodborne infection did not result in the death of any mice during the 5-day observation period. Thus, while the lack of type I IFN signaling was clearly beneficial after i.v. *Lm* infection, it did not alter the progression of foodborne listeriosis.

3.2 I.V. infection induces more robust IFNβ secretion than foodborne infection

In contrast to the rapid nature of i.v. infection, ingested *Lm* must first survive passage through the stomach, invade the intestinal epithelium, and then gain access to the circulation via the lymphatics before reaching the spleen. Depending on the size of the inoculum, this process typically requires 24 to 48 hours after ingestion of contaminated food (35). With this in mind, we hypothesized that the delayed and presumably asynchronous exit of *Lm* from the gastrointestinal tract would trigger a less robust IFNα/β response than a bolus of organisms that arrived in the spleen by i.v. inoculation. Consequently, a phenotype influenced by type I IFN signaling would be more easily observed during i.v. infection than during foodborne infection.

To test this idea, splenocytes were harvested from mice 24 hours after i.v. or foodborne infection (Fig. 3.2A), and lymphocytes were depleted to increase the concentration of macrophages and dendritic cells in the samples. The cells were cultured overnight without further stimulation, allowing for *ex vivo* accumulation of secreted cytokines, and ELISA was used to quantify IFNβ. As shown in Fig. 3.2C, splenocytes from i.v.-infected mice produced more IFNβ than did the splenocytes from mice infected by the foodborne route. However, a considerable disparity existed in the bacterial burdens of these two groups at this time point. The i.v. infected mice averaged 10^6 CFU in the spleen, while the orally challenged mice had less than 200 CFU per spleen (Fig. 3.2B).

To find out if the bacterial burden or the route of transmission was the primary factor influencing IFNβ secretion, we next established an infection model that resulted in colonization of the spleen for similar periods of time with comparable bacterial loads. To accomplish this, the i.v. dose was lowered to approximately 10^3 CFU and spleens were harvested 24 h after injection (Fig. 3.2D). Foodborne infection, however, proceeded for 72 hours to give the bacteria time to exit the G.I. tract and arrive in the spleen. This approach resulted in bacterial burdens of approximately 10^4 CFU in all mice, and in both cases the bacteria had colonized the spleen for approximately 24 hours (Fig. 3.2E). Splenocytes were then harvested and cultured overnight to assess IFNβ production. Despite the similarity in bacterial burdens, splenocytes from i.v.-infected mice still produced significantly more IFNβ than cells from mice that had ingested *Lm* (Fig. 3.2F). Because the murine common type I IFN receptor binds thirteen IFNα subtypes in addition to a single IFNβ (120, 121), it was possible that IFNα secretion could also be influencing the susceptibility of wild type mice to i.v. *Lm* infection. To test this, the splenocyte culture supernatants were also assayed for IFNα; however, little or none was detected (Fig. 3.2G). Thus, as predicted, i.v. infection resulted in a more robust type I IFN response than foodborne infection, even when comparable bacterial burdens were present in the spleen. Furthermore, these results suggested that enhancement of bacterial growth by the mechanisms previously attributed to IFNα/β signaling might not occur during foodborne infection due to decreased production of type I IFN.

3.3 T cell depletion in the spleen is a consequence of i.v., but not foodborne infection

One consequence of i.v. *Lm* infection that has been linked to type I IFN signaling is the extensive loss of splenic lymphocytes that occurs within the first few days after infection. In wild type mice inoculated intravenously with 0.1 LD_{50} of *Lm*, large numbers of splenic T cells upregulated CD69 and underwent apoptosis, with cell death peaking by 3 dpi (190). When type I

IFN signaling was absent, substantially less T cell depletion was observed in the spleen (144). Since oral transmission of *Lm* did not induce robust IFNβ secretion, we hypothesized that there would be little T cell loss in the spleen during foodborne listeriosis. To examine the extent of T cell death, groups of wild type and IFNAR1$^{-/-}$ mice were challenged either i.v. or orally and the total number of TCRβ$^+$ cells in the spleen 3 dpi was compared to the cell counts of uninfected mice. In agreement with previous work, i.v. infection induced an IFNAR1-dependent loss of more than 50% of the TCRβ$^+$ cells in the spleen (Fig. 3.3A). Following foodborne infection, however, there was no significant T cell depletion in either wild type or IFNAR1$^{-/-}$ mice.

The presence of apoptotic cells and cellular debris can trigger the scavenger receptor CD36 on macrophages, causing the cells to shift from a pro-inflammatory to a regulatory state with concomitant production of IL-10 (191, 192). Because significant T cell loss was only observed during i.v. infection, we predicted that i.v., but not foodborne *Lm* infection would result in increased IL-10 production. To investigate this, spleens from infected wild type and IFNAR1$^{-/-}$ mice were homogenized and the amount of IL-10 present was measured directly *ex vivo*. As expected, spleens from wild type mice contained significantly more IL-10 than spleens from IFNAR1$^{-/-}$ mice three days after i.v. infection (Fig. 3.3B). In contrast, splenic IL-10 production did not increase significantly above the concentrations detected in uninfected mice either three or four days after foodborne infection. Together, these results suggested that the IFNβ response induced by foodborne infection was not substantial enough to trigger T cell loss and subsequent increased IL-10 secretion in the spleen.

3.4 IFNα/β signaling does not affect PMN recruitment following foodborne Lm infection

Henry et al. previously showed that IFNAR1-deficient mice recruited significantly higher numbers of PMN to the spleen following intranasal *Francisella* infection compared to wild type mice (105). They proposed that a robust IFNα/β response limited the early influx of PMN by

preventing γδ T cell expansion and production of IL-17, thereby reducing the ability of wild type mice to eliminate bacteria in the early stages of infection. Based on this observation, we hypothesized that the modest IFNβ response triggered by foodborne *Lm* infection would not alter PMN recruitment to the spleen, while robust secretion of IFNβ following i.v. infection would limit this influx.

To test this, the total number of PMN ($Ly6G^{hi}Ly6C^{int}CD11b^{+}$) in the spleens of wild type and IFNAR1-deficient mice was determined by flow cytometry. Spleens were harvested 48 h after i.v. infection and 72 h after foodborne infection. As shown in Fig. 3.4A, i.v. infection of IFNAR1-deficient mice resulted in a greater PMN influx to the spleen compared with wild type mice. Three days after foodborne infection, however, there was no difference in the number of PMN in the spleens of IFNAR1$^{-/-}$ and wild type mice. Thus, PMN recruitment to the spleen was strongly enhanced by the loss of type I IFN signaling during i.v. infection, but not during foodborne infection. These data again suggested that the type I IFN response induced during foodborne listeriosiss was not robust enough to alter the innate immune response necessary for early clearance of *Lm*.

3.5 IFNGR1 expression decreases on splenic macrophages and dendritic cells during both i.v. and foodborne infection

IFNβ was also shown to negatively regulate transcription of the receptor for interferon gamma (IFNGR1), thereby limiting the ability of macrophages to respond to the presence of IFNγ (82, 83). This would presumably result in less killing of intracellular bacteria and provide a more hospitable replicative niche for the growth of *Lm in vivo*. Based on the differential IFNβ secretion we detected, we hypothesized that decreased surface IFNGR1 expression would be observed shortly after i.v. infection, but not following the ingestion of *Lm*-contaminated food.

To test this, splenocytes were harvested from mice 24 hours after i.v. infection, and the mean fluorescence intensity (MFI) of IFNGR1 on the surface of macrophages, dendritic cells, B cells, and T cells was determined directly ex vivo (Fig. 3.5A). Although i.v. infection with 10^3 CFU resulted in robust IFNβ secretion (Fig. 3.2B), little to no decrease in IFNGR1 expression was observed in any of the four cell types examined (Fig. 3.5B). However, in agreement with previous studies, when we increased the inoculum to 10^4 CFU, IFNGR1 expression on CD11c^{hi}F4/80$^{-/lo}$ dendritic cells and F4/80^{hi}CD11c$^{-/lo}$ macrophages decreased to levels that were approximately 50% of that found on uninfected cells. In contrast, B cells showed little to no change in IFNGR1 levels during high titer i.v. infection, and T cells showed an increase above uninfected levels (Fig. 3.5B). These results suggested that dose-dependent decreases in IFNGR1 expression occurred primarily on myeloid-derived antigen-presenting cells and that a bacterial burden of at least 10^5 CFU in the spleen (Fig. 3.5C) was required to observe this effect following i.v. challenge. At 24 hours after foodborne infection, little to no decrease in IFNGR1 MFI was seen on any of the four cell types tested (Fig. 3.5D). This observation was not surprising, since few mice had detectable bacterial loads in the spleen 24 hpi (Fig. 3.5E). By 48 hpi, however, IFNGR1 MFI had decreased by approximately 50% on dendritic cells and macrophages, despite the fact that bacterial burdens in the spleen averaged only 102 CFU at this time point. By 72 hpi, the MFI of IFNGR1 on dendritic cells and macrophages had decreased to levels similar to those seen during high dose i.v. infection. However, as shown in Fig. 3.5D, at this time point the mice had only ~10^4 CFU in the spleen, a bacterial burden that did not trigger changes in IFNGR1 MFI during i.v. infection (Fig. 3.5C). Thus, down regulation of IFNGR1 expression during foodborne infection was dependent on bacterial load in the spleen, but occurred at a significantly lower threshold than during i.v. infection.

3.6 Infection-induced decreases in IFNGR1 expression are not dependent on type I IFN signaling

The changes in IFNGR1 levels observed during foodborne infection in the absence of robust IFNβ secretion hinted that surface expression of this receptor might not be strictly dependent on the presence of a type I IFN signal. To directly assess the role of IFNα/β signaling in down regulation of IFNGR1, groups of wild type and IFNAR1$^{-/-}$ mice were given a high-titer dose of *Lm* intravenously or fed 10^9 CFU of *Lm* and IFNGR1 levels were assessed directly ex vivo by flow cytometry. As shown in Fig. 3.6A, IFNGR1 expression on dendritic cells and macrophages decreased by approximately one-half in IFNAR1$^{-/-}$ mice, equivalent to or in some cases greater than the change seen on cells from wild type mice. For both groups of mice, B cell IFNGR1 expression underwent little change, while expression of this receptor on T cells increased. Thus, infection-induced down-regulation of IFNGR1 was not dependent on type I interferon signaling.

A variety of cells rapidly produce IFNγ during *Lm* infection (81, 193, 194) and the cytokine can be detected in the blood within 24 to 48 hours of either i.v (142, 143) or foodborne (unpublished observation, Bou Ghanem and D'Orazio) transmission. Therefore, it was possible that ligand binding could trigger internalization of IFNGR1 and contribute to the observed decrease in surface expression during the timeframe we tested. If this was the case, then infection-induced decreases in IFNGR1 expression should be greater in wild type mice than in IFNγ-deficient mice (IFNγ$^{-/-}$). To test this, groups of mice were infected i.v. and IFNGR1 expression was assessed 24 hours later. As shown in Fig. 3.6B, dendritic cells and macrophages from IFNγ$^{-/-}$ mice showed significantly less down-regulation of IFNGR1 than did cells from wild type mice. Although IFNγ$^{-/-}$ mice are more susceptible to *Lm* infection over time, there was no significant difference in *Lm* burdens between IFNγ$^{-/-}$ and wild type mice 24 hpi (Fig. 3.6C). Thus, the difference in IFNGR1 expression was not the result of a disparity in bacterial loads.

These results indicated that multiple mechanisms could contribute to decreased surface expression of IFNGR1 during infection, and suggested that this phenotype did not contribute significantly to the enhanced growth of *Lm* in IFNAR1-deficient mice.

3.7 Discussion

Intravenous infection of mice results in a highly reproducible model of systemic listeriosis; however, this method fails to replicate the natural course of infection, which originates in the gastrointestinal tract following the consumption of *Lm*-contaminated foods. Previous studies using i.v. inoculation have suggested that secretion of type I IFN during the early stages of listeriosis may promote growth of *Lm* (142, 143). In this study, we demonstrated that foodborne infection of mice did not elicit a robust type I IFN response in the spleen. Accordingly, the host-detrimental effects caused by IFNα/β signaling were not observed when *Lm* were transmitted by the oral route. The results presented here highlight the necessity of using physiologically relevant infection models to address questions regarding the host immune response to infection.

Intravenous inoculation is widely used for studies of immunity to *Lm* because it produces a robust infection in mice, with up to 90% of the initial inoculum seeding the spleen and liver within 15 minutes (78). *Lm* are thought to be removed from the blood by phagocytes surrounding the marginal zone of the spleen. These cells transport *Lm* to the periarteriolar lymphoid sheath, where increases in bacterial burden can be detected as early as 6 hpi (195). In contrast to the rapid nature of i.v. infection, orally acquired *Lm* typically require 24-48 hours to exit the gastrointestinal tract and begin colonizing the spleen (35, 196, 197). To reach the spleen, *Lm* must survive in the harsh environment of the stomach, invade the intestinal epithelium, disseminate to the mesenteric lymph nodes, and then gain access to the circulation. The specific timing of these events is unclear, but because of the bottlenecks involved in this process small numbers of *Lm* are likely to exit the intestine in waves, rather than as a bolus. It is interesting to note that i.p.

inoculation, which also involves an indirect route of spread to the spleen, does trigger IFNα/β-dependent effects that promote *Lm* growth (144, 198). We speculate that dissemination of *Lm* from the peritoneum to the spleen occurs more rapidly than spread from the intestinal lamina propria, presumably because there are fewer bottlenecks to overcome.

Our results differ from that of Kernbauer et al., who recently concluded that type I IFN signaling promotes resistance to oral *Lm* infection because they found that approximately 30% of IFNAR1^{-/-} mice died within 5 days after intragastric (i.g.) inoculation (189) . There are two key differences between our studies. First, Kernbauer et al. used two separate i.g. injections (200 µl of bicarbonate, and then 200 µl of bacteria) to orally infect mice. I.g. infection is a more physically traumatic method than natural feeding and may promote a pathway of direct bloodstream invasion in a user-dependent manner (57). However, such physical trauma would be expected to result in an infection that mimicked i.v. inoculation, and neither our group, nor O'Connell et al. saw increased death of i.v.-infected IFNAR1^{-/-} mice compared to wildtype animals (143). Thus, the more likely explanation for the unique result in the Kernbauer et al. study is that they used *Lm* LO28, a strain that overexpresses the multidrug efflux pumps MdrM and MdrT due to a spontaneous deletion in the TetR repressor (126, 199, 200). This results in increased secretion of c-di-AMP, greater IRF3 signaling, and hyper-induction of type I IFN compared to either the commonly used laboratory strains EGDe or 10403s or other clinical isolates of *Lm*.

Myeloid-derived cells rapidly initiate IFNβ production after exposure to *Lm*. In vitro infection of bone marrow-derived macrophages and dendritic cells resulted in a clear induction of IFNβ mRNA as early as 4-6 hpi (143, 201), and intracellular cytokine staining of *Lm*-pulsed dendritic cells verified that IFNβ protein was secreted 6 hpi (202). In this study, we manipulated the dose and duration of *Lm* infection to yield similar bacterial burdens in the spleen after oral and i.v. challenge, but found that i.v. inoculation still induced significantly more secretion of IFNβ from splenocytes than foodborne infection. The simplest interpretation of these results is

that the impetus for robust IFNβ secretion is a sudden exposure to a large bolus of bacteria, which infection by the foodborne route would not provide. There are very few published reports that have measured IFNα levels by ELISA during bacterial infection. However, the amount of IFNβ secreted by splenocytes from i.v.-infected mice in this study was similar to that observed in mouse serum after cecal ligation and puncture (203) and from primary mouse lung fibroblasts following in vitro *Chlamydia trachomatis* infection (204). We were unable to detect increased IFNα in the spleen during i.v. or foodborne infection, despite the fact that IFNα subtypes outnumber IFNβ by a large ratio (121). Notably, previous measurements of IFNα concentrations in either serum or spleen ranged from 30-50 pg/mL 24 hours after i.v. *Lm* infection (205, 206). This may indicate that IFNα is produced by cell types that we did not include in high numbers in our splenocyte cultures.

Robust IFNβ secretion following i.v. inoculation of *Lm* triggered significant T cell loss, IL-10 secretion, and a dampening of PMN recruitment in the C57BL/6 mice used in this study. These findings are consistent with previous studies that suggested type I IFN was detrimental to the host during *Lm* infection (105, 142-144). None of these IFNβ-dependent effects were observed during foodborne infection. Surprisingly, down-regulation of IFNGR1, a phenotype that was previously linked to the induction of type I IFN (82, 83), occurred during both i.v. and foodborne infection. Our findings support those of Rayamajhi et al. (83) who found that IFNGR1 down-regulation was primarily observed in myeloid-derived cells. They showed that a soluble factor was responsible for suppression of IFNGR1 expression during in vivo *Lm* infection and used in vitro treatment of bone-marrow derived macrophages to demonstrate that IFNβ could induce this phenotype. Our findings, however, indicate that IFNα/β signaling is not absolutely required for IFNGR1 down-regulation to occur in vivo and suggest that a variety of other signal inputs may influence surface expression of this receptor. For example, IFNγ is quickly produced by a variety of cells in the spleen during *Lm* infection (81, 193, 194), and rapid endocytosis of

IFNGR1 due to ligand binding is likely to occur. Non-ligand based interactions could also promote internalization of IFNGR1, as has been shown to occur on T cells following TCR engagement (207). Prior in vitro work has shown that IFNα/β may act as an antagonist for IFNGR1 (208); however, it is unclear whether in vivo infection would induce the concentrations necessary to achieve these effects.

Type I IFN has traditionally been thought of as an immunostimulatory agent critical for inducing an anti-viral response, but it is also commonly used to treat autoimmune diseases such as relapsing-remitting multiple sclerosis (209). Thus, the actions of type I interferons are context-dependent and may be either pro-inflammatory or anti-inflammatory (210, 211). The timing of IFNα/β secretion, and the concentration present in any given tissue, are likely to be primary factors in determining the downstream effects of a type I IFN response. Future studies of microbial pathogens and the type I IFN response to infection should take into account the impact that route of transmission may have on both the induction and the effects of this uniquely multifunctional family of cytokines.
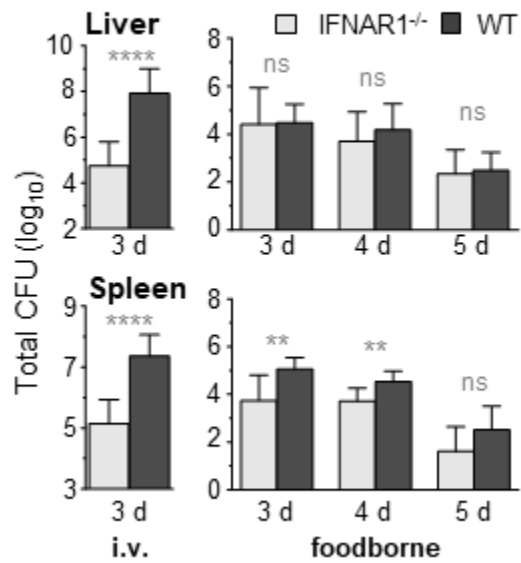
Figure 3.1 Foodborne *Lm* infection of IFNAR1^{-/-} and wild type (WT) C57BL/6J mice results in similar burdens in the liver and spleen.

Mice were infected i.v. with 9.0 x 10^4 CFU or fed 10^9 CFU of *Lm* SD2000. Data from multiple experiments was pooled for a total of 8-10 mice per group except for the 5 dpi time point, which includes 3-6 mice per group. Mean values +/- SD are shown.
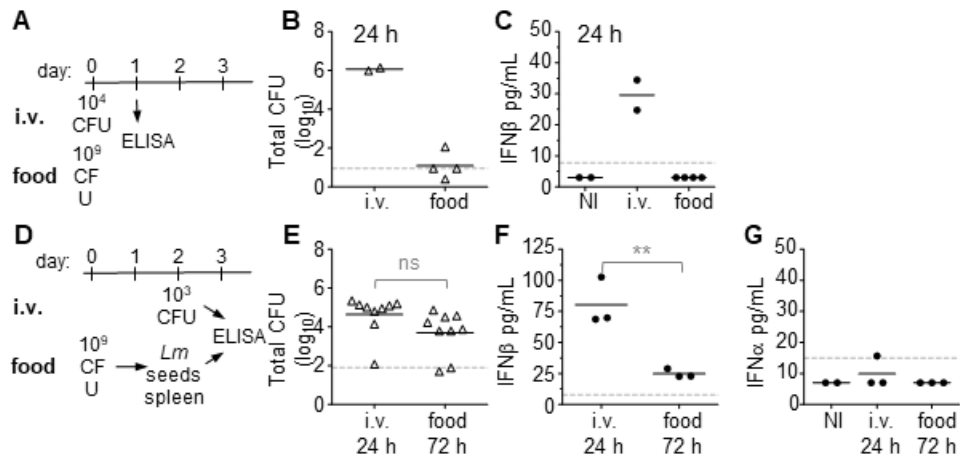
Figure 3.2 Robust IFNβ secretion is induced by i.v., but not foodborne *Lm* infection.
Splenocytes were harvested from infected C57BL/6J mice and a portion was used to determine total CFU burden. B and T cells were depleted from the remaining splenocytes, and the cells were cultured overnight to allow for ex vivo accumulation of secreted IFNα/β. (A), (D), Graphical depictions of infection strategies used are shown. (A) Mice were inoculated i.v. with 5 x 10^4 CFU or fed 10^9 CFU of *Lm* SD2000 and spleens were harvested 24 h later. In panel (D), a lower i.v. dose was used (1 x 10^3 CFU) and spleens were harvested 24 h after i.v. and 72 h after foodborne infection. (B), (E), Total CFU burdens per spleen are shown. (C), (F), (G), IFNβ or IFNα ELISA data are shown. Representative values from one of three (IFNβ) or two (IFNα) separate experiments using 2-3 mice per group are shown. Horizontal lines indicate mean values for each group; dashed lines indicate limits of detection. NI, not infected.
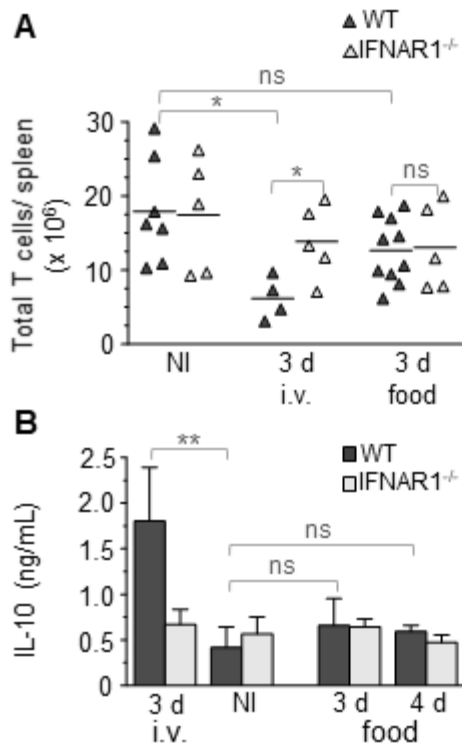
Figure 3.3 IFNα/β signaling does not promote T cell loss or IL-10 induction during foodborne listeriosis.

C57BL/6J (WT) and IFNAR1$^{-/-}$ mice were infected i.v. with 5-6 x 10^4 CFU or fed 10^9 CFU of *Lm* SD2000. Splenocytes were harvested at the indicated time points, and the total number of T cells per spleen **(A)** and the concentration of IL-10 present in clarified spleen homogenates **(B)** was determined. Pooled data from multiple experiments are shown. For panel A, values for each mouse are shown and horizontal lines indicate means for each group. For panel B, mean values +/- SD are shown; n=6-7 mice per group except WT NI, where n=4. NI, not infected.
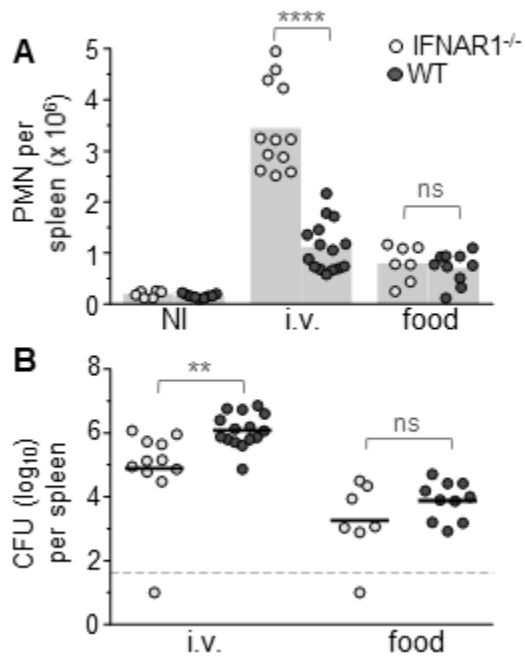
Figure 3.4 A lack of type I IFN signaling enhances PMN recruitment to the spleen during i.v., but not foodborne infection.

Mice were infected i.v. with 1 x 10^4 CFU or fed 10^9 CFU of *Lm* SD2000 and splenocytes were harvested at either 2 dpi (i.v.) or 3 dpi (food).   **A)** The total number of PMN per spleen is shown. **B)** Total *Lm* burdens per spleen are shown; dashed line indicates limit of detection. Data from multiple experiments were pooled; mean values are indicated by grey bars (A) or horizontal lines (B).
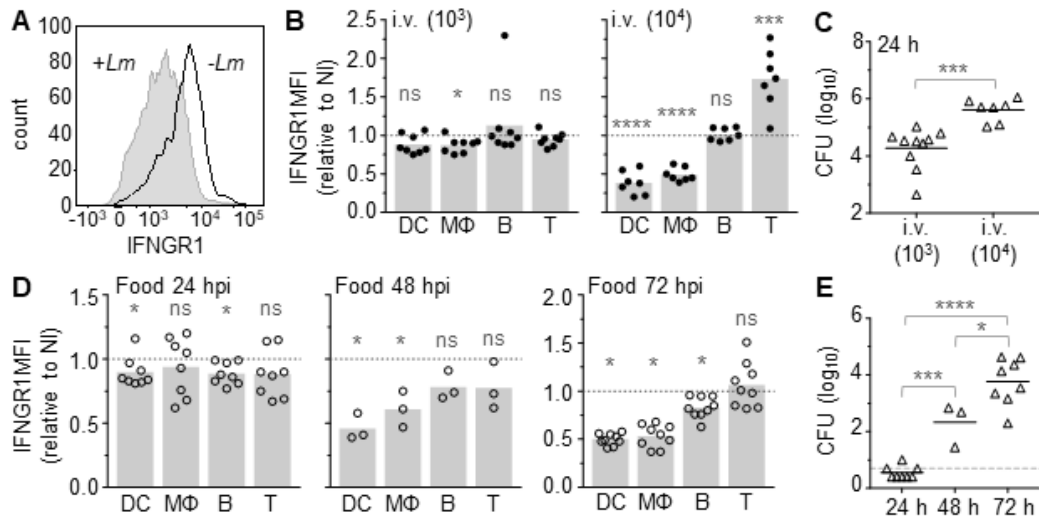
Figure 3.5 *Lm* infection results in decreased IFNGR1 expression on macrophages and dendritic cells.

Mice were infected i.v. with the indicated doses and splenocytes were harvested 24 hpi (B, C) or mice were fed 10^9 CFU, with splenocytes harvested at the indicated time points (D, E). A representative histogram depicting the shift in IFNGR1 expression on dendritic cells 24 h after i.v. infection is shown in panel (A). Mean fluorescence intensity values (MFI) for IFNGR1 were normalized to the MFI for uninfected splenocytes, which is represented by the dotted line at 1.0 (B, D). DC, dendritic cell; MΦ, macrophage. Significance was determined using one-sample t-test; asterisks indicate mean values significantly different from a hypothetical mean of 1.0. (C, E) Total Lm CFU per spleen was determined at indicated time points; dashed line indicates limit of detection.
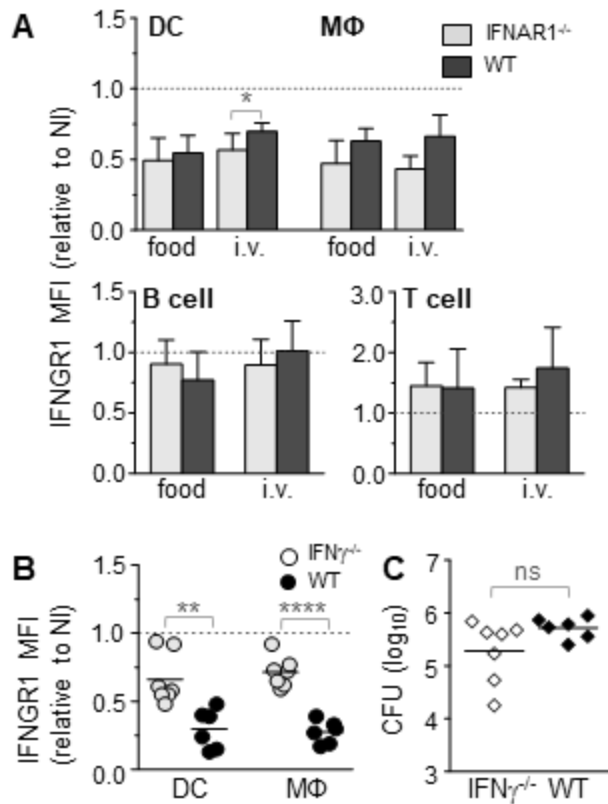
Figure 3.6 Infection-induced decreases in IFNGR1 expression are not type I IFN-dependent.

A) IFNAR1^{-/-} and C57BL/6J (WT) mice were i.v. infected with 4.0×10^3 CFU or fed 10^9 CFU *Lm* SD2000 and spleens were harvested at 24 (i.v.) or 72 (food) hpi. Mean fluorescence intensity values (MFI) for IFNGR1 were normalized to the MFI for uninfected splenocytes, which is represented by the dotted line at 1.0. DC, dendritic cell; MΦ, macrophage. Mean values +/- SD are shown; data was pooled from multiple experiments, n= 4-7 mice per group. **(B, C)** IFNγ^{-/-} and C57BL/6J (WT) mice were i.v. infected with 1×10^4 CFU of *Lm.* Spleens were harvested 24 hours later and IFNGR1 MFI **(B)** and total CFU burden **(C)** was determined.   Data from two experiments was pooled; horizontal lines indicate mean values.

4. **Neutrophils from susceptible and resistant mice efficiently kill opsonized *Listeria monocytogenes***

Summary

Inbred mouse strains differ in their susceptibility to infection with the facultative intracellular bacterium *Listeria monocytogenes* (*Lm*), largely due to delayed or deficient innate immune responses. Previous antibody depletion studies suggested that PMN were particularly important for clearance in the liver, but the ability of PMN from susceptible and resistant mice to directly kill *Lm* has not been examined. In this study, we showed that PMN infiltrated the livers of BALB/c/By/J (BALB/c) and C57BL/6 (B6) mice in similar numbers and both cell types readily migrated towards leukotriene B4 in an *in vitro* chemotaxis assay. However, CFU burdens in the liver were significantly higher in BALB/c mice, suggesting that PMN in the BALB/c liver might not be able to clear *Lm* as efficiently as B6 PMN. Unprimed PMN harvested from either BALB/c or B6 bone marrow killed *Lm* directly *ex vivo*, and pretreatment with autologous serum significantly enhanced killing efficiency for both. *Lm* were internalized within 10 minutes and rapidly triggered intracellular production of reactive oxygen species in a dose-dependent manner. However, PMN from gp91^{phox}-deficient mice also readily killed *Lm*, which suggested that non-oxidative killing mechanisms may be sufficient for bacterial clearance. Together, these results indicate that there is not an intrinsic defect in the ability of PMN from susceptible BALB/c mice

to kill *Lm* and further suggest that if PMN function is impaired in BALB/c mice, it is likely due to locally produced modulating factors present in the liver during infection.

Introduction

Lm are facultative intracellular bacteria that cause foodborne disease in humans. In mouse models of listeriosis, orally transmitted *Lm* establish infection in the gut, and then spread systemically to the spleen, liver, and gall bladder (35, 71). Susceptibility to listeriosis varies among inbred mouse strains; for example, bacterial burdens rise to significantly higher levels and clearance is delayed in BALB/c mice compared to C57BL/6 (B6) or C57BL/10 mice (35, 46, 212). This difference has been attributed primarily to facets of innate immunity, including differential expression of STAT4 and reduced or delayed secretion of TNFα, IL-12, and IFNγ (47-50).

One mechanism for innate clearance of *Lm* is direct killing by neutrophils (PMN). Early work to deplete PMN from mice relied on an antibody (clone RB6-8C5) that was subsequently shown to bind both PMN and monocytes (94-98). More recent depletion strategies designed to avoid this issue yielded conflicting results about the importance of PMN for clearance from the liver (91, 99). PMN in the liver could either kill bacteria released from apoptotic hepatocytes or may directly lyse infected hepatocytes, releasing the bacteria from a protective niche (62, 89, 90). Despite PMN recruitment to the liver, CFU burdens in BALB/c mice increased steadily for approximately 5 days; in contrast, exponential growth of *Lm* was restricted in B6 livers and the number of CFU began to fall after approximately 3 days (35, 46). This suggests that BALB/c PMN might be less efficient at killing *Lm* than B6 PMN.

PMN make up the majority of immune cells in human blood, but only account for about 15% of circulating immune cells in the mouse (102, 113). Since human blood is readily available

in larger quantities than murine blood, human PMN are most commonly used for *in vitro* assays that study interactions of PMN with bacteria. Murine PMN lack defensins and have a low affinity for the prototypical formylated peptide fMLF, but they do possess a strong affinity for formylated peptides derived from *Lm* and *Staphylococcus aureus* (110, 112, 116). Differences in relative speed and migration distance have also been noted when using murine and human PMN were compared in chemotaxis assays (117). The difficulty in obtaining large numbers of PMN from mice and the potential for functional differences with human cells has resulted in a lack of studies using murine PMN. However, PMN isolated from human peripheral blood cannot be used to evaluate how PMN contribute to susceptibility or resistance in mouse models of infection.

It has been estimated that mature PMN remain in the bone marrow of mice for up to 2 days before being released into circulation (101). Boxio et al. first showed that mouse bone marrow is an abundant source of morphologically mature PMN and that these cells release both primary and secondary granules upon stimulation (114). Swamydas et al. further refined the enrichment protocol and showed that PMN harvested from bone marrow could be used for adoptive transfer (115). In this study, we used PMN enriched from the bone marrow of naïve or infected BALB/c and B6 mice and compared the ability of the cells to kill *Lm* directly *ex vivo*. We demonstrate that murine neutrophils efficiently kill serum-opsonized *Lm* using both oxidative and non-oxidative mechanisms. We concluded that there were no intrinsic differences in the capacity of PMN from susceptible BALB/c and resistant B6 mice to directly kill *Lm.*

4.1 Hepatic PMN infiltration after foodborne infection is similar in BALB/c and B6 mice

Using the foodborne model of listeriosis in mice, *Lm* colonize the gut tissue for 24-48 hours and then spread systemically to the spleen and liver (35, 147). Differences in host susceptibility to infection can readily be observed in the liver, where the number of CFU in susceptible BALB/c mice is significantly greater than in the more resistant B6 mice (Fig. 4.1A)

(35). PMN-rich hepatic abscesses containing *Lm* were observed in both BALB/c and B6 mice 24 hours after intravenous infection (53). To verify that PMN were recruited to the liver parenchyma after foodborne infection, livers were harvested after portal vein perfusion to remove blood and Ly6G^{hi} cells were identified by flow cytometry. At 3 dpi, there was a five to ten-fold increase in the number of PMN in the liver, with no significant difference observed between BALB/c and B6 mice (Fig. 4.1A). Thus, a lack of PMN infiltration did not explain the greater CFU burden in the BALB/c liver.

After reaching a tissue such as the liver, PMN must further sense and then migrate towards specific chemoattractants, a process that was recently shown to create a "swarm" at infectious foci (108). To test whether BALB/c cells had a chemotaxis defect, we analyzed the ability of gradient- enriched PMN to migrate towards specific signals using an under-agarose assay. We first tested *Lm*-derived formylated peptides, which were previously shown by Liu et al. to induce chemotaxis from mouse PMN in a Boyden chamber assay (111). A combination of two formylated peptides (1 µM fMIVTLF plus 1µM fMIGWII) did not induce migration in the under-agar assay, despite triggering a burst of intracellular ROS when applied to either BALB/c or B6 PMN, likely a result of low diffusion through the matrix (data not shown). However, leukotriene B4, a lipid-derived chemotactic signal produced by PMN (106), did induce migration of gradient-enriched murine PMN. The maximum distance traveled in three hours was approximately 900 µm for both BALB/c and B6 PMN (Fig. 4.1B). Together, these data indicated that recruitment of circulating PMN and chemotaxis towards PMN-derived stimuli was similar in both susceptible BALB/c mice and resistant B6 mice.

4.2 Unprimed bone marrow PMN rapidly kill Lm in the presence of autologous serum

Although there was no difference in PMN infiltration, increased bacterial growth in BALB/c mice could also be due to an intrinsic defect in the ability of BALB/c PMN to kill *Lm*. To test this, we developed an *in vitro* killing assay using PMN isolated from the bone marrow of

uninfected mice. PMN were enriched using gradient centrifugation, a method that typically yielded a 65-80% pure population of Ly6G^{hi} PMN (Fig. 4.2A). The remaining cells were Ly6C^{hi} monocytes (1-5%), CD19$^+$ B cells (10-20%), and a small number of CD11b$^+$CD64$^-$ cells (data not shown). The enriched PMN were transferred to a 96-well flat-bottom plate and incubated with *Lm* at low MOI for 90 minutes. As shown in Fig. 4.2B, there was only a 20% decrease in detectable CFU within this time frame using PMN from either mouse strain.

Bortolussi et al. previously showed that *Lm* uptake by human PMN was greatly enhanced when serum was present (67). To find out if killing efficiency could be improved by exposure to serum proteins, we pre-treated late stationary phase bacteria with 10% autologous mouse serum for 30 min. prior to the addition of PMN. As shown in Fig. 4.2C, serum pre-treatment significantly increased the killing rate within one hour for both BALB/c and B6 PMN. In contrast, pre-treatment with heat-inactivated serum did not enhance killing of *Lm*. Thus, a heat-labile component found in naïve serum, most likely complement, contributed significantly to the ability of PMN to kill *Lm in vitro*. Accordingly, serum pre-treatment was used for all subsequent killing assays.

In the killing assays described above, the percentage of *Lm* killed was calculated by comparing the number of CFU recovered in the presence of PMN to the number of CFU found in assay wells that contained only bacteria. Incubation of *Lm* in tissue culture media for one hour resulted in an approximate doubling of the bacteria (Fig. 4.2D), a pattern that was consistently observed in all assays. The number of CFU recovered after the addition of gradient-enriched PMN was significantly less than the initial inoculum (dashed line), demonstrating that the PMN were actively killing bacteria within 1 h rather than simply inhibiting growth. However, given that the PMN out-numbered the bacteria in these assays by up to 10-fold, it was surprising that so many viable *Lm* remained in each well. To find out if a longer incubation time would allow the PMN to completely clear the inoculum, the killing assay was extended to four hours. *Lm*

incubated in tissue culture media alone increased more than 30-fold during this time frame (Fig. 4.2D). When PMN were added, the number of *Lm* was five-fold higher than the initial inoculum but this number represented an approximate 80% killing rate compared to bacterial growth without PMN. Thus, prolonged incubation time did not increase the efficiency of killing, and extending the incubation period just allowed any bacteria that evaded contact with PMN to replicate exponentially.

4.3 Sorted bone marrow PMN maintain viability and killing capacity after in vitro culture.

Although gradient centrifugation provided a substantially enriched PMN population to study, it was unknown whether any of the killing observed could be ascribed to the contaminating cells, which typically made up 20-35% of the enriched population. To investigate this, three populations of cells were sorted from BALB/c and B6 bone marrow: $Ly6G^{hi}Ly6C^{+}$ PMN, $Ly6C^{hi}Ly6G^{-}$ monocytes, and the residual $Ly6G^{-}Ly6C^{-}$ cells (Fig. 4.3A). Each population was plated separately and incubated with *Lm* for one hour. As shown in Fig. 4.3B, sorted PMN from both BALB/c and B6 mice killed nearly 80% of the bacteria. Neither monocytes nor the residual population of primarily B cells were capable of killing the bacteria directly *ex vivo*. These results indicated that murine bone marrow PMN could be sorted without deleterious effects and suggested that the killing observed with gradient-enriched cells was attributable only to the PMN.

To assess the functional *ex vivo* lifespan of murine bone marrow PMN, sorted cells were cultured overnight and inoculated with *Lm* the following day. As shown in Fig. 4.3C, PMN remained capable of killing 60 to 70% of the inoculum after 24 hours of *in vitro* culture. However, in contrast to what was observed directly *ex vivo*, $Ly6C^{hi}$ monocytes also killed approximately 60% of bacteria. Surprisingly, even the other cells, which were comprised mainly of $CD19^{+}$ B cells, killed 30-40% of the *Lm* (Fig. 4.3C). Therefore, murine PMN are viable and

retain efficient killing ability for at least 24 hours after isolation from the bone marrow. However, these data indicate that only highly purified sorted PMN should be used for experiments involving cells maintained in culture for more than a few hours.

4.4 Bone marrow PMN rapidly internalize and kill *Lm* intracellularly.

Human PMN are known to phagocytose particulate matter within seconds, followed by rapid closure of the phagosome, which then fuses with granules containing an array of antibacterial compounds (213). Extracellular killing mechanisms such as PMN extracellular traps have also been described (214). To assess the importance of bacterial internalization for *in vitro* killing of *Lm*, sorted PMN were pre-treated with cytochalasin D, an inhibitor of actin polymerization. *Lm* constitutively expressing GFP were added and differential "in/out" staining was performed 10 minutes later. Non-permeabilized cells were stained with Texas Red-conjugated polyclonal anti-*Lm* antibodies such that cell-associated extracellular bacteria appeared yellow (Fig. 4.4A). Bacteria that were internalized by the PMN, and thus, not accessible to the antibodies, appeared green. As shown in Fig. 4.4A, approximately 90% of the cell-associated *Lm* were intracellular 10 minutes after incubation with either BALB/c or B6 PMN. Pre-treatment with cytochalasin D decreased the percentage of intracellular bacteria, but did not completely block uptake. Killing assays performed simultaneously also showed a significant reduction in the percentage of bacteria killed when cytochalasin D was used (Fig. 4.4B). These results indicated that phagocytosis contributes to the ability of mouse bone marrow PMN to efficiently kill serum-opsonized *Lm*.

To investigate the possibility that *Lm* might be efficiently internalized by murine PMN but not killed within the short time period of these assays, a gentamicin protection assay was performed to quantify intracellular bacteria. *Lm* was added to gradient-purified PMN, and gentamicin was added 10 min later. As shown in Fig. 4.4C, 10 ug/ml gentamicin was sufficient

to kill 100% of the 1×10^5 CFU added to each well in the absence of PMN. At t=25 min, 50-200 gentamicin-resistant CFU were detected per well (0.05-0.2% of the initial inoculum). The number of intracellular *Lm* did not change at 35 or 45 minutes post-infection (Fig. 4.4C). These data suggested that a small number of *Lm* may be able to avoid killing and survive intracellularly. However, the negligible number of gentamicin-resistant bacteria were not likely to influence the percent killed calculations in the *in vitro* killing assays.

4.5 *Lm* induces a respiratory burst in unprimed murine PMN

One of the ways PMN can kill bacteria is though targeted release of reactive oxygen species (ROS). To measure the induction of ROS in PMN exposed to *Lm*, dihydrorhodamine 123 (DHR) fluorescence was used. DHR diffuses across the cell membrane and fluoresces when oxidized to rhodamine by either peroxynitrite, a product of nitric oxide and superoxide, or hypochlorous acid (215). The short incubation period of the assays described here was not likely to activate iNOS (216, 217); therefore, in this system, DHR served primarily as a measure of the amount of hypochlorous acid produced by the PMN.

Gradient-enriched PMN from BALB/c and B6 mice were incubated in media for one hour, and then suspended in buffer prior to the addition of serum-opsonized *Lm*. As shown in Fig. 4.5A, when the bacteria were added at a low MOI, less than 25% of the PMN produced ROS within 30 minutes. When 10-fold more bacteria were added, the number of ROS-positive cells increased significantly for both BALB/c and B6 PMN. Thus, unprimed PMN from both mouse strains rapidly responded to the presence of *Lm* by producing ROS in a dose-responsive manner. Although increasing the MOI resulted in a more robust respiratory burst, the killing efficiency remained at 60 to 80% (Fig. 5.5B), as was observed previously for assays using lower MOI (compare to Fig. 2C, 3B, and 4B). Together, these observations suggested that ROS might not be required for efficient killing during the *in vitro* assay.

4.6 Murine PMN use both oxidative and non-oxidative mechanisms to kill *Lm*

To specifically assess the importance of ROS for killing of *Lm*, PMN from gp91[phox]-deficient mice were compared to wild type B6 PMN. These mice lack a functional allele for the large gp91 subunit of NADPH oxidase; thus, the enzyme cannot assemble (218). As shown previously, there was a dose-dependent response for wildtype B6 PMN, with an MOI of 10 inducing more ROS-positive cells than even PMA treatment (Fig. 6A). PMN from gp91[phox]-deficient mice produced no detectable ROS at low MOI or after treatment with PMA, but, 2-5% of the cells became rhodamine-positive when *Lm* was added at an MOI of 10. A simultaneous killing assay done with these cells showed that gp91[phox-/-] PMN were equally capable of killing *Lm* as cells from the wild type NADPH oxidase-sufficient mice, regardless of the MOI used (Fig. 4.6A). Thus, in genetically deficient mice that were unable to produce ROS from birth, non-oxidative mechanisms were sufficient to kill *Lm*.

As an alternate approach to block ROS activity in both BALB/c and B6 mice, 4-hydroxy Tempo (Tempol) was used to scavenge superoxide produced in response to *Lm*. Tempol is a pleiotropic antioxidant with both superoxide dismutase and catalase-like properties (219, 220). Gradient-enriched PMN were pre-treated with Tempol for 90 minutes prior to the addition of *Lm*, and DHR was added to the samples to report generation of ROS. As shown in Fig. 4.6B, approximately 20-30% of either BALB/c or B6 PMN produced high levels of ROS within 30 min, and pre-treatment with Tempol significantly reduced the percentage of ROS^{hi} cells detected. Tempol treatment also resulted in a 10-15% reduction in killing by PMN from both mouse strains (Fig 4.6B). These data indicated that in mice genetically capable of producing ROS, scavenging oxidative intermediates such that less hypochlorous acid was available reduced killing efficiency in PMN. However, these data were also consistent with the conclusion that oxidative killing mechanisms are not required to eliminate *Lm*.

Since oxidative mechanisms were not required to kill *Lm*, we hypothesized that inhibition of proteases such as elastase, cathepsin G, and proteinase 3 would result in at least partial loss of killing capacity. To test this, gradient-enriched PMN were incubated with diisopropylfluorophosphate (DFP), a non-specific serine protease inhibitor. DFP was previously reported to inhibit protease activity without affecting production of ROS (221). Treatment with 5 mM DFP resulted in a significant reduction in PMN killing ability (Fig. 4.6C). However, treatment with 5 mM DFP also completely inhibited the ROS response in PMN exposed to *Lm*. Lowering the concentration to 0.2 mM DFP eliminated the effect on ROS activity, but this concentration did not inhibit bacterial killing (Fig. 4.6C). Therefore, it was not possible to determine whether the loss of killing efficiency was due to a loss of serine protease activity or a reduction in ROS availability in wildtype mice. DFP treatment of PMN from gp91^{phox}-deficient mice, however, did result in a significant loss of killing, suggesting that full protease activity is important for optimal killing in the absence of ROS (Fig. 4.6D).

4.7 PMN harvested from the bone marrow of infected BALB/c and B6 mice kill *Lm* with similar efficiency

Since murine PMN largely stay sequestered in bone marrow until receiving a chemotactic signal to egress into the circulation, the cells used in our *in vitro* assays were likely to be less activated than cells that are primed to infiltrate infected tissues. To assess the ability of activated cells to kill *Lm*, we harvested bone marrow from BALB/c and B6 mice 2 days after foodborne infection with *Lm*. At this time point, there are typically no CFU in the bone marrow; however, there are cells producing IFNγ, and monocytes still in the marrow have undergone inflammatory changes (75). Likewise, PMN in the marrow of both BALB/c and B6 mice had uniformly upregulated CD11b expression (Fig. 4.7A). CD11b is a component of complement receptor 3, and it was previously shown that CD11b increased on the surface of human PMN after activation

(222-224). However, no significant differences were observed for the ability of CD11b^{hi} PMN to kill *Lm in vitro* compared to cells from uninfected mice (Fig. 4.7A). Thus, unprimed cells from the marrow of uninfected mice behaved very similarly to primed cells from the marrow of infected mice.

To assess the ability of activated cells that had already emigrated from the bone marrow, we isolated cells from infected livers. Collagenase-perfused livers were harvested from both BALB/c and B6 mice at 3.5 days after infection. Non-parenchymal cells, including PMN were gradient-enriched and then kanamycin-resistant *Lm* were added. As shown in Fig. 4.7B, these cells killed 30-40% of the added *Lm*. Together, these results suggest that there are no intrinsic differences in the ability of PMN from susceptible BALB/c or resistant B6 mice to clear *Lm* infection.

4.8 Discussion

To begin to address the possibility that susceptibility to listeriosis was determined by an intrinsic defect in PMN function in mice, we developed an *in vitro* killing assay using PMN enriched from murine bone marrow. We found that murine PMN killed opsonized *Lm* efficiently even without being primed with agents such as PMA or IFNγ. Furthermore, murine PMN could be sorted and kept in culture for at least 24 hours without affecting killing ability. We showed that there was no intrinsic difference in the ability of BALB/c and B6 PMN to kill *Lm* directly *ex vivo*. However, it is possible that *in vivo*, there are substances produced in the BALB/c liver that inhibit the function of PMN and thus, contribute to the delayed clearance of *Lm*.

In agreement with previous studies using human PMN (67, 225), we showed that opsonization with naïve serum significantly improved the ability of PMN to kill *Lm*. *In vitro,* complement may be fixed on the surface of *Lm* through the classical or alternative pathway (67,

68). *In vivo*, complement is rapidly activated during inflammation and may also be activated by either proteases or acute-phase proteins present during infection (226). The concentration of specific complement components in the liver during *Lm* infection is unknown, but several studies have found increased expression of complement receptors on activated PMN (222-224). In humans, specific antibodies may also be involved in enhancing uptake and killing of *Lm*. Using a rabbit model, Vahidy et al. demonstrated that *Lm* opsonized with immune serum was internalized to a significantly greater extent than bacteria treated with non-immune serum (227).

The ROS burst has long been thought of as a primary means by which PMN clear microbes, through oxidative damage to bacterial DNA, peroxidation of membrane lipids, and other mechanisms (216). ROS might also increase the K^+ concentration in vacuoles, raising the pH and releasing proteases from an anionic matrix to allow for optimal protease activity (228). Assembly of the multicomponent NADPH oxidase is triggered by the act of phagocytosis, resulting in targeted release of ROS (229, 230). However, in this study, only a high MOI induced robust intracellular ROS production in PMN and increased ROS activity did not result in more efficient killing of *Lm*. PMN from mice genetically unable to make ROS from birth had no defect in killing *Lm*, therefore, non-oxidative killing mechanisms are sufficient. However, in animals capable of triggering an ROS burst, modulation of that response led to reduced bacterial killing. The loss of killing capacity observed after Tempol treatment was likely due to a disruption in the ratio of available oxygen intermediates. Since Tempol has catalase-like activity and also acts as a superoxide dismutase mimetic (219, 220), it presumably depletes the H_2O_2 that would normally be acted upon by myeloperoxidase to form hypochlorous acid, the oxidizing agent for DHR 123 (215).

It is not surprising that *Lm* can be resistant to killing by oxidative mechanisms, as the bacteria are known to produce both catalase and superoxide dismutase as protection against host-derived ROS (231). Previously, stationary phase *Lm* were found to be more vulnerable to killing

73

by human PMN than logarithmic phase bacteria, a result that was attributed to lower catalase production (232). Furthermore, superoxide dismutase was found to be phosphorylated and thus, less active in stationary phase *Lm* (233). However, in our study, we found no significant difference in the ability of murine PMN to kill either logarithmic phase or stationary phase *Lm*, and both cultures produced similar bubbling reactions in the presence of hydrogen peroxide (Pitts, unpublished observation). The *Lm* cytolysin LLO was also shown to inhibit the activation of NADPH oxidase in macrophages (42); however, the toxin may be rapidly degraded in PMN (234).

PMN granules contain a variety of proteins and peptides that provide non-oxidative means of killing bacteria including cathepsin G, elastase, proteinase 3, lactoferrin, and lysozyme (235). Alford et al. showed that purified cathepsin G alone could kill either *S. aureus* or *Lm* (236). Since several of these compounds are serine proteases, (236, 237) we expected to find at least a partial loss of killing efficiency after pretreatment with DFP, a serine protease inhibitor, but this only occurred in a gp91phox^{-/-} background. DFP was previously used to show that serine proteases were important for human PMN to kill *Streptococcus pneumoniae* (238), but ROS activity was not monitored in that study, so we cannot make a direct comparison to our results. DFP was also used to inhibit proteolysis of CD43 on human PMN stimulated with opsonized zymosan; in that study, the DFP did not inhibit ROS generation (221). This suggests that the nature of the phagocytosed particle may determine whether or not DFP impacts the ROS burst.

Circulating PMN are readily obtained from human peripheral blood; however, the cells are easily affected by *ex vivo* isolation and labeling techniques, and are prone to rapid cell death (101, 239-241). In contrast, mature PMN harvested from the bone marrow have a longer half-life, can be maintained in culture for at least 24 hours (114), and as we showed here, are not affected by manipulations such as cell sorting. A key advantage of using unprimed cells, rather than cells that have already egressed from the bone marrow, is the ability to study how specific

74

inflammatory signals alter the functional properties of the PMN. An important challenge for future work will be to understand how signals in infected tissues such as the liver may affect the function of PMN during infection.
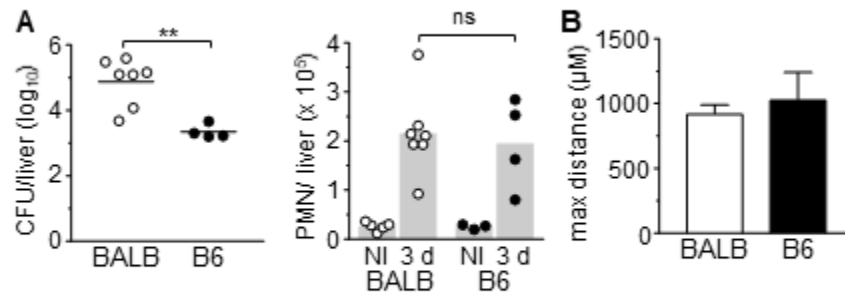
Figure 4.1 PMN recruitment to the liver following foodborne infection is similar in B6 and BALB/c mice

PMN recruitment to the liver following foodborne infection is similar in B6 and BALB/c mice. (A) Mice were fed 3 x 10^8 CFU of *Lm* SD2000. At 3 dpi, livers were perfused and total CFU was determined. Total Ly6G^{hi}Ly6C$^+$ PMN found in the non-parenchymal fraction after tissue digestion in uninfected (NI) or infected (3 d) mice was also determined. Pooled results from three independent experiments are shown. (B) Migration of gradient-enriched PMN toward 100 nM leukotriene B4 was monitored using an under-agarose assay. Representative results from one of three independent experiments are shown (n=4 technical replicates per group).
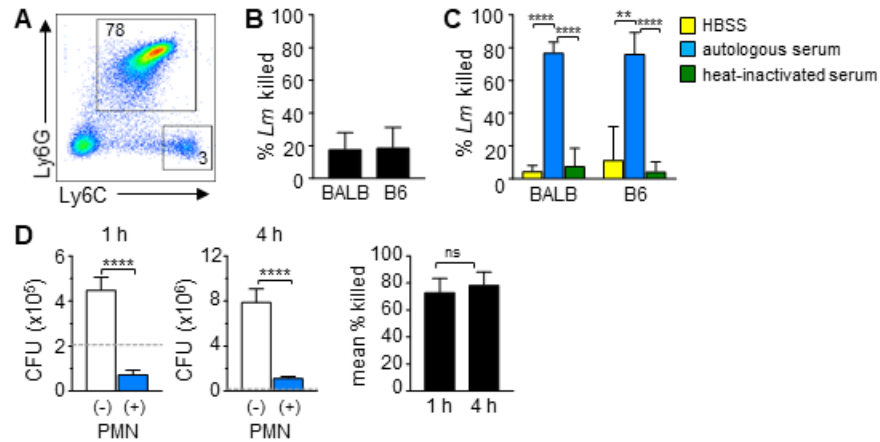
Figure 4.2 Murine PMN kill *Lm* efficiently in the presence of serum.

Gradient-enriched PMN were used to perform in vitro killing assays. (A) Representative dot plot shows the composition of a typical gradient enriched bone marrow prep; live and single cell gates were applied. (B) PMN (n=3 technical replicates) were incubated with *Lm* at a MOI of 0.05 for 90 min. Pooled results from 2 independent experiments are shown. (C) *Lm* were pre-treated as indicated and added to PMN (MOI 0.1) for 60 min. Representative results from one of three independent experiments are shown. (D) Serum-opsonized *Lm* (MOI=2) was added to BALB/c PMN. The absolute number of CFU remaining in the wells at either 1 h or 4 h for a representative experiment is shown in the two left graphs. Dashed lines indicate the number of CFU at t=0. The mean percentage killed at each timepoint (+/- SD) for three independent experiments is shown on the right.
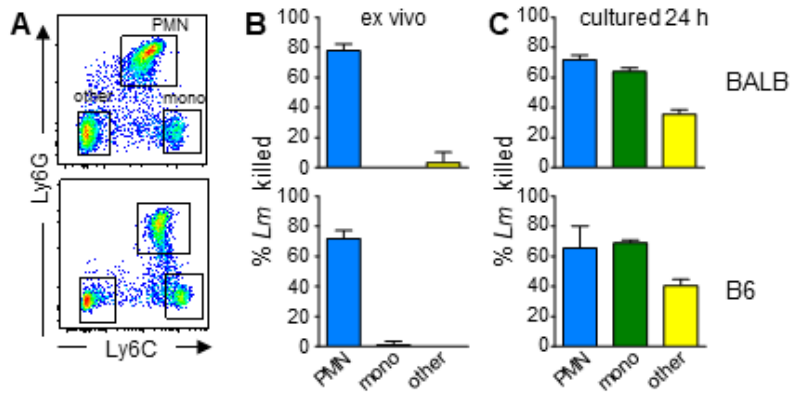
Figure 4.3 Murine PMN rapidly internalize *Lm in vitro*.

Sorted murine PMN efficiently kill *Lm*. (A) Representative plots depict the three populations of cells sorted from marrow of BALB/c (top row) and B6 (bottom row) mice. (B) Sorted cells were plated in media for 1 h and then serum-opsonized *Lm* was added (MOI=0.1); killing efficiency was assessed after 50 min. (C) Sorted cells were cultured overnight at 37°C in 7% CO2. The following day, a killing assay was performed as described above. One of two independent experiments with 3 technical replicates per group is shown.
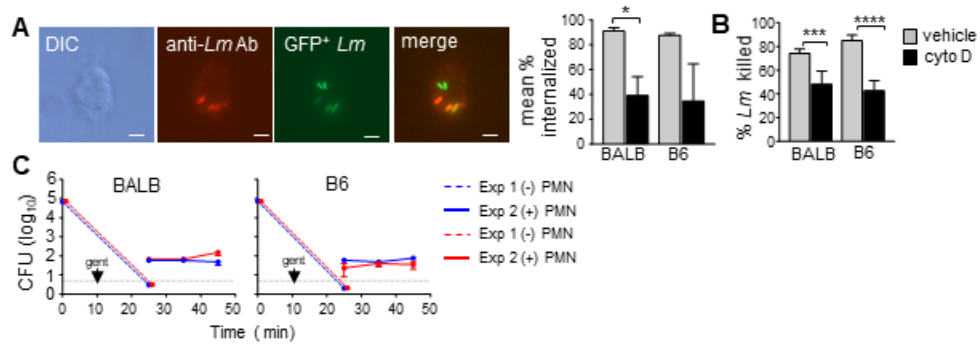
Figure 4.4 Murine PMN rapidly internalize *Lm in vitro*.

(A) Serum-opsonized *Lm* constitutively expressing GFP (*Lm* SD2710) was added to sorted PMN (MOI=1) that were pre-treated for 45 min with either 20 μM cytochalasin D (cyto D) or DMSO (vehicle). Cell-associated *Lm* were visualized by differential in/out staining 10 minutes post infection. Representative images show intracellular (green) and extracellular (yellow) bacteria (scale bar= 2 μM) and the mean percentage of internalized bacteria in three independent experiments is shown. B) A representative killing assay performed at 50 minutes for cells treated as in (A); bars indicate mean +/- SD. C) Gentamicin protection assay performed with serum-opsonized *Lm* and gradient-enriched PMN (n=3 technical replicates) and incubated for 10 min before addition of gentamicin. Gentamicin was added at t=0 as indicated by the arrowheads. Data from two independent experiments (Exp 1, Exp 2) are shown.
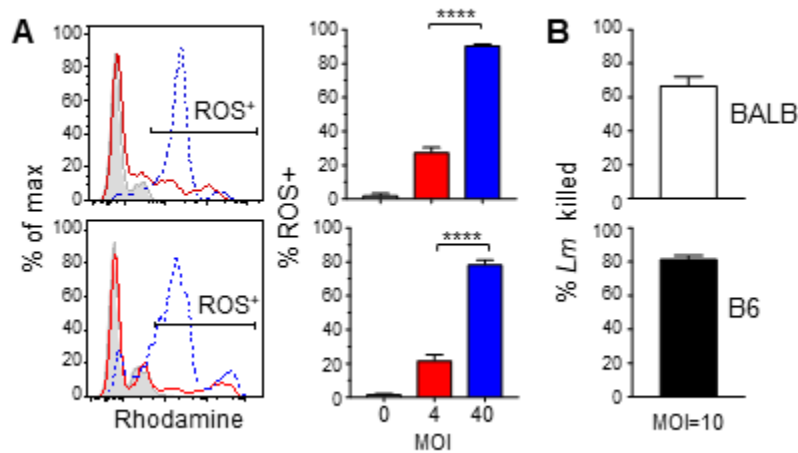
Figure 4.5 *Lm* **induces a dose-dependent ROS burst in murine PMN.**

Gradient-enriched PMN suspended in HBSS were incubated with dihydrorhodamine 123 prior to the addition of *Lm* at MOI=4 (red), MOI=40 (blue); mock infected cells are shown in grey. (A) Representative histograms for cells harvested 30 min after addition of bacteria and total ROS+ Ly6G^{hi}Ly6C^{+} PMN are shown. (B) Gradient-enriched PMN were used for an in vitro killing assay (MOI=10). Killing efficiency was assessed after 50 min. Representative results from one of three experiments using n=3-5 technical replicates per treatment are shown. Bars indicate mean +/- SD.
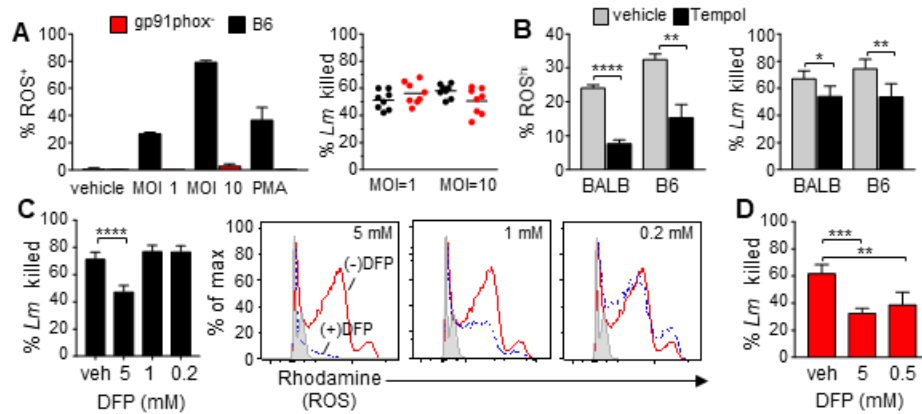
Figure 4.6 ROS is not required for efficient in vitro killing of *Lm*.

(A) Gradient-enriched PMN from gp91[phox-/-] and B6 mice were loaded with DHR prior to addition of either serum-opsonized *Lm* or 20 nM PMA. ROS levels were determined at 30 min and a killing assay as performed at 50 min. Pooled data from two independent experiments are shown; horizontal bars indicate mean +/- SD (B). Gradient-enriched PMN were incubated with 50 μM Tempol or vehicle for 90 min. prior to addition of *Lm* and the percentage of ROS[hi] neutrophils and the killing efficiency for these cells was determined. Data from one of three independent experiments is shown; bars indicate mean +/- SD. (C) Gradient-enriched BALB/c PMN were incubated with DFP for 30 min. at the indicated concentrations prior to addition of *Lm* (MOI=10). ROS activity was determined 30 min later and % killed was determined 50 min after addition of bacteria (n=5). Representative results from one of two independent experiments are shown. Solid grey histogram indicates uninfected. (G) Gradient-enriched PMN from gp91[phox-/-] males were treated with DFP at the indicated concentrations for 30 min. prior to addition of *Lm* (MOI=10) for an *in vitro* killing assay. Bars indicate mean for n=6 replicates from one of two independent experiments
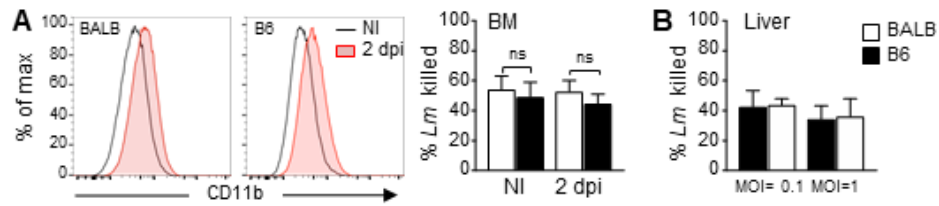
Figure 4.7 Neutrophils harvested from the bone marrow of infected BALB and B6 mice kill
***Lm* with similar efficiency.**

(A) CD11b surface expression on sorted PMN from uninfected mice (NI) or mice fed 3 x 10^8
CFU *Lm* SD2000 (2 dpi) was determined. Representative flow cytometry histograms are shown.
PMN were incubated with *Lm* SD2001 for 50 min and the percentage of kanamycin-resistant
bacteria killed was determined. Bars indicate mean +/- SD for 6 technical replicates from one of
three independent experiments. (B) BALB/c and B6 female mice were fed 1 x 10^9 CFU *L.
monocytogenes* and livers were harvested at 3.5 dpi following collagenase perfusion via the portal
vein. The enriched non-parenchymal fraction was plated and exposed to *Lm* SD2001 at the
indicated MOI for 50 min and the percentage of kanamycin-resistant bacteria killed was
determined. Bars indicate mean +/- SD for 6 technical replicates from one of two independent
experiments.

5. Prostaglandin E2 is a negative regulator of the neutrophil response to *Listeria monocytogenes*

Pitts, MG and D'Orazio, SEF

Summary

During acute *Listeria monocytogenes* (*Lm*) infection, neutrophils (PMN) rapidly infiltrate the liver and begin to remove both free bacteria and infected cells. In the C57BL/6J (B6) mouse, hepatic *Lm* burdens quickly peak and then begin to decline, but in susceptible BALB/cBy/J (BALB) mice the bacterial load continues to increase exponentially despite adequate PMN recruitment. We previously showed that bone marrow PMN from both mice killed *Lm* with similar efficiency. This suggests that the microenvironment in the BALB liver may be modulating PMN function. Prostaglandin E2 (PGE2), an immunomodulatory lipid previously shown to suppress Th2 responses and PMN effector functions, was produced in significantly higher amounts by the mononuclear leukocyte fraction of cells from infected BALB livers than cells from infected B6 livers. PGE2 significantly inhibited *in vitro* killing of *Lm* by both B6 and BALB PMN, and this loss of function was rescued by PGE2 receptor antagonism. We previously found that PMN isolated from mice lacking the gp91 subunit of NADPH oxidase efficiently killed *Lm* within 50 minutes. When these PMN were treated with PGE2, however, no loss in killing was observed, suggesting that PGE2 was impacting oxidative killing mechanisms. Data also suggests that the presence of PGE2 negatively affects PMN migration and internalization of *Lm,* thus affecting production of reactive oxygen species and overall killing efficiency. Thus, an excess of PGE2 secretion in the infected BALB liver negatively impacts PMN ability to kill *Lm* by blunting multiple killing mechanisms, allowing the bacteria to replicate exponentially during critical early stages of the infection.

Introduction

Prostaglandin E2 (PGE2) is a signaling lipid derived by enzymatic modification of arachidonic acid present in the cell membrane. Related compounds, called eicosanoids, include leukotriene B4 (LTB4), thromboxane A4, and prostacyclins. PGE2 is probably best known for its roles in pain and fever; in fact, it is a classic pro-inflammatory mediator with numerous drugs directed at its production. However, there is a growing body of knowledge related to the role of PGE2 in inhibition of innate immune responses, such as aberrant T cell polarization, inhibition of macrophage function, induction of IL-10 secretion, and suppression of PMN effector functions (148-155). The role of PGE2 in the body seems to depend strongly on the tissue, the stimulus causing its induction, and the timing of secretion. In many situations, suppression of innate immunity by PGE2 may outweigh its induction of pro-inflammatory pathways.

Introduction of mechanical trauma or inflammatory stimuli such as bacteria can stimulate production of PGE2, which begins with release of arachidonic acid from the cell membrane by one of three phospholipase A2 enzymes. Two of these, cPLA2 and sPLA2, are inducible, and cPLA2 has been shown to be activated by secretion of the cholesterol-dependent cytolysin LLO (157). Once arachidonic acid is liberated, it may be oxidized by the cyclooxygenase enzymes (COX-1 and COX-2), producing an intermediate prostaglandin that is further enzymatically modified by prostaglandin E synthase (PGES) to produce PGE2. Three isoforms of PGES exist-microsomal PGES (mPGES) 1 and 2 and cytosolic PGES (cPGES). A study using peritoneal macrophages of BALB/c and B6 mice found that BALB/c macrophages express higher levels of mPGES and thus produce more PGE2 when stimulated with LPS (150). Free arachidonic acid can also be metabolized by the lipoxygenase pathway, ultimately resulting in leukotrienes including LTB4, a lipid with chemotactic properties for PMN (106, 107). Activation of 15-lipoxygenase results in secretion of lipoxin A4 (LXA$_4$), a pro-resolution lipid produced during the

plateau phase of PMN swarming (109, 159, 160). Using human PMN, Levy et al. showed that PGE2 exposure switched lipoxygenase activity from predominately 5-LO, producing LTB4, to 15-LO, making LXA_4 within 5 hours (160). This study provided strong evidence that PGE2 could induce downregulation of the PMN inflammatory response.

PGE2 is rapidly removed from circulation and may also be degraded by a dehydrogenase or by albumin (162-165). It binds four G-protein coupled receptors, designated EP1-EP4, which are expressed on a variety of tissues and cells (152, 166, 167). Ligation of EP2 and EP4 stimulates an increase in cyclic adenosine monophosphate (cAMP) through activation of adenylate cyclase (168), and it is ligation of these two receptors that is also thought to result in many of the immunosuppressive effects of PGE2 (152, 162).

Numerous studies examining the effect of PGE2 on innate immune functions have concluded that, given the necessary stimulation and environment, it is an immunosuppressive compound (152, 156, 162). More than thirty years ago, Hutchison and Myers identified PGE2 in splenocyte culture supernatants as a factor that suppressed peritoneal macrophage phagocytosis of *Lm* (177). Since then, PGE2 has been observed to be produced at higher levels by stimulated BALB cells than B6 cells and additionally, BALB mice were found to be more sensitive to its effects than were B6 mice (149, 150). PGE2 is also a potent inhibitor of production of reactive oxygen species and secretion of IL-12 and TNFα from monocytes (151, 153, 242), all of which could have impacts on the course of *Lm* infection.

Following foodborne infection, PMN are robustly recruited to sites of *Lm* colonization including the liver (75, 147, 243). PMN are thought to be necessary for removal of *Lm* from the liver, where they may both lyse infected hepatocytes as well as kill free bacteria (62, 89, 90). We previously showed that bone marrow PMN from susceptible BALB and resistant B6 mice killed *Lm* with similar efficiency *in vitro,* suggesting that any inhibition of PMN function in the liver was an effect of the microenvironment (243). In this study, we show that PGE2 causes a dose-

dependent decrease in PMN killing efficiency *in vitro*, and that PGE2 is produced at higher levels by immune cells harvested from the livers of *Lm*-susceptible BALB mice than cells from resistant B6 mice. These data suggest that PGE2 and its family of eicosanoids should be more closely examined as immune modulators as more is learned about the course of dissemination and growth of *Lm* following foodborne infection.

5.1 *Lm* exposure induces upregulation of COX-2 in myeloid cells *in vitro*

COX-1, thought of as a "housekeeping" enzyme, and COX-2, the inducible cyclooxygenase enzyme, are the first enzymes that act on arachidonic acid to produce prostaglandins once it has been liberated from the cell membrane. Although reports are somewhat contradictory on the levels of COX-2 at basal levels, this enzyme is considered to be induced by inflammatory stimulation (158, 162). To measure *Lm*-mediated stimulation of PGE2 production in myeloid cells, bone marrow-derived monocyte cultures were stimulated with live *Lm* SD2000. Three populations of cells were present, Ly6C^{hi} monocytes, Ly6C$^-$CD64$^+$ macrophages, and a transitioning CD64^{hi}Ly6C$^{lo/med}$ population (Fig. 5.1A). As shown in Fig. 5.1B, COX-2 was expressed in all three populations prior to stimulation. When cells were exposed to heat-killed sonicated *Lm* or infected with live, replicating *Lm,* both the MFI and the COX-2$^+$ percentage of each cell type increased. However a lower percentage of monocytes (GR1$^+$CD64$^-$) was COX-2+ prior to treatment and these cells responded at a lower level to stimulation than macrophages or transitioning cells.

5.2 *Lm* infection induces PGE2 secretion in the livers of BALB/c mice

Since monocytes and PMN infiltrate the liver within three days after foodborne infection (Fig. 5.2A, (243)), we next decided to assess COX-2 expression levels in cells harvested from the

livers of infected mice. At three days after infection, a mixed population of cells was harvested from the livers of BALB and B6 mice and enriched for hematopoietic cells using gradient centrifugation. These cells were stained for intracellular COX-2 expression as well as surface markers for PMN, monocytes, Kupffer cells, and B and T lymphocytes. As shown in Fig. 5.2B, however, intracellular staining for this enzyme did not reveal any conclusive infection-related induction of COX-2, and furthermore did not point to any one cell type as the primary producers of PGE2 in response to *Lm.*

PGE2 is often a locally-acting compound and has both autocrine and paracrine functions (156). Additionally, it is metabolized very rapidly, making *ex vivo* measurement in a mixed population of cells difficult (163, 164). In order to measure PGE2 in the liver, a proxy measurement, prostaglandin E2 metabolite (PGEM) was used. PGEM is a stable converted metabolite of PGE2 useful for determining PGE2 secretion in situations where PGE2 is secreted but also metabolized by neighboring cells. First, mice were fed *Lm* and livers were harvested at 3 dpi and homogenized. When clarified supernatants from liver homogenates were tested, PGEM measurements were low and variable (Fig 5.2C). Because of this, we next depleted parenchymal cells from collagenase-digested livers and cultured the remaining hematopoetic fraction overnight, allowing secretion of PGE2 into the supernatant. A mixed population of non-parenchymal cells was isolated from the livers of infected animals to assess PGE2 secretion following *in vivo* infection. As shown in Fig. 5.2A, this population consisted of neutrophils, monocytes, and numerous other cells not stained by Ly6G and Ly6C markers. Cells from infected BALB/c livers, which contained an average of 10-15-fold higher CFU burdens than B6 livers (Fig. 5.2D), secreted significantly more PGE2 in overnight culture than cells from infected B6 livers (Fig. 5.2E). To address concerns that perhaps the high CFU burden in BALB liver cultures was driving PGE2 secretion and understand what stimulus initiated secretion, uninfected liver cells were exposed to live *Lm* or heat killed, sonicated *Lm*. For comparison, cells from

infected mice were further stimulated with heat killed, sonicated *Lm*. As shown in Fig. 5.2F, the additional stimulation boosted PGE2 secretion from cells obtained from infected livers; however, only cells from infected mice were capable of secreting PGE2 under any of the conditions tested. Thus, *in vivo* conditions in the BALB/c liver initiated PGE2 secretion and that secretion could be increased by further stimulation.

To assess whether the effects of augmented PGE2 signaling or inhibition could be seen on a macroscopic level, mice were treated with either indomethacin, a COX-2 inhibitor, or exogenous 16,16 DM PGE2, a receptor agonist, after infection. However, neither of these treatments had a clear effect on CFU burdens in the liver or spleen at 3 or 4 dpi (Figure 5.2G and H). Interestingly, BALB/c mice receiving indomethacin treatment appeared more active and less ruffled than mice receiving vehicle treatment. PGE2 treatment seemed to have no gross effect on the behavior or appearance of B6 mice, however.

5.3 PGE2 down-regulates PMN killing efficiency through EP2 and EP4 signaling

PGE2 was previously shown to modulate many functions of innate immunity, including macrophage phagocytosis and PMN ROS burst and TNFα secretion (153, 171, 179). It followed, therefore, that overproduction of PGE2 could play a role in the growth of *Lm* observed in BALB/c livers. All of the above-mentioned effects are indirect measures of cell function, however. To directly test the effect of PGE2 on the ability of PMN to kill *Lm*, an *in vitro* killing assay using bone marrow PMN was used as previously described ((243), chapter 4). Gradient enriched bone marrow PMN were plated in tissue culture media and then treated with PGE2 for 30 or 90 min., as indicated, before addition of *Lm*. As shown in Fig. 5.3A, PGE2 treatment yielded a dose-dependent reduction in killing efficiency as compared to vehicle treatment. The highest amounts of inhibition were observed at 1μM after 30 min. of treatment or .1-1 μM after 90 min. of treatment. Wells in which PMN were treated with PGE2 yielded 33-50% more

bacteria than vehicle-treated wells.   As shown in Fig. 5.3B, when the average reduction in killing with 1 μM PGE2 was pooled across many samples, similar results were observed with both BALB and B6 PMN despite variability from assay-to-assay.

Two of the four PGE2 receptors, EP2 and EP4, have previously been shown to be responsible for most of the immune-inhibitory actions of PGE2 signaling (168, 171, 172, 179, 180). Much of this is thought to be a result of intracellular cAMP accumulation; however, little is actually known about how cAMP accumulation affects the direct killing ability of phagocytic cells. To assess the contribution of these two receptors to the PGE2-dependent loss of killing, PMN from BALB/c and B6 mice were treated with EP2 and EP4 receptor antagonists concurrently with PGE2.   As shown in Fig. 5.3C, PGE2 caused a 20-30% loss of killing efficiency.   EP2 antagonism partially rescued this loss of killing, with further rescue observed using EP4 antagonism.   Although some variation was again present, nearly full rescue was observed in many samples. These results suggested that the inhibition of PMN killing caused by PGE2 was dependent on the EP2 and EP4 receptors.

5.4 PGE2 exerts pleiotropic effects on PMN function

EP2 and EP4 ligation mediate an increase in cAMP that was previously shown in murine PMN to result in decreased secretion of TNFα after LPS stimulation (171). Other EP2 and EP4-dependent effects have also been shown in macrophages, including lower phagocytosis efficiency and reduced ROS burst (151, 178). We previously showed that mouse PMN kill *Lm* through redundant oxidative and non-oxidative mechanisms (chapter 4), but how these receptors influence the many mechanisms that PMN use to kill, however, is unknown. Since reductions in killing efficiency after PGE2 treatment averaged 20-30%, we reasoned that there were likely to be several small testable effects within the parameters of using bone marrow PMN that added up to the larger phenotype.

An under-agarose assay was first employed to assess the effect of PGE2 treatment on PMN chemotaxis toward a 1000 nM LTB4 gradient. Enriched bone marrow PMN from BALB/c and B6 mice were suspended in media containing 1 µM PGE2, incubated for 5 min., and added to the assay gel. After 2 hours, maximum distance traveled under the agarose was measured. As shown in Fig. 5.4A, untreated cells traveled 19-35% farther than cells treated with PGE2. Because deficiencies in chemotaxis could result in lower bacterial internalization, in/out staining after PGE2 pre-treatment was next used to assess the efficiency of phagocytosis. To obtain a pure population of PMN to study, cells were sorted using Ly6G and Ly6C markers. GFP-expressing bacteria were added to PMN that had been pretreated with PGE2, and in/out staining was performed at 10 mpi, a point at which it was already known that most cell-associated bacteria could be found intracellularly ((243), chapter 4). At this point, approximately 10-12% fewer cell-associated bacteria were found to be intracellular when cells were PGE2-treated (Fig 5.4B).

Since internalization of bacteria in PMN results in ROS generation, we next used M-cherry expressing *Lm* together with dihydrorhodamine (DHR), which is oxidized to rhodamine and fluoresces comparably to FITC in the presence of ROS. Treatment of cells with 1µM PGE2 prior to addition of bacteria caused a 5-7% reduction in the percentage of cells detected to contain M-cherry bacteria and a comparable reduction in ROS positivity at the same time point (Fig. 5.4C). Importantly, however, further assays to detect reductions in ROS due to PGE2 exposure were unsuccessful. It is difficult to say whether reagent breakdown or compensation of the colors led to the differences. The initial experiment, however, was performed using sorted cells and subsequent experiments used gradient-enriched cells with surface staining after exposure to bacteria and DHR. Other than incidental mouse-to-mouse variation, it seems likely that the differences in the particular parameters of the initial experiment vs subsequent experiments led to the lack of positive results from the latter.

We previously showed that gp91*phox*^{-/-} PMN had no defect in killing *Lm* despite complete lack of ROS burst ((243), chapter 4). Furthermore, the data in chapter 4 suggested that ROS in wild type mice, a reduction in ROS could result in a small but significant reduction in killing efficiency. To understand if the effect of PGE2 on ROS extended beyond the initial 10-minute time point and affected killing efficiency, gp91*phox*^{-/-} PMN were incubated in 1 μM PGE2 for 90 min before addition of Lm. As shown in Fig. 5.4D, PGE2 pretreatment resulted in an approximate 15% decrease in wild type PMN killing efficiency but had no effect on the ROS-deficient PMN, indicating that it indeed was affecting ROS in the wild type cells. Together, these data suggest that PGE2 has numerous small effects on the multiple methods that PMN use to kill *Lm*.

5.5 Discussion

PMN are recruited to *Lm*-infected liver and thought to be necessary for hepatic clearance of *Lm,* yet the connection of PMN killing efficiency to susceptibility in listeriosis has not been previously explored. Our lab previously showed that bone marrow PMN from susceptible BALB/c and resistant B6 mice killed *Lm* with similar efficiency, indicating that upon egress from the marrow, these cells were likely to be in a similar state of readiness and suggesting that in the liver, they encounter an environment that changes their functional capacities. In this study, we examine the effects of PGE2, an immunomodulatory lipid, and show that it is both produced at higher levels in the livers of susceptible animals and that PMN are less able to kill *Lm* in its presence.

It was not surprising to find PGE2 produced by fractionated BALB liver immune cells; however, it was unexpected to find that infection appeared not to induce PGE2 secretion in samples from B6 mice. Whether this was due to a differential cell infiltrate at 3 dpi is unknown. Previous studies using macrophages have indicated that BALB cells possess more PGE2 binding

sites and produce more PGE2 after stimulation than B6 or C3H/HeN macrophages (149, 150), but to the best of our knowledge this is the first study to find differential secretion in the context of infection. Unfortunately, we were unable to verify induction of COX-2 in response to *in vivo* infection. However, two explanations exist for this. First, a low percentage of total cells are likely to be infected at any given time in the liver after foodborne transmission. It seems likely that COX-2 induction and/or PGE2 secretion are dependent on the presence of bacteria in neighboring cells, if not within the producing cell itself. Furthermore, the extensive processing required to fractionate immune cells from the liver could easily negatively impact this staining.

The impact of PGE2 pretreatment on the ability of PMN to kill *Lm* was, on average, a 20-30% loss of killing efficiency. This means that in comparison with vehicle-treated cells, approximately 25% more bacteria escaped killing, remaining alive and able to replicate after 50 min of contact with PMN. Since PMN are likely to accumulate in the liver over the course of several days after foodborne infection and be exposed to tonic as well as acute PGE2 secretion, these results are suggestive that the *in vitro* phenotype could also be observed *in vivo*. Levy et al. proposed the idea of an "eicosanoid switch," a process by which PMN are exposed to PGE2 for several hours and then begin to modulate their own dispersal by producing pro-resolution lipoxin A4 (160). These results were supported by the recent work of Reategui et al. in which swarming PMN produced lipoxin A4 during the plateau phase of the swarm, thus changing their behavior pattern (109).

Many of these results are supportive of results others have obtained using other cell types and other forms of stimulation after PGE2 treatment. The small but significant effects on chemotaxis, bacterial internalization, and ROS are also supportive of the larger phenotype, a defect in overall killing capacity in PMN. Together, these results point to an immunomodulatory role for PGE2 during the context of bacterial infection that could easily play a part in other opportunistic infections. Further work with the foodborne infection model and refinement of

techniques to measure PGE2 in the infected host will be required to elucidate the effects of PGE2

on clearance of *Lm*.
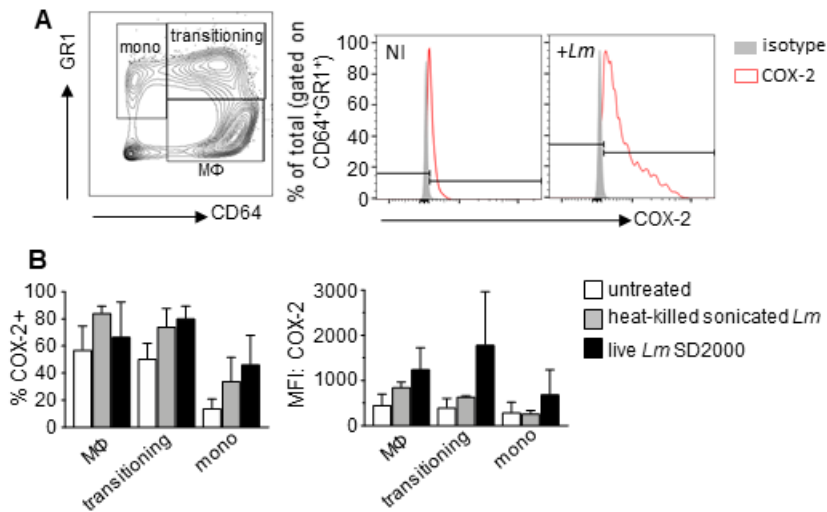
Figure 5.1 *In vitro* infection induces COX-2 upregulation

Bone marrow-derived monocytes (GR1$^+$CD64$^-$), transitioning cells (GR1$^+$CD64$^+$), and macrophages (CD64$^+$GR1$^-$) were infected for 2 hr with *Lm* SD2000 (MOI=1) for 2 hr followed by addition of 25μg/ mL gentamicin. COX-2 expression was assessed after overnight incubation. (A) A representative plot depicts the three cell types in culture at day four. On the right, a representative COX-2 histogram for transitioning cells is shown with uninfected cells on the left and infected cells on the right.   (B) Percent COX-2+ cells for each cell type and COX-2 mean fluorescence intensity (MFI) and are shown. Pooled results from three independent experiments are shown; bars indicate mean +/- SD.
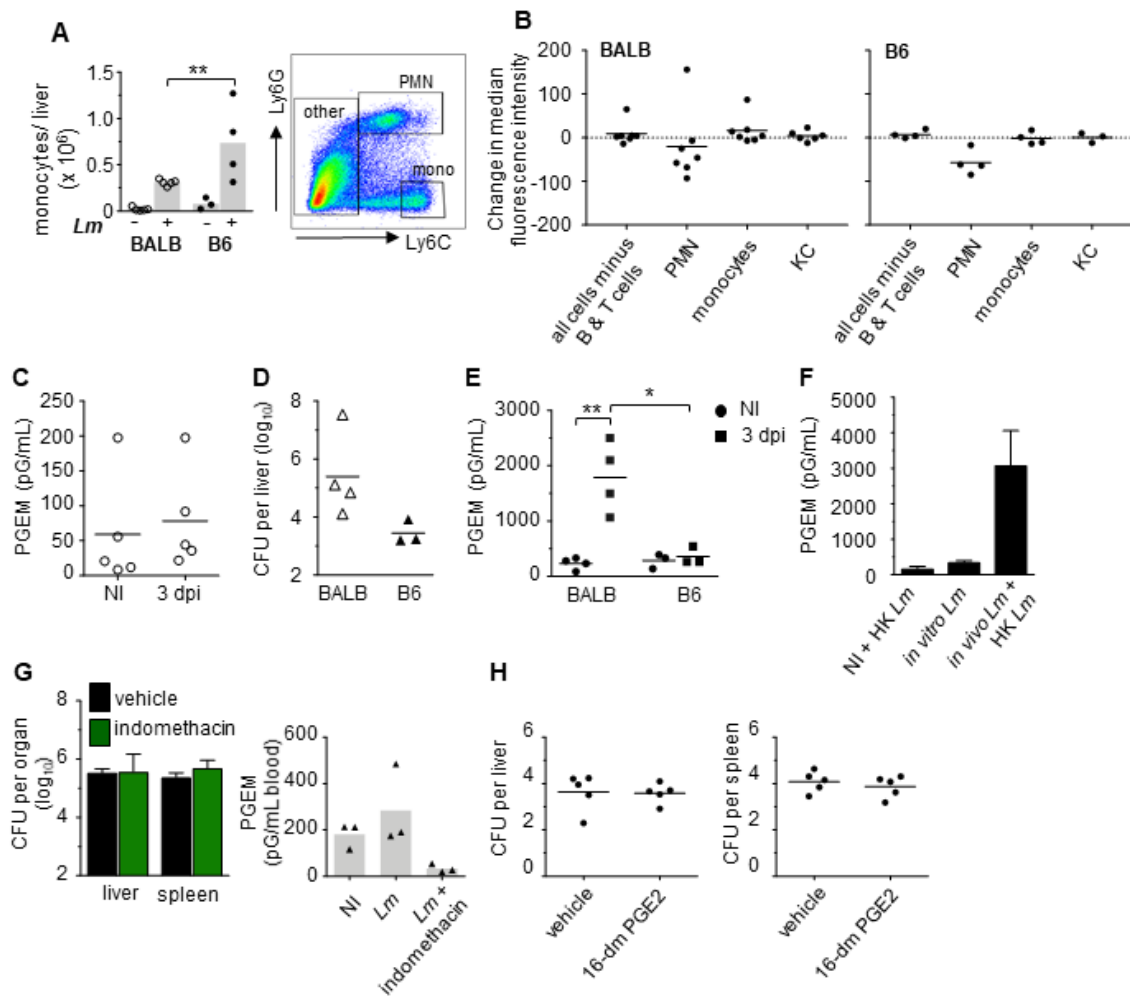
Figure 5.2 *In vivo Lm* **infection stimulates PGE2 secretion from liver non-parenchymal cells**
BALB and B6 female mice were fed 5 x 10^8 CFU *Lm* SD2000 and livers were harvested 3 dpi
following collagenase perfusion. (A) Left- Monocyte infiltrate in the livers of uninfected (-) or
infected (+) mice. Each symbol represents one mouse; three pooled experiments are shown.
Right- an example of a typical FACS profile of liver non-parenchymal cells is shown. Live,
singlet, and CD45+ gates were incorporated prior to applying Ly6G and Ly6C gating. (B) Liver
non-parenchymal cells were harvested from infected mice and stained for markers of B and T
lymphocytes, PMN, monocytes, and Kupffer cells (KC). COX-2 median fluorescence intensity is
shown as change compared to uninfected cells. Each symbol represents one mouse; three pooled
experiments are shown. (C) Prostaglandin E Metabolite (PGEM) was measured from supernatant
of clarified BALB liver homogenates. Pooled results from two experiments are shown. (D, E)
Livers were harvested from infected mice after perfusion and collagenase digestion. CFU burden

was determined from a portion of cells prior to depletion of hepatocytes (D) and the remainder was cultured overnight at 37°C in 7% CO_2 for determination of secreted PGE2 (E). Pooled results from three independent experiments; n=1-2 mice per repeat are shown. (F) Non-parenchymal cells from uninfected or infected BALB livers were stimulated by exposure to heat-killed, sonicated *Lm* or infected *in vitro*. (G) BALB females were treated with indomethacin every 12h beginning 24 hpi. Organs and blood were harvested at 72 hpi. (H) Female B6 mice were treated with 16,16 dmPGE2 once daily beginning immediately after infection and organs were harvested at 4 dpi. Results from one experiment are shown, bars indicate mean +/- SD.
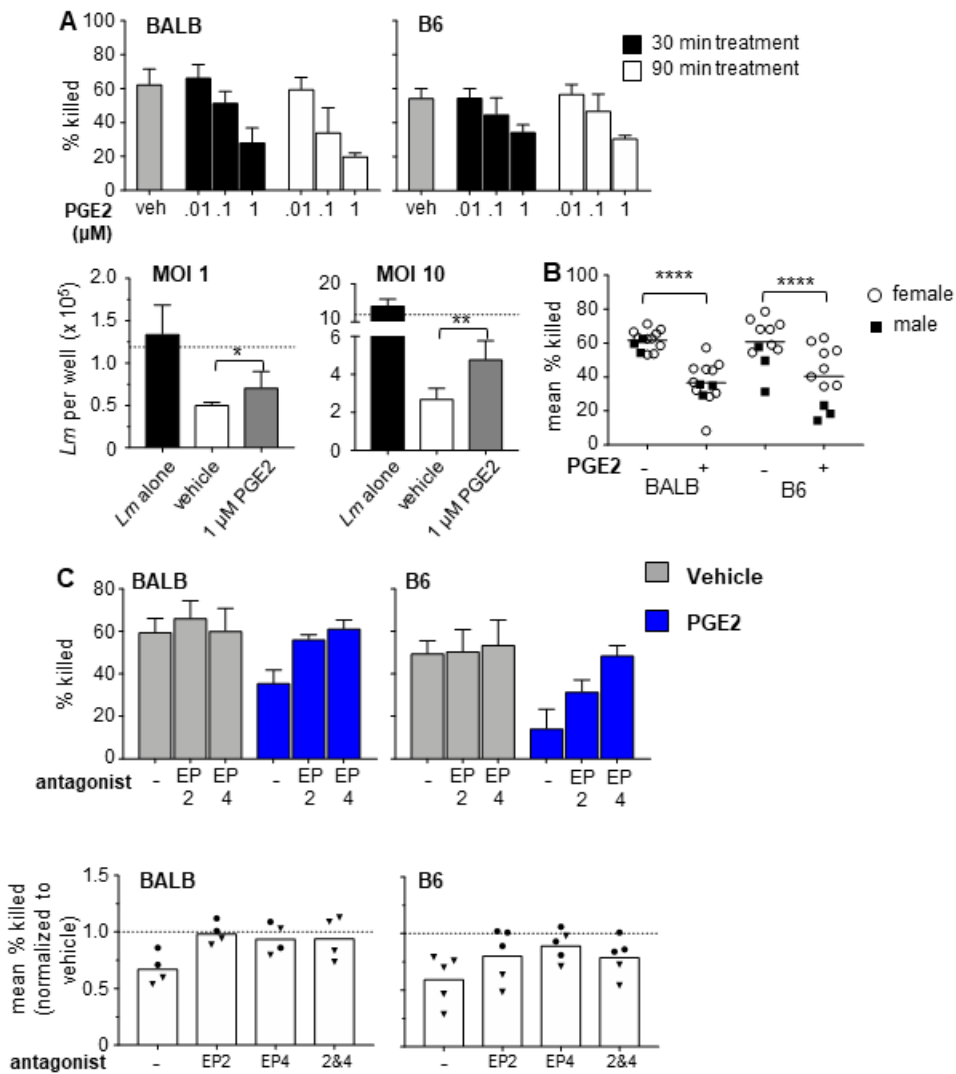
Figure 5.3 PGE2 pretreatment results in a dose-dependent loss of killing efficiency in murine PMN

(A) BALB/c and B6 PMN were incubated with the indicated concentrations of PGE2 for 30 or 90 min. before 50 min incubation with *Lm* (MOI=1).   Representative results; n=4 replicates per treatment, are shown. Bars indicate mean +/- SD. Below this, the number of CFU per well are shown for one representative experiment in which *Lm* (MOI=1 or 10) were either incubated for 50 min alone to measure growth, with PMN that had received vehicle treatment, or with PMN that were pretreated with 1μM PGE2. Dotted line indicates initial inoculum. Representative results are shown for one of two independent experiments; n=5 technical replicates per treatment, bars indicate mean +/- SD. (B) Pooled results are shown for experiments where PMN were incubated with 1 μM PGE2 for 60-90 min. Each symbol represents the mean for one experiment.

(C) (Top) BALB and B6 PMN were incubated with 1 uM PGE2 concurrently with 100 nM EP-2 antagonist PF-04418948 or EP4-antagonist L-161,982 prior to addition of *Lm* (MOI=1). Representative results for a killing assay are shown; n=3 technical replicates per treatment. Bars indicate mean +/- SD. (Bottom) Pooled, normalized results for three independent experiments with three technical replicates per treatment are shown. Each symbol represents the mean of one experiment.
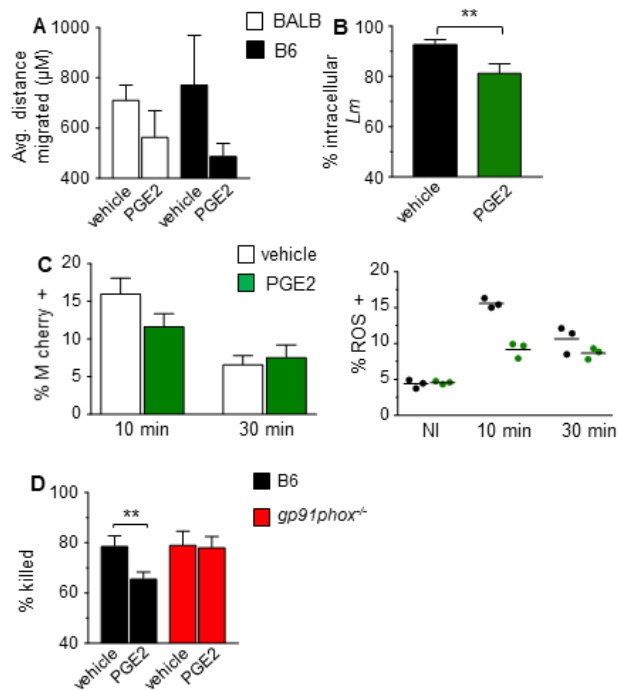
Figure 5.4 PGE2 exerts pleiotropic effects on PMN function

(A) Gradient enriched PMN were suspended in media containing 1 uM PGE2, incubated for 5 min, and applied to an under-agarose assay with 1000 nM LTB4 as the attractant in a well that was 1mM away from the wells containing cells. Results from one experiment are shown; n= 4 technical replicates per treatment. (B) FACS-sorted BALB/c PMN were incubated in 1 μM PGE2 for 90 min prior to addition of *Lm* SD2710. Percent of cell-associated bacteria at 10 mpi found intracellularly using in/out staining is shown. Results from one experiment are shown; n=3 technical replicates per treatment. (C) FACS-sorted PMN were incubated in 1 μM PGE2 for 90 min prior to addition of DHR and M-cherry expressing *Lm*. Percent of PMN positive for M-cherry at 10 and 30 mpi is shown on the left, and percent of ROS+ cells is shown on the right. Representative results for one of two experiments are shown (D) Bone marrow PMN from B6 and gp91*phox*^{-/-} mice were sorted, exposed to 1 μM PGE2 for 90 min, and then incubated with *Lm*. Percent of inoculum killed at 50 mpi is shown; n=5 technical replicates per treatment, representative results from one of two experiments. In all cases, bars indicate mean +/- SD.

6.   Discussion, conclusions, and future directions

Listeriosis in humans is lethal in approximately 25% of all diagnosed cases (12, 13), yet surprisingly little is known about its natural course of infection. Some of this is due to listeriosis being a relatively "new" recognized disease. In fact, although the bacterium was described in 1926 (244) and there were periodic outbreaks of illness attributed to foodstuffs, research on *Lm* as a serious human pathogen did not begin until the mid-1980s.   For years, however, *Lm* was used as a tool for immunology discovery rather than studied as an important foodborne pathogen. *Lm* has been considered a model intracellular pathogen for years, and intravenous infection of mice with *Lm* has yielded results that are now pillars of immunology and pathogenesis knowledge. Much of what we now know regarding how intracellular bacteria invade cells and escape phagosomal killing, as well as the necessity of IFNγ for clearance of intracellular bacteria can be attributed to use of *Lm.*

Intravenous infection has also been a method used to skirt the problem that mice are not a natural host for *Lm*. Doses in excess of 10^{10} *Lm* could be given to wild type mice via gavage with no impact on survival (29), while significantly lower doses of ~10^3-10^4 bacteria were required to observe liver and spleen invasion and even rapid death using intravenous inoculation (46, 212) This was because of a single amino acid mismatch between a key virulence determinant needed for entry of non-phagocytic cells, InlA, and E-cadherin, its receptor on enterocytes (30). To improve the efficiency of murine infection by the oral route, Lecuit et al. created a "humanized" mouse expressing enterocyte-restricted human E-cadherin (29) and later Wollert et al. created a "murinized" version of InlA, termed "InlA^m" (58). These groups and many others, however, still used gavage, a sometimes-traumatic method by which bacteria are delivered directly to the stomach, for infections. When Bou Ghanem et al. later developed a method of foodborne transmission of *Lm* in mice, InlA was not found to be required to establish intestinal infection, but

InlA^m enhanced persistence in the underlying intestinal tissue and spread to the mesenteric lymph nodes (35).

Still, however, little of the pathway from the stomach to the intestinal lamina propria to the extra-intestinal organs has been explained. Melton-Witt et al. orally infected guinea pigs with tagged *Lm* clones and used mathematical modeling to conclude that only approximately 1 in 10^6 *Lm* will invade the intestinal epithelium (72). Becattini et al. recently showed that in mice with a healthy microbiota, *Lm* was significantly less able to invade and disseminate to other organs than in mice which had received antibiotic treatment, indicating an important role for intestinal microbiota and their products in protection against pathogenic bacteria (181). These data indicate that very low numbers of *Lm* will be able to successfully pass through the cadre of immune cells waiting in the lamina propria and subsequently be transported to the liver and spleen. Despite encountering multiple barriers to invasion and dissemination bottlenecks, *Lm* causes very serious disease when it overcomes initial barriers. Thus, it is important to understand how dissemination occurs and the host immune responses that occur at each step of the pathway.

The area that I chose to focus on for my dissertation work was host immune responses, first in the spleen and then in the liver. Much is known about how intravenously inoculated *Lm* are taken up by the liver and spleen (64, 76, 78), but relatively little has been determined regarding the immune responses that are triggered when (presumably) small numbers of stress-adapted bacteria arrive to these organs after foodborne infection. Apart from the clear necessity for IFNγ for *Lm* clearance, even less is known about what local and systemic mediators are induced by dissemination of foodborne bacteria and how these mediators influence the course of infection. Some of these mediators can have opposing effects depending on their timing, tissue, and stimulus, which could be important as a pathogen like *Lm* moves slowly out of the intestine and into the peripheral organs. Therefore, chose to examine type I IFN and PGE2, two mediators

more classically-known as pro-inflammatory but which had previously been shown to have anti-inflammatory roles in certain tissues and environments.

Initially, I focused on the "type I IFN response" to *Lm* in the spleen, a phenotype that was first observed when IFNAR1$^{-/-}$ mice were found to be more resistant to intravenous *Lm* infection than their wild type counterparts (142, 143, 145). Later however, another group concluded that type I IFN signaling was necessary for defense against *Lm* infection after intragastric inoculation of *Lm* LO28, a strain that causes hyper-induction of IFNβ secretion (126, 189). Much of the resistance phenotype found after i.v. infection was attributed to IFNα/β-dependent downregulation of IFNγR1, which was thought to decrease macrophage activation (83). The results presented in chapter three, however, suggest that type I IFN is inconsequential in the course of foodborne listeriosis. This work showed that IFNAR1$^{-/-}$ mice were not resistant to foodborne *Lm* infection in comparison to wild type B6 controls and that little, if any, type I IFN was produced in the spleen after foodborne infection. Importantly, this work also showed that downregulation of the IFNγ receptor was a consequence of infection, rather than a consequence of type I IFN signaling. It seems likely that during the course of infection, IFNγ is naturally secreted and the receptor is simply internalized after binding its ligand. It is undisputed that type I IFN *can* cause downregulation of IFNGR1; however, this appears to only be of importance in high dose experimental i.v. infection thus far.

Overall, the results shown in chapter three indicate that while type I IFN can play an important role in the pathogenesis of *Lm* infection, its induction is strongly dependent on the route of infection. If work in the *Listeria* field were to move forward with type I IFN, it seems reasonable to ask if type I IFN is routinely found in samples from positively diagnosed patients. IFNα/β secretion is a part of innate immunity, however, meaning that it is produced early in the course of infection, therefore finding it in patients days to weeks after consumption of contaminated foods could prove difficult. The most relevant scenario might actually be maternal-

fetal transmission, which occurs via the bloodstream or invasion of the placenta. Interestingly, Cappelletti et al. recently found that stimulation of type I IFN signaling in pregnant mice induced preterm birth (245), suggesting that a pathogen that invades the placenta and causes robust IFNα/β signaling could be the cause of some miscarriages and spontaneous abortions.

PGE2 is a lipid mediator well-known for its roles in pain and fever; however emerging evidence has pointed to PGE2 as an anti-inflammatory compound in certain settings (152, 153, 162). I hypothesized that PGE2 played an anti-inflammatory role in the liver after foodborne infection by blunting the effector functions of PMN, which are recruited to the liver after infection and necessary for *Lm* clearance (53, 91, 93, 94). In turn, this lack of bacterial killing in the early phase of *Lm* colonization of the liver contributed significantly to the susceptibility observed in BALB mice, particularly in the liver. In order to understand how PGE2 affected PMN in the context of infection, it was necessary to first understand how PMN interacted with and killed *Lm.* This provided an opportunity to study PMN from both *Listeria*-susceptible BALB mice and resistant B6 mice and to determine if any key differences existed between PMN from these two strains. Most differences in susceptibility to intracellular bacteria between these two strains have been attributed to facets of innate immunity including differential secretion of IFNγ (48-50), yet the ability of PMN to directly kill *Lm* had not been examined. I hypothesized that PMN from both mice would kill *Lm* similarly, but that BALB PMN encountered a suppressive microenvironment in the liver, thus blunting their normally highly bactericidal effector functions. Mouse PMN are not routinely used in studies of bacteria-PMN interactions, both because PMN are easily obtained from human blood samples as well as because of perceived differences between murine and human PMN. The results shown in chapter 4 suggest that for pathogens which elicit a strong PMN response such as *Francisella tularensis* and *Streptococcus pyogenes*, studies using mouse bone marrow PMN would provide useful information on how these pathogens are killed by or evade PMN killing. In particular, *Francisella tularensis*, another

intracellular pathogen, elicits a robust PMN response to the lungs but is also one of the few

pathogens known to parasitize PMN (for a review, see Allen, L.A. 2016, *Frontiers in Cellular*

and Infection Microbiology). The *Francisella* field has also undergone some of the same

evolution of knowledge regarding the necessity for PMN in early clearance as *Listeria* has. With

the knowledge that mouse bone marrow PMN are relatively long-lived an amenable to sorting

and other manipulations, it would be worthwhile to understand how the functional "age" (i.e.

relatively young bone marrow PMN vs "older" circulating PMN) and activation markers affect

this unusual phenotype.

With regard to continuing this research line with *Listeria*, the possibilities are almost

endless. Understanding how the tissue microenvironment affects PMN expression of homing

markers CXCR1, CXCR2, receptors for leukotriene B4, and the formyl peptide receptors should

be of foremost importance, as PMN are needed for clearance but also contribute to tissue damage

in listeriosis. The under-agarose assay is a crude measure of chemotaxis, and other, more

sophisticated methods should be considered including simple microfluidic assays. Although it

provided a useful measure of movement, the under-agarose assay lacks the ability to control for

the weight of the agarose or small variations in the thickness and purity of the agarose that could

impede movement. I was also unable to verify *Listeria*-specific chemotaxis, as the

chemoattractant used in these assays must be able to rapidly diffuse into the agarose to create a

concentration gradient. Use of purified liver PMN rather than bone marrow PMN to assess

chemotaxis would also improve the physiological relevance of this data; however, this will

require a method to cleanly extract PMN from the liver, however, without inadvertently providing

activation or apoptosis signals.

Although it provided the data necessary to answer the question at hand, Figure 4.4 also

raises some interesting questions also that should be answered in the future. In Figure 4.4C, a

very small percentage of inoculated bacteria are intracellular at 25 mpi. This in itself is not

impressive, as PMN are likely to initiate killing mechanisms nearly as soon as the phagocytic vacuole closes, thus most of the bacteria phagocytosed early were already degraded. The time points after this, though, show that the number of intracellular bacteria remains low but steady, suggesting some level of survival inside PMN. Importantly, however, the cells used in these two assays were gradient-enriched, meaning that a significant percentage of the cells were not PMN and could potentially allow *Lm* to exist or grow. A follow-up experiment to this should include sorted PMN and time points of 15 min-2 hr after inoculation.

The role of PGE2 in *Lm* pathogenesis is potentially far more complex than that of type I IFN and is something that should be further explored. Even as it plays important roles in regulation of blood pressure, kidney function, and induction of IL-6 (173, 174, 246), PGE2 could be playing a pathogenic role in the progression of listeriosis. Most study of the effects of PGE2 has dealt with isolated capabilities of phagocytes, such as showing decreased phagocytosis, or a reduction in TNFα secretion (153, 177). Here, I attempted to look at the whole picture and hypothesized that PGE2 was secreted at high levels in the BALB liver after infection and was thereby able to decrease the killing efficiency of PMN recruited to this site of infection. A cartoon depicting the overall hypothesis for this research is depicted in Fig. 6.1. PMN are primary effector cells in a variety of situations, including listeriosis, tularemia, candidiasis, and even cuts and scrapes. If PMN exit the bone marrow able to effectively neutralize virulent bacteria, and then encounter a microenvironment that downregulates that ability to kill before they have done their job, it is almost certain that this decreased capability will be apparent in higher disease burdens. Likewise, PMN have to be controlled so as to prevent inadvertent tissue damage as a result of their many methods of neutralizing bacteria. This could be of special importance in cases of immune compromise, where eicosanoid secretion is likely to be dysregulated already.

I found that PGE2 was both produced at higher levels by liver cells from susceptible BALB animals than from B6 animals and that PGE2 effectively down-modulated the killing efficiency of unprimed bone marrow PMN. These results are supportive of numerous other reports showing inhibition of cell functions such as phagocytosis in macrophages and decreased production of ROS in PMN (153, 177), but to the best of my knowledge, this is the first report of PGE2 exposure decreasing the ability of any cell to kill a pathogenic bacterium. The especially intriguing part of these results, however, may be that PGE2 did not just have one effect on PMN. Instead, these data suggest that PGE2 may modulate PMN motility, internalization of bacteria, and production of reactive oxygen species. These may all represent a target for therapeutic intervention in the liver and beyond as we look for ways to augment human immunity to disease without the use of antibiotics.

This research could be taken in several different directions. The connection of PGE2 secretion to aging and susceptibility to listeriosis should be more fully explored in particular. Experiments could include PMN behavior tracking using bone marrow from aged mice, foodborne infection of aged mice, and blood samples from elderly human donors. Given the known roles for PGE2 in aging and inflammation, I would hypothesize that PMN from elderly samples are sensitive to the effects of PGE2 and are less able to migrate toward and kill bacteria than PMN from young samples.

The best way to elucidate the effects of PGE2 on PMN function in the context of the liver might actually be an adoptive transfer. PMN could be antibody depleted from BALB/c mice and PMN from congenic mice adoptively transferred in at the time of infection. The time course of foodborne infection along with PMN recruitment to the liver might present some challenges, but performing this experiment using i.v infection would yield some context as to whether further efforts should be undertaken to do the depletion for foodborne infection or not.

The idea presented by Levy et al. of an "eicosanoid switch" (160) should also be explored. Are PMN in the liver, in the presence of high levels of PGE2, induced to secrete lipoxin A4, thus resulting in resolution of PMN swarming? Does "resolution" happen before it should, or do B6 mice resolve PMN-mediated inflammation early on, thus alleviating the prospect of tissue damage? A first step in these experiments would be to sort PMN and treat with PGE2 for 6-8 hours before assessing killing ability. I would hypothesize that a very long exposure to PGE2, possibly with "boosters" would result in severe down regulation of PMN chemotaxis and killing, coinciding with increased transcription of 15-lipoxygenase. Following this set of experiments, lipoxin A4 could be measured by EIA and also added exogenously.

Much of the immune response to foodborne bacteria remains underexplored. Overall, the results presented in these chapters suggest that immune mediators during foodborne infection can have very different roles given unique stimuli, tissue environments, and timing. More so than any other infection route, infections acquired from consumption of contaminated foods are likely to cause unique immune responses in multiple areas of the host as they disseminate and colonize their preferred tissues. Future study of foodborne infections should take into account the unique role of local and systemic mediators not traditionally considered to be a major factor in bacterial pathogenesis.
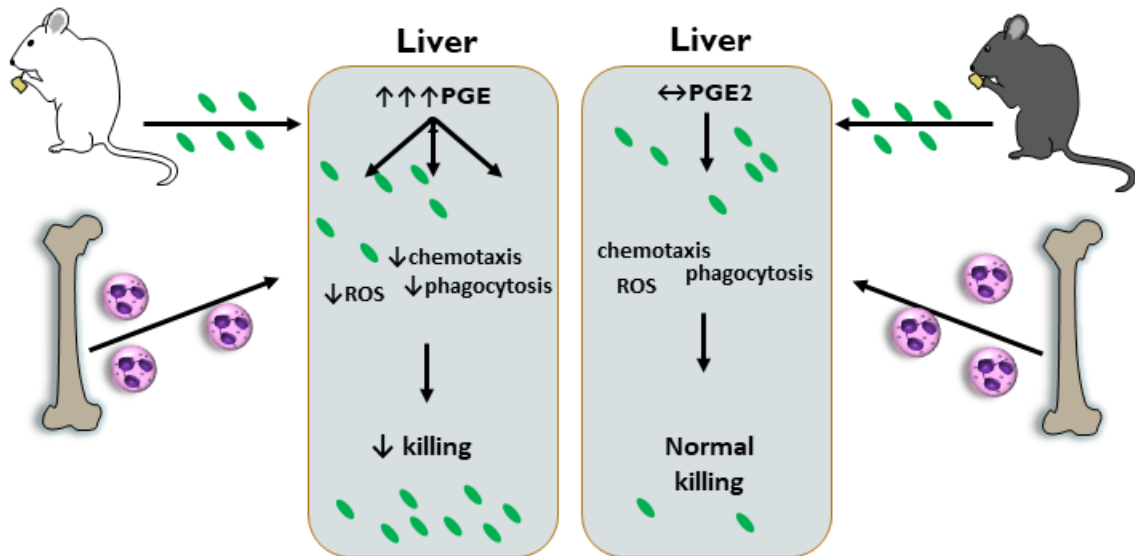
Figure 6.1 Hypothesis: Overproduction of PGE2 in the BALB liver decreases PMN killing efficiency

BALB and B6 mice both consume *Lm*, which invades the intestine and disseminates to the liver in similar numbers in both mice. The bacterial insult triggers recruitment of PMN to the livers of both mice that emerge from the bone marrow similarly able to kill bacteria In the BALB mouse, however, the arrival of the bacteria triggers overproduction of PGE2 that is not observed in the B6 mouse. This PGE2 then causes a reduction in multiple parameters of PMN function, leading to a decrease in overall PMN killing efficiency in the BALB liver.

Appendix I: List of abbreviations

AMP/ c-di-AMP= adenosine monophosphate/ cyclic-di-adenosine monophosphate

BALB/ BA= BALBcBy/J mouse, a strain of mouse that is susceptible to *Listeria* infection

B6= C57BL/6J mouse, a strain of mouse that is relatively resistant to *Listeria* infection

BHI= brain heart infusion (broth or agar)

CD (e.g. CD4, CD86)= cluster of differentiation

CFU= colony forming units

COX-2= cyclooxygenase enzyme 2

DHR= dihydrorhodamine 123

DNA= deoxyribonucleic acid

dpi= days post infection

EIA= enzyme immunoassay

ELISA= enzyme-linked immunosorbent assay

FACS= fluorescence activated cell sorting

hpi= hours post infection

IFN= interferon

IFNAR= interferon alpha/beta receptor

IFNγR= interferon gamma receptor

i.g.= intragastric

Inl (A/B)= internalin

KC= Kupffer cell

IL= interleukin

i.p.= intraperitoneal

i.v.= intravenous

JAK= Janus kinase

Lm = Listeria monocytogenes

LO/ LOX= lipoxygenase

LSEC= liver sinusoidal endothelial cell

LTB4= leukotriene B4

M= molar (micro, nano)

mΦ= macrophage

MAPK= mitogen-activated protein kinase

MFI= mean fluorescence intensity

MHC= major histocompatibility complex

mPGES= microsomal prostaglandin E synthase

mpi= minutes post infection

NI= not infected

NK cell= natural killer cell

NSAID= non-steroidal anti-inflammatory drug

PG/ PGE2= prostaglandin/ prostaglandin E2

PLA2= phospholipase A2

PMN= neutrophil polymorphonuclear leukocyte

PrfA= positive regulatory factor A

RNA= ribonucleic acid

ROS= reactive oxygen species

SD= standard deviation

STAT= signal transducer and activator of transcription

STING= stimulator of interferon-related genes

TLR= toll-like receptor

TRAIL= tumor necrosis factor alpha apoptosis-inducing ligand

TNFα= tumor necrosis factor alpha

TYK= tyrosine kinase

UTR= untranslated region

VCAM= vascular cell adhesion molecule

VLA4= very late antigen 4

WT= wild-type

α= alpha

β= beta

Δ= delta, deletion

γ= gamma

κ= kappa

μ= micro

σ= sigma

References

1.	Welshimer HJ, Donker-Voet J. 1971. Listeria monocytogenes in nature. Appl Microbiol 21:516-9.

2.	Locatelli A, Spor A, Jolivet C, Piveteau P, Hartmann A. 2013. Biotic and abiotic soil properties influence survival of Listeria monocytogenes in soil. PLoS One 8:e75969.

3.	Maury MM, Tsai YH, Charlier C, Touchon M, Chenal-Francisque V, Leclercq A, Criscuolo A, Gaultier C, Roussel S, Brisabois A, Disson O, Rocha EPC, Brisse S, Lecuit M. 2016. Uncovering Listeria monocytogenes hypervirulence by harnessing its biodiversity. Nat Genet 48:308-313.

4.	Grif K, Patscheider G, Dierich MP, Allerberger F. 2003. Incidence of fecal carriage of Listeria monocytogenes in three healthy volunteers: a one-year prospective stool survey. Eur J Clin Microbiol Infect Dis 22:16-20.

5.	Beach C. 2018. South African agency 99.99 percent sure of Listeria source. http://www.foodsafetynews.com/2018/04/south-african-agency-99-99-percent-sure-of-listeria-source/#.WsbcoogbPIW. Accessed April 5, 2018.

6.	Administration USFaD. April 17, 2017 2017. Summary of Recall Cases in Calendar Year 2016. https://www.fsis.usda.gov/wps/portal/fsis/topics/recalls-and-public-health-alerts/recall-summaries. Accessed Sept. 07.

7.	Prevention CfDCa. July 15, 2016 2016. Multistate Outbreak of Listeriosis Linked to Frozen Vegetables (Final Update). https://www.cdc.gov/listeria/outbreaks/frozen-vegetables-05-16/index.html. Accessed Sept 07.

8.	Prevention CfDCa. July 13, 2015 2015. Multistate Outbreak of Listeriosis Linked to Blue Bell Creameries Products (Final Update). https://www.cdc.gov/listeria/outbreaks/ice-cream-03-15/index.html. Accessed Sept 07.

9.	Allerberger F, Wagner M. 2010. Listeriosis: a resurgent foodborne infection. Clin Microbiol Infect 16:16-23.

10.	Scharff RL. 2012. Economic burden from health losses due to foodborne illness in the United States. J Food Prot 75:123-31.

11.   Charlier C, Perrodeau E, Leclercq A, Cazenave B, Pilmis B, Henry B, Lopes A, Maury MM, Moura A, Goffinet F, Dieye HB, Thouvenot P, Ungeheuer MN, Tourdjman M, Goulet V, de Valk H, Lortholary O, Ravaud P, Lecuit M, group Ms. 2017. Clinical features and prognostic factors of listeriosis: the MONALISA national prospective cohort study. Lancet Infect Dis 17:510-519.

12.   Prevention CfDCa. June 29, 2017 2017. Listeriosis: Information for Health Professionals and Laboratories. https://www.cdc.gov/listeria/technical.html. Accessed Sept 07 2017.

13.   de Noordhout CM, Devleesschauwer B, Angulo FJ, Verbeke G, Haagsma J, Kirk M, Havelaar A, Speybroeck N. 2014. The global burden of listeriosis: a systematic review and meta-analysis. Lancet Infect Dis 14:1073-1082.

14.   Pouillot R, Klontz KC, Chen Y, Burall LS, Macarisin D, Doyle M, Bally KM, Strain E, Datta AR, Hammack TS, Van Doren JM. 2016. Infectious Dose of Listeria monocytogenes in Outbreak Linked to Ice Cream, United States, 2015. Emerg Infect Dis 22:2113-2119.

15.   Farber JM, Ross WH, Harwig J. 1996. Health risk assessment of Listeria monocytogenes in Canada. Int J Food Microbiol 30:145-56.

16.   Goulet V, King LA, Vaillant V, de Valk H. 2013. What is the incubation period for listeriosis? BMC Infect Dis 13:11.

17.   Welshimer HJ. 1960. Survival of Listeria monocytogenes in soil. J Bacteriol 80:316-20.

18.   Mengaud J, Dramsi S, Gouin E, Vazquez-Boland JA, Milon G, Cossart P. 1991. Pleiotropic control of Listeria monocytogenes virulence factors by a gene that is autoregulated. Mol Microbiol 5:2273-83.

19.   Wiedmann M, Arvik TJ, Hurley RJ, Boor KJ. 1998. General stress transcription factor sigmaB and its role in acid tolerance and virulence of Listeria monocytogenes. J Bacteriol 180:3650-6.

20.   Johansson J, Mandin P, Renzoni A, Chiaruttini C, Springer M, Cossart P. 2002. An RNA thermosensor controls expression of virulence genes in Listeria monocytogenes. Cell 110:551-61.

21.   de las Heras A, Cain RJ, Bielecka MK, Vazquez-Boland JA. 2011. Regulation of Listeria virulence: PrfA master and commander. Curr Opin Microbiol 14:118-27.

22.   Portnoy DA, Jacks PS, Hinrichs DJ. 1988. Role of hemolysin for the intracellular growth of Listeria monocytogenes. J Exp Med 167:1459-71.

23.   Nadon CA, Bowen BM, Wiedmann M, Boor KJ. 2002. Sigma B contributes to PrfA-mediated virulence in Listeria monocytogenes. Infect Immun 70:3948-52.

24.   Gaillard JL, Berche P, Frehel C, Gouin E, Cossart P. 1991. Entry of L. monocytogenes into cells is mediated by internalin, a repeat protein reminiscent of surface antigens from gram-positive cocci. Cell 65:1127-41.

25.   Lecuit M, Ohayon H, Braun L, Mengaud J, Cossart P. 1997. Internalin of Listeria monocytogenes with an intact leucine-rich repeat region is sufficient to promote internalization. Infect Immun 65:5309-19.

26.   Mengaud J, Lecuit M, Lebrun M, Nato F, Mazie JC, Cossart P. 1996. Antibodies to the leucine-rich repeat region of internalin block entry of Listeria monocytogenes into cells expressing E-cadherin. Infect Immun 64:5430-3.

27.   Mengaud J, Ohayon H, Gounon P, Mege RM, Cossart P. 1996. E-cadherin is the receptor for internalin, a surface protein required for entry of L. monocytogenes into epithelial cells. Cell 84:923-32.

28.   Pentecost M, Otto G, Theriot JA, Amieva MR. 2006. Listeria monocytogenes invades the epithelial junctions at sites of cell extrusion. PLoS Pathog 2:e3.

29.   Lecuit M, Vandormael-Pournin S, Lefort J, Huerre M, Gounon P, Dupuy C, Babinet C, Cossart P. 2001. A transgenic model for listeriosis: role of internalin in crossing the intestinal barrier. Science 292:1722-5.

30.   Lecuit M, Dramsi S, Gottardi C, Fedor-Chaiken M, Gumbiner B, Cossart P. 1999. A single amino acid in E-cadherin responsible for host specificity towards the human pathogen Listeria monocytogenes. EMBO J 18:3956-63.

31.   Bierne H, Cossart P. 2002. InlB, a surface protein of Listeria monocytogenes that behaves as an invasin and a growth factor. J Cell Sci 115:3357-67.

32.   Cossart P, Lecuit M. 1998. Interactions of Listeria monocytogenes with mammalian cells during entry and actin-based movement: bacterial factors, cellular ligands and signaling. EMBO J 17:3797-806.

33.   Gregory SH, Sagnimeni AJ, Wing EJ. 1996. Expression of the inlAB operon by Listeria monocytogenes is not required for entry into hepatic cells in vivo. Infect Immun 64:3983-6.

34.   Bierne H, Mazmanian SK, Trost M, Pucciarelli MG, Liu G, Dehoux P, Jansch L, Garcia-del Portillo F, Schneewind O, Cossart P, European Listeria Genome C. 2002. Inactivation of the srtA gene in Listeria monocytogenes inhibits anchoring of surface proteins and affects virulence. Mol Microbiol 43:869-81.

35.   Bou Ghanem EN, Jones GS, Myers-Morales T, Patil PD, Hidayatullah AN, D'Orazio SE. 2012. InlA promotes dissemination of Listeria monocytogenes to the mesenteric lymph nodes during food borne infection of mice. PLoS Pathog 8:e1003015.

36.   Corr S, Hill C, Gahan CG. 2006. An in vitro cell-culture model demonstrates internalin- and hemolysin-independent translocation of Listeria monocytogenes across M cells. Microb Pathog 41:241-50.

37.   Drolia R, Tenguria S, Durkes AC, Turner JR, Bhunia AK. 2018. Listeria Adhesion Protein Induces Intestinal Epithelial Barrier Dysfunction for Bacterial Translocation. Cell Host Microbe doi:10.1016/j.chom.2018.03.004.

38.   Bielecki J, Youngman P, Connelly P, Portnoy DA. 1990. Bacillus subtilis expressing a haemolysin gene from Listeria monocytogenes can grow in mammalian cells. Nature 345:175-6.

39.   Gaillard JL, Berche P, Sansonetti P. 1986. Transposon mutagenesis as a tool to study the role of hemolysin in the virulence of Listeria monocytogenes. Infect Immun 52:50-5.

40.   Camilli A, Goldfine H, Portnoy DA. 1991. Listeria monocytogenes mutants lacking phosphatidylinositol-specific phospholipase C are avirulent. J Exp Med 173:751-4.

41.   Smith GA, Marquis H, Jones S, Johnston NC, Portnoy DA, Goldfine H. 1995. The two distinct phospholipases C of Listeria monocytogenes have overlapping roles in escape from a vacuole and cell-to-cell spread. Infect Immun 63:4231-7.

42.   Lam GY, Fattouh R, Muise AM, Grinstein S, Higgins DE, Brumell JH. 2011. Listeriolysin O suppresses phospholipase C-mediated activation of the microbicidal NADPH oxidase to promote Listeria monocytogenes infection. Cell Host Microbe 10:627-34.

43.   Kocks C, Gouin E, Tabouret M, Berche P, Ohayon H, Cossart P. 1992. L. monocytogenes-induced actin assembly requires the actA gene product, a surface protein. Cell 68:521-31.

44.   Tilney LG, Portnoy DA. 1989. Actin filaments and the growth, movement, and spread of the intracellular bacterial parasite, Listeria monocytogenes. J Cell Biol 109:1597-608.

45.   Cheers C, McKenzie IF. 1978. Resistance and susceptibility of mice to bacterial infection: genetics of listeriosis. Infect Immun 19:755-62.

46.   Cheers C, McKenzie IF, Pavlov H, Waid C, York J. 1978. Resistance and susceptibility of mice to bacterial infection: course of listeriosis in resistant or susceptible mice. Infect Immun 19:763-70.

47. Liu T, Nishimura H, Matsuguchi T, Yoshikai Y. 2000. Differences in interleukin-12 and -15 production by dendritic cells at the early stage of Listeria monocytogenes infection between BALB/c and C57 BL/6 mice. Cell Immunol 202:31-40.

48. Watanabe H, Numata K, Ito T, Takagi K, Matsukawa A. 2004. Innate immune response in Th1- and Th2-dominant mouse strains. Shock 22:460-6.

49. Bou Ghanem EN, Nelson CC, D'Orazio SE. 2011. T cell-intrinsic factors contribute to the differential ability of CD8+ T cells to rapidly secrete IFN-gamma in the absence of antigen. J Immunol 186:1703-12.

50. Kuroda E, Kito T, Yamashita U. 2002. Reduced expression of STAT4 and IFN-gamma in macrophages from BALB/c mice. J Immunol 168:5477-82.

51. Plant J, Glynn AA. 1974. Natural resistance to Salmonella infection, delayed hypersensitivity and Ir genes in different strains of mice. Nature 248:345-7.

52. Gervais F, Stevenson M, Skamene E. 1984. Genetic control of resistance to Listeria monocytogenes: regulation of leukocyte inflammatory responses by the Hc locus. J Immunol 132:2078-83.

53. Boyartchuk VL, Broman KW, Mosher RE, D'Orazio SE, Starnbach MN, Dietrich WF. 2001. Multigenic control of Listeria monocytogenes susceptibility in mice. Nat Genet 27:259-60.

54. Qi Z, Wang J, Han X, Yang J, Zhao G, Cao Y. 2014. Listr1 locus regulates innate immunity against Listeria monocytogenes infection in the mouse liver possibly through Cxcl11 polymorphism. Immunogenetics 66:231-42.

55. Wang N, Elso CM, Mackin L, Mannering SI, Strugnell RA, Wijburg OL, Brodnicki TC. 2014. Congenic mice reveal genetic epistasis and overlapping disease loci for autoimmune diabetes and listeriosis. Immunogenetics 66:501-6.

56. Pasche B, Kalaydjiev S, Franz TJ, Kremmer E, Gailus-Durner V, Fuchs H, Hrabe de Angelis M, Lengeling A, Busch DH. 2005. Sex-dependent susceptibility to Listeria monocytogenes infection is mediated by differential interleukin-10 production. Infect Immun 73:5952-60.

57. D'Orazio SE. 2014. Animal models for oral transmission of Listeria monocytogenes. Front Cell Infect Microbiol 4:15.

58. Wollert T, Pasche B, Rochon M, Deppenmeier S, van den Heuvel J, Gruber AD, Heinz DW, Lengeling A, Schubert WD. 2007. Extending the host range of Listeria monocytogenes by rational protein design. Cell 129:891-902.

59. Tsai YH, Disson O, Bierne H, Lecuit M. 2013. Murinization of internalin extends its receptor repertoire, altering Listeria monocytogenes cell tropism and host responses. PLoS Pathog 9:e1003381.

60. Alam MS, Costales M, Cavanaugh C, Pereira M, Gaines D, Williams K. 2016. Oral exposure to Listeria monocytogenes in aged IL-17RKO mice: A possible murine model to study listeriosis in susceptible populations. Microb Pathog 99:236-246.

61. Jones GS, Bussell KM, Myers-Morales T, Fieldhouse AM, Bou Ghanem EN, D'Orazio SEF. 2015. Intracellular Listeria monocytogenes comprise a minimal but vital fraction of the intestinal burden following foodborne infection. Infection and Immunity doi:10.1128/iai.00503-15.

62. Conlan JW, North RJ. 1991. Neutrophil-mediated dissolution of infected host cells as a defense strategy against a facultative intracellular bacterium. J Exp Med 174:741-4.

63. Gregory SH, Sagnimeni AJ, Wing EJ. 1996. Bacteria in the bloodstream are trapped in the liver and killed by immigrating neutrophils. J Immunol 157:2514-20.

64. Mackaness GB. 1962. Cellular resistance to infection. J Exp Med 116:381-406.

65. D'Orazio SE, Halme DG, Ploegh HL, Starnbach MN. 2003. Class Ia MHC-deficient BALB/c mice generate CD8+ T cell-mediated protective immunity against Listeria monocytogenes infection. J Immunol 171:291-8.

66. Pizarro-Cerda J, Kuhbacher A, Cossart P. 2012. Entry of Listeria monocytogenes in mammalian epithelial cells: an updated view. Cold Spring Harb Perspect Med 2.

67. Bortolussi R, Issekutz A, Faulkner G. 1986. Opsonization of Listeria monocytogenes type 4b by human adult and newborn sera. Infect Immun 52:493-8.

68. Bennett M, Baker EE. 1977. Marrow-dependent cell function in early stages of infection with Listeria monocytogenes. Cell Immunol 33:203-10.

69. Croize J, Arvieux J, Berche P, Colomb MG. 1993. Activation of the human complement alternative pathway by Listeria monocytogenes: evidence for direct binding and proteolysis of the C3 component on bacteria. Infect Immun 61:5134-9.

70. MacGowan AP, Peterson PK, Keane W, Quie PG. 1983. Human peritoneal macrophage phagocytic, killing, and chemiluminescent responses to opsonized Listeria monocytogenes. Infect Immun 40:440-3.

71. Hardy J, Francis KP, DeBoer M, Chu P, Gibbs K, Contag CH. 2004. Extracellular replication of Listeria monocytogenes in the murine gall bladder. Science 303:851-3.

72.   Melton-Witt JA, Rafelski SM, Portnoy DA, Bakardjiev AI. 2012. Oral infection with signature-tagged Listeria monocytogenes reveals organ-specific growth and dissemination routes in guinea pigs. Infect Immun 80:720-32.

73.   Glomski IJ, Decatur AL, Portnoy DA. 2003. Listeria monocytogenes mutants that fail to compartmentalize listerolysin O activity are cytotoxic, avirulent, and unable to evade host extracellular defenses. Infect Immun 71:6754-65.

74.   Jones GS, Bussell KM, Myers-Morales T, Fieldhouse AM, Bou Ghanem EN, D'Orazio SE. 2015. Intracellular Listeria monocytogenes comprises a minimal but vital fraction of the intestinal burden following foodborne infection. Infect Immun 83:3146-56.

75.   Jones GS, D'Orazio SE. 2017. Monocytes Are the Predominant Cell Type Associated with Listeria monocytogenes in the Gut, but They Do Not Serve as an Intracellular Growth Niche. J Immunol 198:2796-2804.

76.   Conlan JW. 1996. Early pathogenesis of Listeria monocytogenes infection in the mouse spleen. J Med Microbiol 44:295-302.

77.   O'Donnell H, Pham OH, Benoun JM, Ravesloot-Chavez MM, McSorley SJ. 2015. Contaminated water delivery as a simple and effective method of experimental Salmonella infection. Future Microbiol 10:1615-27.

78.   Conlan JW. 1999. Early host-pathogen interactions in the liver and spleen during systemic murine listeriosis: an overview. Immunobiology 201:178-87.

79.   Carrero JA, Calderon B, Unanue ER. 2006. Lymphocytes are detrimental during the early innate immune response against Listeria monocytogenes. J Exp Med 203:933-40.

80.   Bou Ghanem EN, McElroy DS, D'Orazio SE. 2009. Multiple mechanisms contribute to the robust rapid gamma interferon response by CD8+ T cells during Listeria monocytogenes infection. Infect Immun 77:1492-501.

81.   Berg RE, Cordes CJ, Forman J. 2002. Contribution of CD8+ T cells to innate immunity: IFN-gamma secretion induced by IL-12 and IL-18. Eur J Immunol 32:2807-16.

82.   Kearney SJ, Delgado C, Eshleman EM, Hill KK, O'Connor BP, Lenz LL. 2013. Type I IFNs Downregulate Myeloid Cell IFN-γ Receptor by Inducing Recruitment of an Early Growth Response 3/NGFI-A Binding Protein 1 Complex That Silences ifngr1 Transcription. The Journal of Immunology 191:3384-3392.

83.   Rayamajhi M, Humann J, Penheiter K, Andreasen K, Lenz LL. 2010. Induction of IFN-alphabeta enables Listeria monocytogenes to suppress macrophage activation by IFN-gamma. J Exp Med 207:327-37.

84.   Crispe IN. 2003. Hepatic T cells and liver tolerance. Nat Rev Immunol 3:51-62.

85. Ebe Y, Hasegawa G, Takatsuka H, Umezu H, Mitsuyama M, Arakawa M, Mukaida N, Naito M. 1999. The role of Kupffer cells and regulation of neutrophil migration into the liver by macrophage inflammatory protein-2 in primary listeriosis in mice. Pathol Int 49:519-32.

86. Jenne CN, Kubes P. 2013. Immune surveillance by the liver. Nat Immunol 14:996-1006.

87. Hyun Y-M, Hong C-W. 2017. Deep insight into neutrophil trafficking in various organs. Journal of Leukocyte Biology 102:617-629.

88. Holub M, Cheng CW, Mott S, Wintermeyer P, van Rooijen N, Gregory SH. 2009. Neutrophils sequestered in the liver suppress the proinflammatory response of Kupffer cells to systemic bacterial infection. J Immunol 183:3309-16.

89. Conlan JW, Dunn PL, North RJ. 1993. Leukocyte-mediated lysis of infected hepatocytes during listeriosis occurs in mice depleted of NK cells or CD4+ CD8+ Thy1.2+ T cells. Infect Immun 61:2703-7.

90. Rogers HW, Callery MP, Deck B, Unanue ER. 1996. Listeria monocytogenes induces apoptosis of infected hepatocytes. J Immunol 156:679-84.

91. Carr KD, Sieve AN, Indramohan M, Break TJ, Lee S, Berg RE. 2011. Specific depletion reveals a novel role for neutrophil-mediated protection in the liver during Listeria monocytogenes infection. Eur J Immunol 41:2666-76.

92. Leist M, Gantner F, Bohlinger I, Germann PG, Tiegs G, Wendel A. 1994. Murine hepatocyte apoptosis induced in vitro and in vivo by TNF-alpha requires transcriptional arrest. J Immunol 153:1778-88.

93. Conlan JW, North RJ. 1994. Neutrophils are essential for early anti-Listeria defense in the liver, but not in the spleen or peritoneal cavity, as revealed by a granulocyte-depleting monoclonal antibody. J Exp Med 179:259-68.

94. Conlan JW. 1997. Critical roles of neutrophils in host defense against experimental systemic infections of mice by Listeria monocytogenes, Salmonella typhimurium, and Yersinia enterocolitica. Infect Immun 65:630-5.

95. Czuprynski CJ, Brown JF, Maroushek N, Wagner RD, Steinberg H. 1994. Administration of anti-granulocyte mAb RB6-8C5 impairs the resistance of mice to Listeria monocytogenes infection. J Immunol 152:1836-46.

96. Czuprynski CJ, Theisen C, Brown JF. 1996. Treatment with the antigranulocyte monoclonal antibody RB6-8C5 impairs resistance of mice to gastrointestinal infection with Listeria monocytogenes. Infect Immun 64:3946-9.

97.   Rakhmilevich AL. 1995. Neutrophils are essential for resolution of primary and secondary infection with Listeria monocytogenes. J Leukoc Biol 57:827-31.

98.   Rogers HW, Unanue ER. 1993. Neutrophils are involved in acute, nonspecific resistance to Listeria monocytogenes in mice. Infect Immun 61:5090-6.

99.   Shi C, Hohl TM, Leiner I, Equinda MJ, Fan X, Pamer EG. 2011. Ly6G+ neutrophils are dispensable for defense against systemic Listeria monocytogenes infection. J Immunol 187:5293-8.

100.   Martin C, Burdon PC, Bridger G, Gutierrez-Ramos JC, Williams TJ, Rankin SM. 2003. Chemokines acting via CXCR2 and CXCR4 control the release of neutrophils from the bone marrow and their return following senescence. Immunity 19:583-93.

101.   Pillay J, den Braber I, Vrisekoop N, Kwast LM, de Boer RJ, Borghans JA, Tesselaar K, Koenderman L. 2010. In vivo labeling with 2H2O reveals a human neutrophil lifespan of 5.4 days. Blood 116:625-7.

102.   Furze RC, Rankin SM. 2008. Neutrophil mobilization and clearance in the bone marrow. Immunology 125:281-8.

103.   Meeks KD, Sieve AN, Kolls JK, Ghilardi N, Berg RE. 2009. IL-23 is required for protection against systemic infection with Listeria monocytogenes. J Immunol 183:8026-34.

104.   Hamada S, Umemura M, Shiono T, Tanaka K, Yahagi A, Begum MD, Oshiro K, Okamoto Y, Watanabe H, Kawakami K, Roark C, Born WK, O'Brien R, Ikuta K, Ishikawa H, Nakae S, Iwakura Y, Ohta T, Matsuzaki G. 2008. IL-17A produced by gammadelta T cells plays a critical role in innate immunity against listeria monocytogenes infection in the liver. J Immunol 181:3456-63.

105.   Henry T, Kirimanjeswara GS, Ruby T, Jones JW, Peng K, Perret M, Ho L, Sauer JD, Iwakura Y, Metzger DW, Monack DM. 2010. Type I IFN signaling constrains IL-17A/F secretion by gammadelta T cells during bacterial infections. J Immunol 184:3755-67.

106.   Ford-Hutchinson AW, Bray MA, Doig MV, Shipley ME, Smith MJ. 1980. Leukotriene B, a potent chemokinetic and aggregating substance released from polymorphonuclear leukocytes. Nature 286:264-5.

107.   Palmblad J, Malmsten CL, Uden AM, Radmark O, Engstedt L, Samuelsson B. 1981. Leukotriene B4 is a potent and stereospecific stimulator of neutrophil chemotaxis and adherence. Blood 58:658-61.

108. Lammermann T, Afonso PV, Angermann BR, Wang JM, Kastenmuller W, Parent CA, Germain RN. 2013. Neutrophil swarms require LTB4 and integrins at sites of cell death in vivo. Nature 498:371-5.

109. Reategui E, Jalali F, Khankhel AH, Wong E, Cho H, Lee J, Serhan CN, Dalli J, Elliott H, Irimia D. 2017. Microscale arrays for the profiling of start and stop signals coordinating human-neutrophil swarming. Nat Biomed Eng 1.

110. Gao JL, Lee EJ, Murphy PM. 1999. Impaired antibacterial host defense in mice lacking the N-formylpeptide receptor. J Exp Med 189:657-62.

111. Liu M, Chen K, Yoshimura T, Liu Y, Gong W, Wang A, Gao JL, Murphy PM, Wang JM. 2012. Formylpeptide receptors are critical for rapid neutrophil mobilization in host defense against Listeria monocytogenes. Sci Rep 2:786.

112. Southgate EL, He RL, Gao JL, Murphy PM, Nanamori M, Ye RD. 2008. Identification of formyl peptides from Listeria monocytogenes and Staphylococcus aureus as potent chemoattractants for mouse neutrophils. J Immunol 181:1429-37.

113. Doeing DC, Borowicz JL, Crockett ET. 2003. Gender dimorphism in differential peripheral blood leukocyte counts in mice using cardiac, tail, foot, and saphenous vein puncture methods. BMC Clin Pathol 3:3.

114. Boxio R, Bossenmeyer-Pourie C, Steinckwich N, Dournon C, Nusse O. 2004. Mouse bone marrow contains large numbers of functionally competent neutrophils. J Leukoc Biol 75:604-11.

115. Swamydas M, Lionakis MS. 2013. Isolation, purification and labeling of mouse bone marrow neutrophils for functional studies and adoptive transfer experiments. J Vis Exp doi:10.3791/50586:e50586.

116. Eisenhauer PB, Lehrer RI. 1992. Mouse neutrophils lack defensins. Infect Immun 60:3446-7.

117. Jones CN, Hoang AN, Martel JM, Dimisko L, Mikkola A, Inoue Y, Kuriyama N, Yamada M, Hamza B, Kaneki M, Warren HS, Brown DE, Irimia D. 2016. Microfluidic assay for precise measurements of mouse, rat, and human neutrophil chemotaxis in whole-blood droplets. J Leukoc Biol 100:241-7.

118. Heit B, Kubes P. 2003. Measuring chemotaxis and chemokinesis: the under-agarose cell migration assay. Sci STKE 2003:PL5.

119. Isaacs A, Lindenmann J, Valentine RC. 1957. Virus interference. II. Some properties of interferon. Proc R Soc Lond B Biol Sci 147:268-73.

120. Platanias LC. 2005. Mechanisms of type-I- and type-II-interferon-mediated signalling. Nat Rev Immunol 5:375-386.

121. Pestka S, Krause CD, Walter MR. 2004. Interferons, interferon-like cytokines, and their receptors. Immunol Rev 202:8-32.

122. Schreiber G. 2017. The molecular basis for differential type I interferon signaling. J Biol Chem 292:7285-7294.

123. Ishikawa H, Barber GN. 2008. STING is an endoplasmic reticulum adaptor that facilitates innate immune signalling. Nature 455:674-8.

124. Parvatiyar K, Zhang Z, Teles RM, Ouyang S, Jiang Y, Iyer SS, Zaver SA, Schenk M, Zeng S, Zhong W, Liu ZJ, Modlin RL, Liu YJ, Cheng G. 2012. The helicase DDX41 recognizes the bacterial secondary messengers cyclic di-GMP and cyclic di-AMP to activate a type I interferon immune response. Nat Immunol 13:1155-61.

125. Woodward JJ, Iavarone AT, Portnoy DA. 2010. c-di-AMP secreted by intracellular Listeria monocytogenes activates a host type I interferon response. Science 328:1703-5.

126. Schwartz KT, Carleton JD, Quillin SJ, Rollins SD, Portnoy DA, Leber JH. 2012. Hyperinduction of host beta interferon by a Listeria monocytogenes strain naturally overexpressing the multidrug efflux pump MdrT. Infect Immun 80:1537-45.

127. Sauer JD, Sotelo-Troha K, von Moltke J, Monroe KM, Rae CS, Brubaker SW, Hyodo M, Hayakawa Y, Woodward JJ, Portnoy DA, Vance RE. 2011. The N-ethyl-N-nitrosourea-induced Goldenticket mouse mutant reveals an essential function of Sting in the in vivo interferon response to Listeria monocytogenes and cyclic dinucleotides. Infect Immun 79:688-94.

128. Barchet W, Cella M, Colonna M. 2005. Plasmacytoid dendritic cells--virus experts of innate immunity. Semin Immunol 17:253-61.

129. Stockinger S, Kastner R, Kernbauer E, Pilz A, Westermayer S, Reutterer B, Soulat D, Stengl G, Vogl C, Frenz T, Waibler Z, Taniguchi T, Rulicke T, Kalinke U, Muller M, Decker T. 2009. Characterization of the interferon-producing cell in mice infected with Listeria monocytogenes. PLoS Pathog 5:e1000355.

130. Dresing P, Borkens S, Kocur M, Kropp S, Scheu S. 2010. A Fluorescence Reporter Model Defines "Tip-DCs" as the Cellular Source of Interferon β in Murine *Listeriosis*. PLoS ONE 5:e15567.

131. Muller U, Steinhoff U, Reis LF, Hemmi S, Pavlovic J, Zinkernagel RM, Aguet M. 1994. Functional role of type I and type II interferons in antiviral defense. Science 264:1918-21.

132.   Chawla-Sarkar M, Lindner DJ, Liu YF, Williams BR, Sen GC, Silverman RH, Borden EC. 2003. Apoptosis and interferons: role of interferon-stimulated genes as mediators of apoptosis. Apoptosis 8:237-49.

133.   Stark GR, Kerr IM, Williams BR, Silverman RH, Schreiber RD. 1998. How cells respond to interferons. Annu Rev Biochem 67:227-64.

134.   Hervas-Stubbs S, Perez-Gracia JL, Rouzaut A, Sanmamed MF, Le Bon A, Melero I. 2011. Direct Effects of Type I Interferons on Cells of the Immune System. Clinical Cancer Research 17:2619-2627.

135.   Fink K, Lang KS, Manjarrez-Orduno N, Junt T, Senn BM, Holdener M, Akira S, Zinkernagel RM, Hengartner H. 2006. Early type I interferon-mediated signals on B cells specifically enhance antiviral humoral responses. European Journal of Immunology 36:2094-2105.

136.   Davidson S, Crotta S, McCabe TM, Wack A. 2014. Pathogenic potential of interferon alphabeta in acute influenza infection. Nat Commun 5:3864.

137.   Fujikura D, Chiba S, Muramatsu D, Kazumata M, Nakayama Y, Kawai T, Akira S, Kida H, Miyazaki T. 2013. Type-I interferon is critical for FasL expression on lung cells to determine the severity of influenza. PLoS One 8:e55321.

138.   Mancuso G, Midiri A, Biondo C, Beninati C, Zummo S, Galbo R, Tomasello F, Gambuzza M, Macri G, Ruggeri A, Leanderson T, Teti G. 2007. Type I IFN signaling is crucial for host resistance against different species of pathogenic bacteria. J Immunol 178:3126-33.

139.   Manca C, Tsenova L, Bergtold A, Freeman S, Tovey M, Musser JM, Barry CE, 3rd, Freedman VH, Kaplan G. 2001. Virulence of a Mycobacterium tuberculosis clinical isolate in mice is determined by failure to induce Th1 type immunity and is associated with induction of IFN-alpha /beta. Proc Natl Acad Sci U S A 98:5752-7.

140.   Stanley SA, Johndrow JE, Manzanillo P, Cox JS. 2007. The Type I IFN Response to Infection with Mycobacterium tuberculosis Requires ESX-1-Mediated Secretion and Contributes to Pathogenesis. The Journal of Immunology 178:3143-3152.

141.   Perkins DJ, Rajaiah R, Tennant SM, Ramachandran G, Higginson EE, Dyson TN, Vogel SN. 2015. Salmonella Typhimurium Co-Opts the Host Type I IFN System To Restrict Macrophage Innate Immune Transcriptional Responses Selectively. Journal of Immunology 195:2461-2471.

142. Auerbuch V, Brockstedt DG, Meyer-Morse N, O'Riordan M, Portnoy DA. 2004. Mice Lacking the Type I Interferon Receptor Are Resistant to Listeria monocytogenes. The Journal of Experimental Medicine 200:527-533.

143. O'Connell RM, Saha SK, Vaidya SA, Bruhn KW, Miranda GA, Zarnegar B, Perry AK, Nguyen BO, Lane TF, Taniguchi T, Miller JF, Cheng G. 2004. Type I interferon production enhances susceptibility to Listeria monocytogenes infection. J Exp Med 200:437-45.

144. Carrero JA, Calderon B, Unanue ER. 2004. Type I interferon sensitizes lymphocytes to apoptosis and reduces resistance to Listeria infection. J Exp Med 200:535-40.

145. Fehr T, Schoedon G, Odermatt B, Holtschke T, Schneemann M, Bachmann MF, Mak TW, Horak I, Zinkernagel RM. 1997. Crucial role of interferon consensus sequence binding protein, but neither of interferon regulatory factor 1 nor of nitric oxide synthesis for protection against murine listeriosis. J Exp Med 185:921-31.

146. Eshleman EM, Delgado C, Kearney SJ, Friedman RS, Lenz LL. 2017. Down regulation of macrophage IFNGR1 exacerbates systemic L. monocytogenes infection. PLoS Pathog 13:e1006388.

147. Pitts MG, Myers-Morales T, D'Orazio SE. 2016. Type I IFN Does Not Promote Susceptibility to Foodborne Listeria monocytogenes. J Immunol 196:3109-16.

148. Betz M, Fox BS. 1991. Prostaglandin E2 inhibits production of Th1 lymphokines but not of Th2 lymphokines. J Immunol 146:108-13.

149. Kuroda E, Sugiura T, Zeki K, Yoshida Y, Yamashita U. 2000. Sensitivity difference to the suppressive effect of prostaglandin E2 among mouse strains: a possible mechanism to polarize Th2 type response in BALB/c mice. J Immunol 164:2386-95.

150. Kuroda E, Yamashita U. 2003. Mechanisms of enhanced macrophage-mediated prostaglandin E2 production and its suppressive role in Th1 activation in Th2-dominant BALB/c mice. J Immunol 170:757-64.

151. Serezani CH, Chung J, Ballinger MN, Moore BB, Aronoff DM, Peters-Golden M. 2007. Prostaglandin E2 suppresses bacterial killing in alveolar macrophages by inhibiting NADPH oxidase. Am J Respir Cell Mol Biol 37:562-70.

152. Hata AN, Breyer RM. 2004. Pharmacology and signaling of prostaglandin receptors: multiple roles in inflammation and immune modulation. Pharmacol Ther 103:147-66.

153. Grainger JR, Wohlfert EA, Fuss IJ, Bouladoux N, Askenase MH, Legrand F, Koo LY, Brenchley JM, Fraser ID, Belkaid Y. 2013. Inflammatory monocytes regulate pathologic responses to commensals during acute gastrointestinal infection. Nat Med 19:713-21.

154. Miao CM, Jiang XW, He K, Li PZ, Liu ZJ, Cao D, Ou ZB, Gong JP, Liu CA, Cheng Y. 2016. Bone marrow stromal cells attenuate LPS-induced mouse acute liver injury via the prostaglandin E 2-dependent repression of the NLRP3 inflammasome in Kupffer cells. Immunol Lett 179:102-113.

155. Takano M, Nishimura H, Kimura Y, Washizu J, Mokuno Y, Nimura Y, Yoshikai Y. 1998. Prostaglandin E2 protects against liver injury after Escherichia coli infection but hampers the resolution of the infection in mice. J Immunol 161:3019-25.

156. Harizi H. 2013. The immunobiology of prostanoid receptor signaling in connecting innate and adaptive immunity. Biomed Res Int 2013:683405.

157. Noor S, Goldfine H, Tucker DE, Suram S, Lenz LL, Akira S, Uematsu S, Girotti M, Bonventre JV, Breuel K, Williams DL, Leslie CC. 2008. Activation of cytosolic phospholipase A2alpha in resident peritoneal macrophages by Listeria monocytogenes involves listeriolysin O and TLR2. J Biol Chem 283:4744-55.

158. Zidar N, Odar K, Glavac D, Jerse M, Zupanc T, Stajer D. 2009. Cyclooxygenase in normal human tissues--is COX-1 really a constitutive isoform, and COX-2 an inducible isoform? J Cell Mol Med 13:3753-63.

159. Kienle K, Lammermann T. 2016. Neutrophil swarming: an essential process of the neutrophil tissue response. Immunol Rev 273:76-93.

160. Levy BD, Clish CB, Schmidt B, Gronert K, Serhan CN. 2001. Lipid mediator class switching during acute inflammation: signals in resolution. Nat Immunol 2:612-9.

161. Russel FG, Koenderink JB, Masereeuw R. 2008. Multidrug resistance protein 4 (MRP4/ABCC4): a versatile efflux transporter for drugs and signalling molecules. Trends Pharmacol Sci 29:200-7.

162. Kalinski P. 2012. Regulation of immune responses by prostaglandin E2. J Immunol 188:21-8.

163. Forstermann U, Neufang B. 1983. Elimination from the circulation of cats of 6-keto-prostaglandin E1 compared with prostaglandins E2 and I2. J Pharm Pharmacol 35:724-8.

164. Hamberg M, Samuelsson B. 1971. On the metabolism of prostaglandins E 1 and E 2 in man. J Biol Chem 246:6713-21.

165. Yang J, Petersen CE, Ha CE, Bhagavan NV. 2002. Structural insights into human serum albumin-mediated prostaglandin catalysis. Protein Sci 11:538-45.

166. Dey I, Lejeune M, Chadee K. 2006. Prostaglandin E2 receptor distribution and function in the gastrointestinal tract. Br J Pharmacol 149:611-23.

167. Narumiya S. 1994. Prostanoid receptors. Structure, function, and distribution. Ann N Y Acad Sci 744:126-38.

168. Regan JW. 2003. EP2 and EP4 prostanoid receptor signaling. Life Sci 74:143-53.

169. Fujino H, West KA, Regan JW. 2002. Phosphorylation of glycogen synthase kinase-3 and stimulation of T-cell factor signaling following activation of EP2 and EP4 prostanoid receptors by prostaglandin E2. J Biol Chem 277:2614-9.

170. Sugimoto Y, Narumiya S. 2007. Prostaglandin E receptors. J Biol Chem 282:11613-7.

171. Yamane H, Sugimoto Y, Tanaka S, Ichikawa A. 2000. Prostaglandin E(2) receptors, EP2 and EP4, differentially modulate TNF-alpha and IL-6 production induced by lipopolysaccharide in mouse peritoneal neutrophils. Biochem Biophys Res Commun 278:224-8.

172. Tilley SL, Coffman TM, Koller BH. 2001. Mixed messages: modulation of inflammation and immune responses by prostaglandins and thromboxanes. J Clin Invest 108:15-23.

173. Downey GP, Gumbay RS, Doherty DE, LaBrecque JF, Henson JE, Henson PM, Worthen GS. 1988. Enhancement of pulmonary inflammation by PGE2: evidence for a vasodilator effect. J Appl Physiol (1985) 64:728-41.

174. Hinson RM, Williams JA, Shacter E. 1996. Elevated interleukin 6 is induced by prostaglandin E2 in a murine model of inflammation: possible role of cyclooxygenase-2. Proc Natl Acad Sci U S A 93:4885-90.

175. Baratelli F, Lin Y, Zhu L, Yang SC, Heuze-Vourc'h N, Zeng G, Reckamp K, Dohadwala M, Sharma S, Dubinett SM. 2005. Prostaglandin E2 induces FOXP3 gene expression and T regulatory cell function in human CD4+ T cells. J Immunol 175:1483-90.

176. Hock BD, McKenzie JL, Keenan JI. 2017. Helicobacter pylori outer membrane vesicles inhibit human T cell responses via induction of monocyte COX-2 expression. Pathog Dis 75.

177. Hutchison DL, Myers RL. 1987. Prostaglandin-mediated suppression of macrophage phagocytosis of Listeria monocytogenes. Cell Immunol 110:68-76.

178. Pereira PAT, Assis PA, Prado MKB, Ramos SG, Aronoff DM, Paula-Silva FWG, Sorgi CA, Faccioli LH. 2017. Prostaglandins D2 and E2 Have Opposite Effects on Alveolar Macrophage Infected with Histoplasma capsulatum. J Lipid Res doi:10.1194/jlr.M078162.

179. Aronoff DM, Canetti C, Peters-Golden M. 2004. Prostaglandin E2 inhibits alveolar macrophage phagocytosis through an E-prostanoid 2 receptor-mediated increase in intracellular cyclic AMP. J Immunol 173:559-65.

180. Armstrong RA. 1995. Investigation of the inhibitory effects of PGE2 and selective EP agonists on chemotaxis of human neutrophils. Br J Pharmacol 116:2903-8.

181. Becattini S, Littmann ER, Carter RA, Kim SG, Morjaria SM, Ling L, Gyaltshen Y, Fontana E, Taur Y, Leiner IM, Pamer EG. 2017. Commensal microbes provide first line defense against Listeria monocytogenes infection. J Exp Med 214:1973-1989.

182. Quereda JJ, Dussurget O, Nahori MA, Ghozlane A, Volant S, Dillies MA, Regnault B, Kennedy S, Mondot S, Villoing B, Cossart P, Pizarro-Cerda J. 2016. Bacteriocin from epidemic Listeria strains alters the host intestinal microbiota to favor infection. Proc Natl Acad Sci U S A 113:5706-11.

183. Conlan JW, North RJ. 1991. Neutrophil-mediated dissolution of infected host cells as a defense strategy against a facultative intracellular bacterium. Journal of Experimental Medicine 174:741-744.

184. Pitts MG, D'Orazio SEF. 2018. A Comparison of Oral and Intravenous Mouse Models of Listeriosis. Pathogens 7.

185. Cao Y-A, Wagers AJ, Beilhack A, Dusich J, Bachmann MH, Negrin RS, Weissman IL, Contag CH. 2004. Shifting foci of hematopoiesis during reconstitution from single stem cells. Proceedings of the National Academy of Sciences 101:221-226.

186. Jones GS, D'Orazio SE. 2013. Listeria monocytogenes: cultivation and laboratory maintenance. Curr Protoc Microbiol 31:9B 2 1-7.

187. Bou Ghanem EN, Myers-Morales T, D'Orazio SE. 2013. A mouse model of foodborne Listeria monocytogenes infection. Curr Protoc Microbiol 31:9B 3 1-9B 3 16.

188. Bou Ghanem EN, Myers-Morales T, Jones GS, D'Orazio SE. 2013. Oral transmission of Listeria monocytogenes in mice via ingestion of contaminated food. J Vis Exp doi:10.3791/50381:e50381.

189. Kernbauer E, Maier V, Rauch I, Muller M, Decker T. 2013. Route of Infection Determines the Impact of Type I Interferons on Innate Immunity to Listeria monocytogenes. PLoS One 8:e65007.

190. Jiang J, Lau LL, Shen H. 2003. Selective depletion of nonspecific T cells during the early stage of immune responses to infection. J Immunol 171:4352-8.

191. Filardy AA, Pires DR, Nunes MP, Takiya CM, Freire-de-Lima CG, Ribeiro-Gomes FL, DosReis GA. 2010. Proinflammatory Clearance of Apoptotic Neutrophils Induces an IL-12lowIL-10high Regulatory Phenotype in Macrophages. The Journal of Immunology 185:2044-2050.

192. Voll RE, Herrmann M, Roth EA, Stach C, Kalden JR, Girkontaite I. 1997. Immunosuppressive effects of apoptotic cells. Nature 390:350-351.

193. Thale C, Kiderlen AF. 2005. Sources of interferon-gamma (IFN-gamma) in early immune response to Listeria monocytogenes. Immunobiology 210:673-83.

194. Yin J, Ferguson TA. 2009. Identification of an IFN-gamma-producing neutrophil early in the response to Listeria monocytogenes. J Immunol 182:7069-73.

195. Aoshi T, Carrero JA, Konjufca V, Koide Y, Unanue ER, Miller MJ. 2009. The cellular niche of Listeria monocytogenes infection changes rapidly in the spleen. European Journal of Immunology 39:417-425.

196. MacDonald TT, Carter PB. 1980. Cell-mediated immunity to intestinal infection. Infect Immun 28:516-23.

197. Monk IR, Casey PG, Hill C, Gahan CG. 2010. Directed evolution and targeted mutagenesis to murinize Listeria monocytogenes internalin A for enhanced infectivity in the murine oral infection model. BMC Microbiol 10:318.

198. Kernbauer E, Maier V, Rauch I, Muller M, Decker T. 2013. Route of Infection Determines the Impact of Type I Interferons on Innate Immunity to. PLoS One 8:e65007.

199. Reutterer B, Stockinger S, Pilz A, Soulat D, Kastner R, Westermayer S, Rulicke T, Muller M, Decker T. 2008. Type I IFN are host modulators of strain-specific Listeria monocytogenes virulence. Cell Microbiol 10:1116-29.

200. Yamamoto T, Hara H, Tsuchiya K, Sakai S, Fang R, Matsuura M, Nomura T, Sato F, Mitsuyama M, Kawamura I. 2012. Listeria monocytogenes strain-specific impairment of the TetR regulator underlies the drastic increase in cyclic di-AMP secretion and beta interferon-inducing ability. Infect Immun 80:2323-32.

201. Pontiroli F, Dussurget O, Zanoni I, Urbano M, Beretta O, Granucci F, Ricciardi-Castagnoli P, Cossart P, Foti M. 2012. The timing of IFNbeta production affects early innate responses to Listeria monocytogenes and determines the overall outcome of lethal infection. PLoS One 7:e43455.

202. Feng H, Zhang D, Palliser D, Zhu P, Cai S, Schlesinger A, Maliszewski L, Lieberman J. 2005. Listeria-infected myeloid dendritic cells produce IFN-beta, priming T cell activation. J Immunol 175:421-32.

203. Dejager L, Vandevyver S, Ballegeer M, Van Wonterghem E, An LL, Riggs J, Kolbeck R, Libert C. 2014. Pharmacological inhibition of type I interferon signaling protects mice against lethal sepsis. J Infect Dis 209:960-70.

204. Barker JR, Koestler BJ, Carpenter VK, Burdette DL, Waters CM, Vance RE, Valdivia RH. 2013. STING-dependent recognition of cyclic di-AMP mediates type I interferon responses during Chlamydia trachomatis infection. MBio 4:e00018-13.

205. Calame DG, Mueller-Ortiz SL, Morales JE, Wetsel RA. 2014. The C5a anaphylatoxin receptor (C5aR1) protects against Listeria monocytogenes infection by inhibiting type 1 IFN expression. J Immunol 193:5099-107.

206. Serbina NV, Salazar-Mather TP, Biron CA, Kuziel WA, Pamer EG. 2003. TNF/iNOS-producing dendritic cells mediate innate immune defense against bacterial infection. Immunity 19:59-70.

207. Skrenta H, Yang Y, Pestka S, Fathman CG. 2000. Ligand-independent down-regulation of IFN-gamma receptor 1 following TCR engagement. J Immunol 164:3506-11.

208. Ling PD, Warren MK, Vogel SN. 1985. Antagonistic effect of interferon-beta on the interferon-gamma-induced expression of Ia antigen in murine macrophages. J Immunol 135:1857-63.

209. Kasper LH, Reder AT. 2014. Immunomodulatory activity of interferon-beta. Ann Clin Transl Neurol 1:622-31.

210. Carrero JA. 2013. Confounding roles for type I interferons during bacterial and viral pathogenesis. Int Immunol 25:663-9.

211. Gough DJ, Messina NL, Clarke CJ, Johnstone RW, Levy DE. 2012. Constitutive type I interferon modulates homeostatic balance through tonic signaling. Immunity 36:166-74.

212. Mandel TE, Cheers C. 1980. Resistance and susceptibility of mice to bacterial infection: histopathology of listeriosis in resistant and susceptible strains. Infect Immun 30:851-61.

213. Segal AW, Dorling J, Coade S. 1980. Kinetics of fusion of the cytoplasmic granules with phagocytic vacuoles in human polymorphonuclear leukocytes. Biochemical and morphological studies. J Cell Biol 85:42-59.

214. Ermert D, Urban CF, Laube B, Goosmann C, Zychlinsky A, Brinkmann V. 2009. Mouse neutrophil extracellular traps in microbial infections. J Innate Immun 1:181-93.

215. Crow JP. 1997. Dichlorodihydrofluorescein and dihydrorhodamine 123 are sensitive indicators of peroxynitrite in vitro: implications for intracellular measurement of reactive nitrogen and oxygen species. Nitric Oxide 1:145-57.

216. Fang FC. 2004. Antimicrobial reactive oxygen and nitrogen species: concepts and controversies. Nat Rev Microbiol 2:820-32.

217. Stuehr DJ, Marletta MA. 1985. Mammalian nitrate biosynthesis: mouse macrophages produce nitrite and nitrate in response to Escherichia coli lipopolysaccharide. Proc Natl Acad Sci U S A 82:7738-42.

218. Pollock JD, Williams DA, Gifford MA, Li LL, Du X, Fisherman J, Orkin SH, Doerschuk CM, Dinauer MC. 1995. Mouse model of X-linked chronic granulomatous disease, an inherited defect in phagocyte superoxide production. Nat Genet 9:202-9.

219. Wilcox CS. 2010. Effects of tempol and redox-cycling nitroxides in models of oxidative stress. Pharmacol Ther 126:119-45.

220. Francischetti IM, Gordon E, Bizzarro B, Gera N, Andrade BB, Oliveira F, Ma D, Assumpcao TC, Ribeiro JM, Pena M, Qi CF, Diouf A, Moretz SE, Long CA, Ackerman HC, Pierce SK, Sa-Nunes A, Waisberg M. 2014. Tempol, an intracellular antioxidant, inhibits tissue factor expression, attenuates dendritic cell function, and is partially protective in a murine model of cerebral malaria. PLoS One 9:e87140.

221. Remold-O'Donnell E, Parent D. 1995. Downregulation of neutrophil CD43 by opsonized zymosan. Blood 85:337-42.

222. Gordon DL, Rice JL, McDonald PJ. 1989. Regulation of human neutrophil type 3 complement receptor (iC3b receptor) expression during phagocytosis of Staphylococcus aureus and Escherichia coli. Immunology 67:460-5.

223. Kay AB, Glass EJ, Salter DM. 1979. Leucoattractants enhance complement receptors on human phagocytic cells. Clin Exp Immunol 38:294-9.

224. Berger M, O'Shea J, Cross AS, Folks TM, Chused TM, Brown EJ, Frank MM. 1984. Human neutrophils increase expression of C3bi as well as C3b receptors upon activation. J Clin Invest 74:1566-71.

225. Rowan NJ, Kirf D, Tomkins P. 2009. Studies on the susceptibility of different culture morphotypes of Listeria monocytogenes to uptake and survival in human polymorphonuclear leukocytes. FEMS Immunol Med Microbiol 57:183-92.

226. Kolev M, Le Friec G, Kemper C. 2014. Complement--tapping into new sites and effector systems. Nat Rev Immunol 14:811-20.

227. Vahidy R, Jehan F. 1996. Enhanced in vitro engulfment of Listeria monocytogenes by rabbit polymorphonuclear leukocytes in the presence of sera from immune rabbits. FEMS Immunol Med Microbiol 14:103-7.

228. Reeves EP, Lu H, Jacobs HL, Messina CG, Bolsover S, Gabella G, Potma EO, Warley A, Roes J, Segal AW. 2002. Killing activity of neutrophils is mediated through activation of proteases by K+ flux. Nature 416:291-7.

229. Minakami R, Sumimotoa H. 2006. Phagocytosis-coupled activation of the superoxide-producing phagocyte oxidase, a member of the NADPH oxidase (nox) family. Int J Hematol 84:193-8.

230. Nauseef WM. 2004. Assembly of the phagocyte NADPH oxidase. Histochem Cell Biol 122:277-91.

231. Camejo A, Buchrieser C, Couve E, Carvalho F, Reis O, Ferreira P, Sousa S, Cossart P, Cabanes D. 2009. In vivo transcriptional profiling of Listeria monocytogenes and mutagenesis identify new virulence factors involved in infection. PLoS Pathog 5:e1000449.

232. Bortolussi R, Vandenbroucke-Grauls CM, van Asbeck BS, Verhoef J. 1987. Relationship of bacterial growth phase to killing of Listeria monocytogenes by oxidative agents generated by neutrophils and enzyme systems. Infect Immun 55:3197-203.

233. Archambaud C, Nahori MA, Pizarro-Cerda J, Cossart P, Dussurget O. 2006. Control of Listeria superoxide dismutase by phosphorylation. J Biol Chem 281:31812-22.

234. Arnett E, Vadia S, Nackerman CC, Oghumu S, Satoskar AR, McLeish KR, Uriarte SM, Seveau S. 2014. The pore-forming toxin listeriolysin O is degraded by neutrophil metalloproteinase-8 and fails to mediate Listeria monocytogenes intracellular survival in neutrophils. J Immunol 192:234-44.

235. Borregaard N, Cowland JB. 1997. Granules of the human neutrophilic polymorphonuclear leukocyte. Blood 89:3503-21.

236. Alford CE, Amaral E, Campbell PA. 1990. Listericidal activity of human neutrophil cathepsin G. J Gen Microbiol 136:997-100.

237. Odeberg H, Olsson I. 1975. Antibacterial activity of cationic proteins from human granulocytes. J Clin Invest 56:1118-24.

238. Standish AJ, Weiser JN. 2009. Human neutrophils kill Streptococcus pneumoniae via serine proteases. J Immunol 183:2602-9.

239. Basu S, Hodgson G, Katz M, Dunn AR. 2002. Evaluation of role of G-CSF in the production, survival, and release of neutrophils from bone marrow into circulation. Blood 100:854-61.

240. Lord BI, Molineux G, Pojda Z, Souza LM, Mermod JJ, Dexter TM. 1991. Myeloid cell kinetics in mice treated with recombinant interleukin-3, granulocyte colony-stimulating factor (CSF), or granulocyte-macrophage CSF in vivo. Blood 77:2154-9.

241. Tak T, Tesselaar K, Pillay J, Borghans JA, Koenderman L. 2013. What's your age again? Determination of human neutrophil half-lives revisited. J Leukoc Biol 94:595-601.

242. van der Pouw Kraan TC, Boeije LC, Smeenk RJ, Wijdenes J, Aarden LA. 1995. Prostaglandin-E2 is a potent inhibitor of human interleukin 12 production. J Exp Med 181:775-9.

243. Pitts MG, Combs TA, D'Orazio SEF. 2018. Neutrophils from Both Susceptible and Resistant Mice Efficiently Kill Opsonized Listeria monocytogenes. Infect Immun 86.

244. Murray EGD, Webb RA, Swann MBR. 1926. A disease of rabbits characterised by a large mononuclear leucocytosis, caused by a hitherto undescribed bacillus Bacterium monocytogenes (n.sp.). The Journal of Pathology and Bacteriology 29:407-439.

245. Cappelletti M, Presicce P, Lawson MJ, Chaturvedi V, Stankiewicz TE, Vanoni S, Harley IT, McAlees JW, Giles DA, Moreno-Fernandez ME, Rueda CM, Senthamaraikannan P, Sun X, Karns R, Hoebe K, Janssen EM, Karp CL, Hildeman DA, Hogan SP, Kallapur SG, Chougnet CA, Way SS, Divanovic S. 2017. Type I interferons regulate susceptibility to inflammation-induced preterm birth. JCI Insight 2:e91288.

246. Negishi M, Sugimoto Y, Ichikawa A. 1993. Prostanoid receptors and their biological actions. Prog Lipid Res 32:417-34.

Vita

Michelle Georgiana Pitts graduated from the University of Kentucky in 2006 with a Bachelor of Science in Animal Science. She originally came to Kentucky after winning a position in the Kentucky Equine Management Internship program, which places college students on Lexington area horse farms for an intensive period of training, in 2002. Michelle worked at Rood and Riddle Equine Hospital as an ICU technician while completing her undergraduate degree. After graduation, she held management positions at several area horse farms before deciding to obtain graduate education.

Michelle entered the Integrated Biomedical Sciences program in 2012 and the laboratory of Dr. Sarah D'Orazio in the Department of Microbiology, Immunology, and Molecular Genetics in May of 2013. She was invited to speak at the 2017 Phagocytes Gordon Research Seminar, awarded the 2017 UK Women's Club Fellowship, and was also named winner of the 2017 UK Infectious Diseases Research Day Three Minute Thesis competition.

At the time of submission of this document, Michelle is an author on three published papers: Pitts, et al. 2018 (*Infection and Immunity*), Pitts, et al. 2018 (*Pathogens*) and Pitts, et al. 2016 (*Journal of Immunology*).